STRUCTURAL AND FUNCTIONAL ANALYSIS ON HUMAN INO80 CHROMATIN REMODELING COMPLEXES

BY

LU CHEN

Submitted to the graduate degree program in

Biochemistry and Molecular Biology and

the Graduate faculty of the University of Kansas Medical Center
in partial fulfillment for the degree of
Doctor of Philosophy.

_____
Co-chairperson: Joan Conaway, Ph.D.

_____
Co-chairperson: Aron Fenton, Ph.D.

_____
Kenneth Peterson, Ph.D.

_____
Joseph Fontes, Ph.D.

_____
Joe Lutkenhaus, Ph.D.

Date defended: 09/10/2013

The Dissertation Committee for Lu Chen certifies

that this is the approved version of the following dissertation:

STRUCTURAL AND FUNCTIONAL ANALYSIS ON HUMAN INO80 CHROMATIN REMODELING COMPLEXES

Committee:

_____

Co-chairperson: Joan Conaway, Ph.D.

_____

Co-chairperson: Aron Fenton, Ph.D.

Date approved: 09/12/2013

ABSTRACT

The Conaway lab previously identified and purified a human ATP-dependent chromatin remodeling complex with similarity to the *Saccharomyces cerevisiae* INO80 complex (65) and demonstrated that it is composed of (i) a Snf2 family ATPase (hIno80) related in sequence to the *S. cerevisiae* Ino80 ATPase, (ii) 7 additional evolutionarily conserved subunits orthologous to yeast INO80 complex subunits, and (iii) 6 apparently metazoan-specific subunits. In the first part of my thesis, we present evidence that the human INO80 complex is composed of three modules that assemble with three distinct domains of the hIno80 ATPase. These modules include (i) one that is composed of the N-terminus of the hIno80 protein and all of the metazoan-specific subunits and is not required for ATP-dependent nucleosome remodeling, (ii) a second that is composed of the hIno80 HSA/PTH domain, the actin-related proteins Arp4 and Arp8, and the GLI-Kruppel family transcription factor YY1, and (iii) a third that is composed of the hIno80 Snf2 ATPase domain, the Ies2 and Ies6 proteins, the AAA+ ATPases Tip49a and Tip49b, and the actin-related protein Arp5. Through purification and characterization of hINO80 complex subassemblies, we demonstrate that ATP-dependent nucleosome remodeling by the hINO80 complex is catalyzed by a core complex comprised of the hIno80 protein HSA/PTH and Snf2 ATPase domains acting in concert with YY1 and the complete set of its evolutionarily conserved subunits.

In the follow-up chapter, we seek to define the requirement for assembling core subunits Ies2, Ies6, Arp5, Tip49a and Tip49b, and distinguish their functional contribution to INO80 chromatin remodeling process. We obtained evidence that the ATPase insertion regions of INO80 family ATPases are necessary and sufficient for assembling all of the five ATPase-associating subunits Ies2, Ies6, Arp5, Tip49a and Tip49b. The missing or inclusion of this insertion module correlates

with loss or gain of nucleosome binding capacity of the INO80 subcomplexes, suggesting they contribute to nucleosome binding. Consistent with this hypothesis, the subcomplexes missing the insertion module were not able to bind to nucleosome, thus they were deficient in nucleosome-stimulated ATPase and ATP dependent nucleosome remodeling activities. Within the insertion module, Ies6 and Arp5 form a heterodimer, and are mutually dependent for assembly into INO80. The heterodimer is dispensable for INO80's ATPase activity, but is required for the optimal nucleosome remodeling, presumably via its contribution in nucleosome binding. On the contrary, Ies2 assembles independently of the Arp5-Ies6 dimer, and is absolutely required for the catalytic activities of the INO80 complex, while dispensable for the binding affinity to nucleosomes. Our studies described in this thesis shed light on the structure and function of the human INO80 chromatin remodeling complex.

ACKNOWLEDGEMENTS

To reach this chapter of my graduate study and my life, I can not express enough gratitude to my mentors, Drs. Joan and Ronald Conaways. First of all, they made it all possible by letting me join the Conaway lab, and embark on the research of human INO80. Moreover, throughout my training in the lab, they opened the doors and show me the way to the wonderful world of protein science and biochemistry. Joan, who I initially met in her transcription lecture to 1st year IGPBS students, introduced me the history of the transcription field and made me re-live those days and nights of experimental effort by Joan and Ron that led to the purification and identification of general transcription factors for the eukaryotic transcription system. Ron, though not heavily involved in teaching duties, kept giving me important lessons that essentially shaped my way of thinking of molecular biology. He shared with me his strong belief in the power of *in vitro* well-defined biochemical approaches and their potential contribution to medicine and biology. He also taught me his "smart" strategies of identifying interesting projects, and how to prioritize them.

I have to say Joan and Ron's way of mentoring is simply amazing, because they seldom tell you what you should or should not do, and never point finger at your naiveness and mistake. Instead, they patiently lead and teach with their own example, by "silently" demonstrating to us their enthusiasm toward science, honest and rigorous standard in evaluating science, and hardworking ethics in weekends and holidays. To me, all of these are contagious. As a result, I have been quietly transformed from a green newbie (only equivalent to a western robot) to a trained biochemistry phD who is capable of designing and conducting controlled biochemistry experiments, and interpret results in a rigorous and cautious way. Additionally, I was allowed to freely explore and mature in a research environment without much pressure and worries, so that I

can test my ideas, follow my heart and interests, and carry out my research projects with all the support and freedom that I need in the world. More importantly, at the moment of finishing my study, I still appreciate and believe in hard work, the beauty and power of mechanistic studies and biochemistry.

Besides talking about their science, you can not simply do without appreciating how great of people Joan and Ron really are. They treat people with respect, generosity, kindness, humor and great deal of fairness. During my darker and stormy days of my graduate studies, Joan and Ron lent me unconditional supports; whenever I made really silly mistakes in the lab, the bad ink has always been embraced and diluted by their smiles and immense tolerance. I think that my learning from them on how to be a responsible, honest, and independently functioning individual is another huge part of the wealth that I inherited from my tenure in the Conaway lab.

My graduate school studies started and end with, and punctuated by interactions with my wonderful graduate committee. Beside Dr. Joan Conaway, Dr. Aron Fenton is the co-chair, who taught me metabolism in my IGPBS module 1 class. Then, Dr. Kenneth Peterson, Dr. Joseph Fontes, Dr. Joe Lutkenhaus, together with Joan, were the lecturers in the IGPBS module 2 molecular biology course, which was one of my favorite. I appreciate their teaching both in the classrooms, and their continued input and support in my comprehensive exam, every one of my committee meetings, the dissertation writing, and my final defense. Special thanks go to Joan and Joe for their critical revision of my thesis. Also, I want to thank Dr. Philippe Prochasson, the ex-member of the committee, for help and suggestions during our meetings as well. Their professionalism and helpful contributions are the ones that I will always be thankful, which keeps up the belief that working hard can always help you reach your destination.

Last but not the least, I want to thank the IGPBS program of Kansas University Medical Center for the opportunity that allowed me to come to and pursue my study in the U.S.; I want to thank Stowers Institute for Medical Research and all the outstanding core facilities for making my research possible, and the department of Biochemistry and Molecular Biology @KUMC for seminars and supports. Also, I, myself, am and my work is in debt to help from all Conaway lab members, past and present, especially Drs. Yong Cai and Jingji Jin, Dr. Dotan Sela, and Dr. Aaron Gottschalk. In addition, my lovely wife, Mengmeng Li, has been offering me great support, courage and positivity along in my sunny and not so bright days.

I am ready to turn to a new chapter of my career and life, but these thank you and cherished memories will always be there deep in my heart.

Lu Chen

2013-09-18

TABLE OF CONTENTS

TABLE OF FIGURES

Chapter I. Introduction and literature review

Nucleosome is the basic unit of the chromatin structure

The existence of histones was first recognized more than a century ago by Kossel et al. (73) in 1884. Histones were initially identified as universal components of eukaryotic chromosomes with a mass level very similar to that of the DNA; therefore, histones at that time were reckoned as candidate for carrier of the genetic material. Subsequently, histones were thought to exist in diverse forms, thus were considered as a good candidate for regulating gene expression. The proposed diversity, however, turned out to be an artifact of the histone purification procedure. High salt was used to extract histones from thymus tissue, whose abundant proteases can readily degrade histones into different "forms". The degradation problem was circumvented when acid extraction was appliedand 5 types of histones, namely H3, H4, H2A, H2B, and H1, were evident (102). People then realized that histones are among the most evolutionarily conserved, invariant proteins. Meanwhile, histones were notoriously hard to study due to their sticky nature – they bind to DNA and one another avidly, and form aggregates. Histones were then regarded as passive coating material of DNAs.

A major breakthrough in understanding the organizing principles of histones came from Kornberg *et al*. (72), who observed that a periodic pattern of 205 bp of DNA repeats was obtained by nuclease digestion of the chromatin of rat livers(58, 91), providing the first evidence supporting the model that the nucleosome is the basic repeating unit of the chromatin structure. In addition, histone proteins, under mild extraction condition, were cleanly separated into two groups, H3/H4, and H2A/H2B (133). Through combining the results of equilibirum ultracentrifugation and chemical cross-linking analyses, Kornberg

et al. (72) proposed the histone octamer model, in which a nucleosome is composed of an H3/H4 tetramer, and two H2A/H2B dimers. The observation of a repeated histone octamers was then supported by electron microscopic image of particles corresponding to the repeating nucleosome structure (93).

A high-resolution structure of the nucleosome particle was solved by Luger *et al*. (84), validating the nucleosome model. This important study demonstrated the globular nature of histone octamers and detailed interactions between histones and DNA, which locate to the phosphodiester backbones of the inner surface of the DNA superhelix (Figure 1). Notably, no contact with the bases of DNA was observed, suggesting histone-DNA interactions lack DNA sequence specificity, providing a mechanistic explanation for the observation that a histone octamer can package essentially any given piece of DNA. In addition, the basic amino-terminal tails of all 4 core histones pass through the DNA superhelix without structural hindrance and protrude outward from the histone octamer. These unstructured histone tails are highly flexible and carry rich information in the form of reversible chemical modifications. The specific combination of various post-translational modifications on the histone tails creates various nucleosomal interfaces, enabling downstream interaction with wide variety of chromatin proteins, ranging from neighboring histones to other regulatory enzymes.

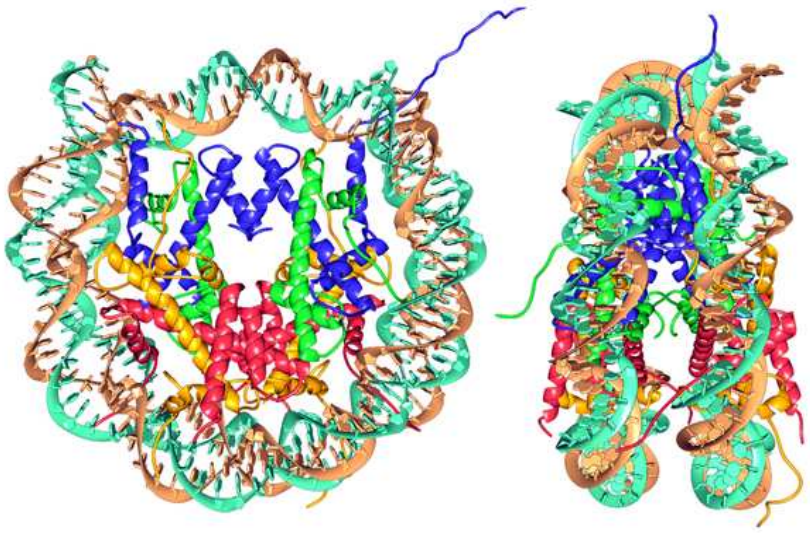

Figure 1 Nucleosome core particle structure.

The nucleosome is the fundamental repeating unit of chromatin. Both its internal and higher-order structures are crucial to the functioning of DNA in the nucleus. This structure contains 147 base pairs of DNA and two copies of each of the four core histone proteins: ribbon traces for the DNA phosphodiester backbones (brown and turquoise) and eight histone proteins (blue: H3; green: H4; yellow: H2A; red: H2B) Figure adapted from Luger, K *et al*..

The first level of chromatin compaction is the organization of the nucleosome structure. Native chromatin has been shown to appear as 11 nm beads-on-a-string by electron microscopy under conditions of low ionic strength (94). With the addition of salt, chromatin array appears to become more compact and resemble fiber-like structures with a diameter of approximately 30 nm (110). This 30 nm chromatin fiber constitutes the second level of chromatin compaction. A further level of chromatin and DNA compaction can be attained in the metaphase chromosome (Figure 2). How nucleosomes are arranged in the chromatin fiber is still a hotly debated question. Most models suggest the 30 nm fiber is made of a helical assembly of a string of zigzagging nucleosomes (39). Among many contributors to higher order chromatin compaction, histone H1, also called the linker histone, promotes coiling or folding of 30 nm chromatin fibers (105). In

addition, histone tails can form contacts with neighboring nucleosomes, thus promoting higher order compaction of chromatin fibers. Indeed, supporting evidence from the aforementioned crystal structure of the nucleosome by Luger *et al*. suggests H4 tails may contact a patch on the H2A-H2B dimer of the neighboring nucleosome. Conceivably, posttranslational modification of the histone tails can either facilitate or abolish these inter-nucleosomal interactions; thereby modulating the organization and accessibility of chromatin for other chromatin-templated transactions (128).

Figure 2. The nucleosome, fundamental particle of the eukaryotic chromosome.

Schematic shows the coiling of DNA around a set of eight histones in the nucleosome, the further coiling in condensed (transcriptionally inactive) chromatin, and uncoiling for interaction with the RNA pol II transcription machinery.

Nucleosomes inhibit access to DNA

The wrapping of DNA around histone octamers occlude one face of the DNA double helix and was initially hypothesized to interfere with many nuclear transactions, including transcription, replication, DNA damage repair and recombination. Indeed, early work showed that packaging promoter sequences with nucleosomes inhibits transcription initiation events by both bacterial and eukaryotic RNA polymerases *in vitro* (80). A similar inhibitory effect on transcription *in vivo* was also evident from genetic experiments in yeast (53). These and other observations led to the model that histones and nucleosomes in general repress transcription.

Two mechanisms have been proposed to contribute to transcription repression by chromatin structure: (i) at the level of a chromatin fiber, histone tails interactions play a vital role in establishing the higher order architecture of chromatin, and posttranslational modifications on histone tails regulate this process; (ii) at the level of single nucleosome, the contacts between the histone fold domain and DNA pose a hindrance for the basal transcription machinery to access the DNA bases, especially at key promoter and/or enhancer sequences. Condensation of the chromatin fiber may be relieved by an increase in histone acetylation level catalyzed by histone acetyltransferases (HATs), and be re-established by the counteracting histone deacetyltransferases (HDACs). On the other hand, the hindrance pose by interactions within a nucleosome core particle can be counteracted by a family of enzymes, namely ATP-dependent chromatin remodeling factors, which will be the main focus of this thesis work.

Nucleosome and its modification play a regulatory role in nuclear transactions

The discovery of various combinations of histone modifications and their correlation with transcriptional outcome has provided evidence to support a regulatory role of nucleosomes for gene expression. Acetylation of multiple lysine residues in the histone tails is associated with active transcription. Additionally, heterochromatic regions of the genome lack acetylation and are constitutively inactive for transcription. Moreover, substitution of H4 lysines with un-acetylatable arginines abolished the expression of a group of inducible genes (8). Finally, many previously identified transcriptional coactivators, such as SAGA and CBP/p300, actually contain HAT activity.

The connection between histone acetylation and transcription is further supported by the finding that histone deacetylation caused by HDACs can repress transcription (123). Several corepressor complexes have been shown to possess HDAC activity, such as Rpd3, and HDAC1. Arguing that histone deaceylases alone are sufficient to confer transcription repression, yeast and mammalian Rpd3s can be directly fused with a heterologous DNA-binding domain and can sufficiently mediate transcription repression, which is sensitive to inhibitors of histone deacetylases. In the physiological setting, all HDACs identified so far reside in large multi-protein complexes with other non-catalytic subunits playing an essential role in regulating and targeting HDAC activity.

Besides acetylation, histone globular domains and tails are subject to a wide variety of posttranslational modifications, which include methylation of arginine (R) and lysine (K) residues; acetylation, ubiquitination, sumolation, and ADP-ribosylation; and phosphorylation of serines (S) and threonines (T) (Figure 3). Much evidence has

suggested a correlative relationship between certain types of modification and the transcriptional outcome of the underlying gene. Active transcription is usually associated with acetylation of multiple residues in H3 and H4, and with di- or tri-methylation of H3 at lysine 4 position; heterochromatic and intergenic regions of the genome often are transcriptionally inactive and are commonly associated with H3 K9 methylation and H3 K27 methylation (74).

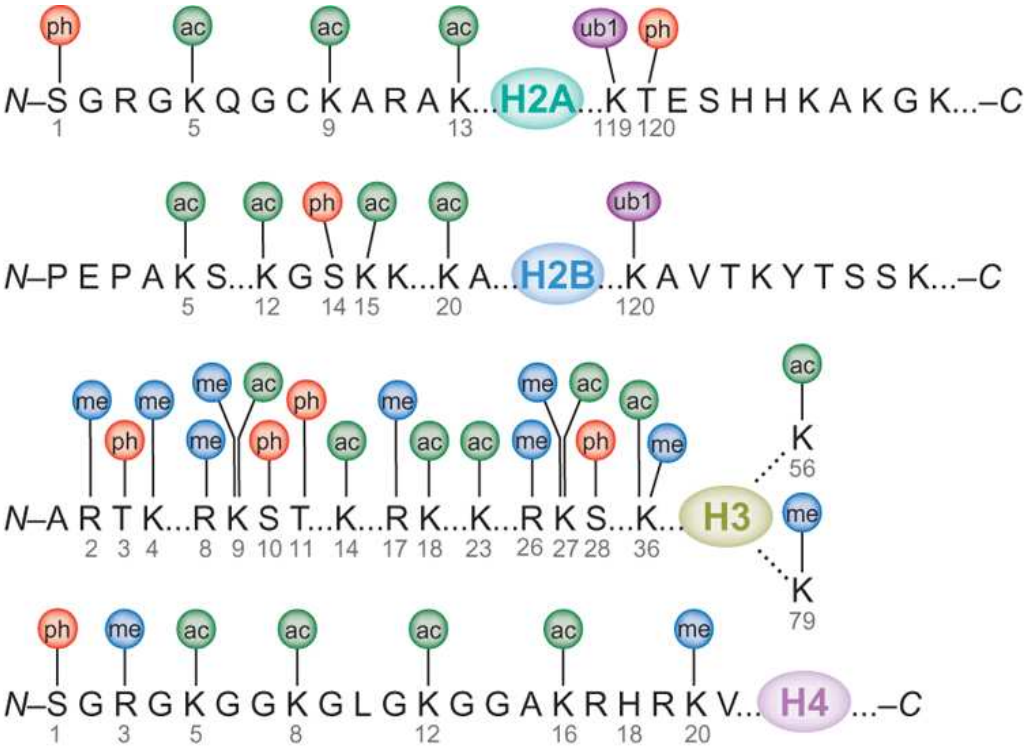

Figure 3. Post-translational modifications of human nucleosomal histones

The modifications include acetylation (ac), methylation (me), phosphorylation (ph) and ubiquitination (ub1). Most of the known histone modifications occur on the N-terminal tails of histones, with some exceptions including ubiquitination of the C-terminal tails of H2A and H2B and acetylation and methylation of the globular domain of H3 at K56 and K79, respectively. Globular domains of each core histone are represented as colored ovals. Figure adapted from Bhaumik et al. (7)

Specific histone modification patterns annotate the metazoan genome and holds predicative power for transcriptional outcome temporally and spatially. Silenced, but developmental poised, genes have shown to be enriched for a specific modification

pattern of overlapping H3K4 methylation and H3K27 methylation in their promoter nucleosomes, the so-called bivalent domains (6). Additionally, H3K4 mono methylation and H3K27 acetylation have been identified as the predominant modifications deposited at nucleosomes flanking enhancer elements, and have been successfully used as a key signature to isolate enhancer sequences at a genome wide scale (20).

The complexity in the type and combination of histone modifications resembles a "histone code" that may define functional states of chromatin and regulate various chromatin-templated transactions. The detailed mechanisms by which cells may interpret this histone code are subjects under intense investigation. Two non-mutually exclusive models have been proposed: the first "direct model" describes the scenario that histone modification may directly affect chromatin condensation and decondensation, as mentioned above in the case of acetylation on histone tails. Mechanistically, the addition of an acetate group reduces the positive charge of the lysine side chain, thus attenuating the favorable interactions between basic histone proteins and the negative charge of DNA (118, 119, 131). Histone phosphorylation would serve as another example of the direct model (1). A second "reader-effector" model proposed that various histone modifications are "read" by effector proteins carrying specific recognition pockets, facilitating downstream biological events via the recruitment or stabilization of other chromatin remodeling and/or modifying complexes (e.g. HATs, HDACs), or general transcription machineries (RNA polymerases, general transcription factors)(114). Biochemical and biophysical methods have uncovered a wide range of modular protein domains that specifically recognize histone modifications in a way that is dependent on both modification state and position within a histone protein. Histone tails carry a rich

combination of posttranslational modifications, creating endless possibilities to be recognized by downstream effector proteins. Thus, modifications of histones may provide an integrative platform, permitting chromatin complexes to receive information from upstream signaling cascades (24).

The history and logic of chromatin remodeling

As introduced earlier, nucleosome packaging *per se* is inhibitory to transcription, presumably because it blocks the access of the basal transcription apparatus and activator proteins to DNA. However, at actively transcribed genes *cis* regulatory DNA sequences, such as promoters and enhancers, have been reported to be hypersensitive to nuclease digestion and are likely to be devoid of nucleosomes suggesting a requirement for an active mechanism by which nucleosome structure and occupancy in key regions of the eukaryotic genome can be controlled and regulated.

The most well studied histone modifications so far are those that occur on the amino terminal tails of histones. As introduced previously, histone tail modifications play important roles in regulating higher order chromatin organization and in recruiting downstream effectors, but they are less likely to have a major impact on nucleosome core structure, since the tails protrude away from the core particle, and do not contribute directly to any histone core-DNA interaction.

An understanding of mechanisms responsible for controlling nucleosome occupancy began to emerge with the discovery of ATP-dependent chromatin remodeling factors as essential regulators of chromatin structure and gene expression. The first chromatin remodeling factor identified was the yeast SWI/SNF complex (switch/sucrose

nonfermermentable). The realization of the function of a group of genes encoding subunits of SWI/SNF complexes was initially obscured by the fact that multiple phenotypic traits were observed when these genes were mutagenized in several screens conducted in the budding yeasts. These diverse phenotypes include the inability to undergo mating-type switching (51); increase the mutation rate of mitochondrial genes (45); and defects in sugar fermentation (88). The first evidence to suggest that these *swi/snf* genes may affect gene transcription *via* altering chromatin structure came from the work by Hirschorn *et al*. (59). First, these authors observed that the transcriptional defects in strains lacking these swi/snf genes could be suppressed by genetically deleting one of the two sets of genes encoding histone H2A and H2B; second, in two swi/snf mutants, they observed an altered nuclease digestion pattern of the SUC2 promoter, suggestive of a change in chromatin structure. The altered chromatin structure could be rescued by reducing expression of H2A-H2B, but not upon inhibiting specific transcription initiation from the SUC2 promoter by mutating its TATA box.

Laurent *et al*. and Cairns *et al*.. provided evidence that several of the SWI/SNF proteins physically associate with each other during immunoprecipitation and chromatographic separation, including SWI1/ADR6, SWI2/SNF2, SWI3, SNF5, and SNF6 (19, 76). This multi-subunit complex, referred to as the SWI/SNF complex, was the first chromatin remodeling complex to be identified. Yeast SWI/SNF complexes were subsequently shown to be required for transcription by DNA-specific activator proteins, including yeast GAL4 and the glucocorticoid receptor expressed in yeast (100, 145). A mechanistic explanation was provided by Cote *et al*. (30), who showed that the binding of GAL4 to nucleosomal DNA could be dramatically enhanced by SWI/SNF complexes in a reaction

that depends on ATP hydrolysis and the presence of the catalytically active SWI2 subunit. Moreover, SNF2, SNF5, and SNF6 were found to be sufficient to activate transcription when tethered to DNA by fusing with a LexA DNA binding domain (75). Therefore, the SWI/SNF remodeling complex was proposed to be generally a transcriptional coactivator complex that can alter the structure of promoter chromatin in an ATP-dependent way, thus facilitating activities of sequence-specific transactivators and the RNA transcription machinery.

The SWI/SNF chromatin remodeling complex is evolutionarily conserved, with homologous subunits having been identified in many species, from yeast to flies, plants, and mammals. Supporting the role of the SWI/SNF chromatin remodeling complex as a transcription coactivator, the *Drosophila* homolog of SWI2/SNF2, Brahma (BRM), was identified in a screen for genes that suppress the body segmentation defects caused by polycomb mutations (70). Such suppressor genes were designated trithorax group genes, among which are other chromatin remodeling factors (e.g. ISWI), and histone modifying proteins (e.g. trithorax/MLL). It is known that reduced expression of the Hox gene locus can lead to the kind of homeotic transformation phenotype that was evident in BRM mutants, suggesting BRM plays a role in maintaining the proper expression of Hox genes. Proteins encoded by the Polycomb group of genes were demonstrated to co-associate and assemble into multi-protein complexes known as PRC1 and PRC2, which are well known gene repressors capable of modulating histone modification and chromatin structure (120). Therefore, BRM and other chromatin remodeling factor can antagonize the silencing effect by well-known chromatin modulators, strengthening the idea that they regulate gene expression via modulating chromatin structure. Subsequently,

it was observed that the BRM complex (i) was associated with regions of actively transcribed regions that were not bound by polycomb group proteins and (ii) was required for the association of RNA polymerase II with salivary gland chromosomes (3).

Structural Characteristics of SWI/SNF2-like ATPase motor

The yeast SWI2/SNF2 gene encodes a protein that is homologous to other ATP-dependent DNA and/or RNA helicases (77). Helicases can be subdivided into 6 helicase-like superfamilies (SF1-SF6) on the basis of primary sequence similarity. SF1 and SF2 share sequence similarity in their common core, which is comprised of two RecA-like domains (124), whereas SF3-SF6 are ring-forming helicases. The budding yeast Snf2 protein and proteins with similar primary sequence have been categorized as members of the SF2 superfamily (43).

The two RecA-like domains of SF2 helicases are each comprised of 7 short but ordered helicase motifs, designated motifs I, Ia, II, III, IV, V, and VI (49), which adopt a bi-lobular structural fold with a central opening cleft as its active site (Figure 4, model built based on the published crystal structure of zebrafish Rad54A [pdb 1Z3I (127)]). Motif I contains the "Walker A" motif and is responsible for binding of the triphosphate tail of ATP (99); Motif Ia forms the edge of a shallow groove across the surface of the protein and may be involved in binding to DNA; Motif II is the DEAD box motif (111), also part of the "Walker B" motif, and has been implicated in binding of Mg^{2+}, which is required for ATP hydrolysis by both DNA and RNA helicases (15); Motif III functions as a hydrolysis sensor, and is likely involved in the coupling of ATP hydrolysis to helicase activity (99); Motif IV forms the linkage between the two RecA like domains, running underneath and then forming a part of the ATP binding site. Motifs V and VI contribute

both to the sides of the ATP binding site and domain interface and could be important for regulating the helicase activity of the protein (124). The collective function of the two RecA-like domains has been proposed to orchestrate transformation of chemical energy released from ATP hydrolysis to mechanical forces, driving the translocation of these RecA-like helicase motors on a nucleic acid substrate. This model may represent a more general mechanism used by many other RecA domain containing enzymes (144).

The inclusion of a Snf2-like motor ATPase has been a defining feature for all ATP-dependent chromatin remodeling machineries. The most remarkable feature of the Snf2 family structure compared to other known SF2 members are several additional structural elements grafted onto the RecA-like core structure (Figure 4B-F). These Snf2-specific features comprise: 1) Two anti-parallel alpha helical protrusions 1 and 2 (Figure 4C), with protrusion 1 sticking out from the RecA-like domain 1 (snf2-N), and protrusion 2 sticking out from the RecA-like domain 2 (snf2-C). 2) A structured linker between the two RecA-like domains (Figure 4D), which connects the two protrusions. The two helical protrusions and the linker are all encoded within an enlarged span between motif III and IV (Figure 4G). 3) A triangular "brace motif" (Figure 4F) is packed against protrusion 2 and encoded by sequences immediately downstream of motif VI, the last conserved motif of the snf2-like ATPase region. 4) A major insertion site is also located next to the protrusion 2 (Figure 4E, 4G). The presence of insertions of variable lengths led to the description of Snf2 family proteins as “split” ATPases. The discontinuity of the RecA-like ATPase domain defines itself as a bipartite combination of SNF2_N and Helicase_C (43).

Snf2-like proteins are not only ubiquitous in eukaryotes but also are present in eubacteria and archaea. A homology search of the human genome against yeast Snf2 reveals a high degree of homology with 26 other ATPase domain-containing proteins. Despite the similarity in the core Snf2-like domain, these human Snf2-like proteins are genetically non-redundant *in vivo*, indicating they play specialized and diverse functions (56).

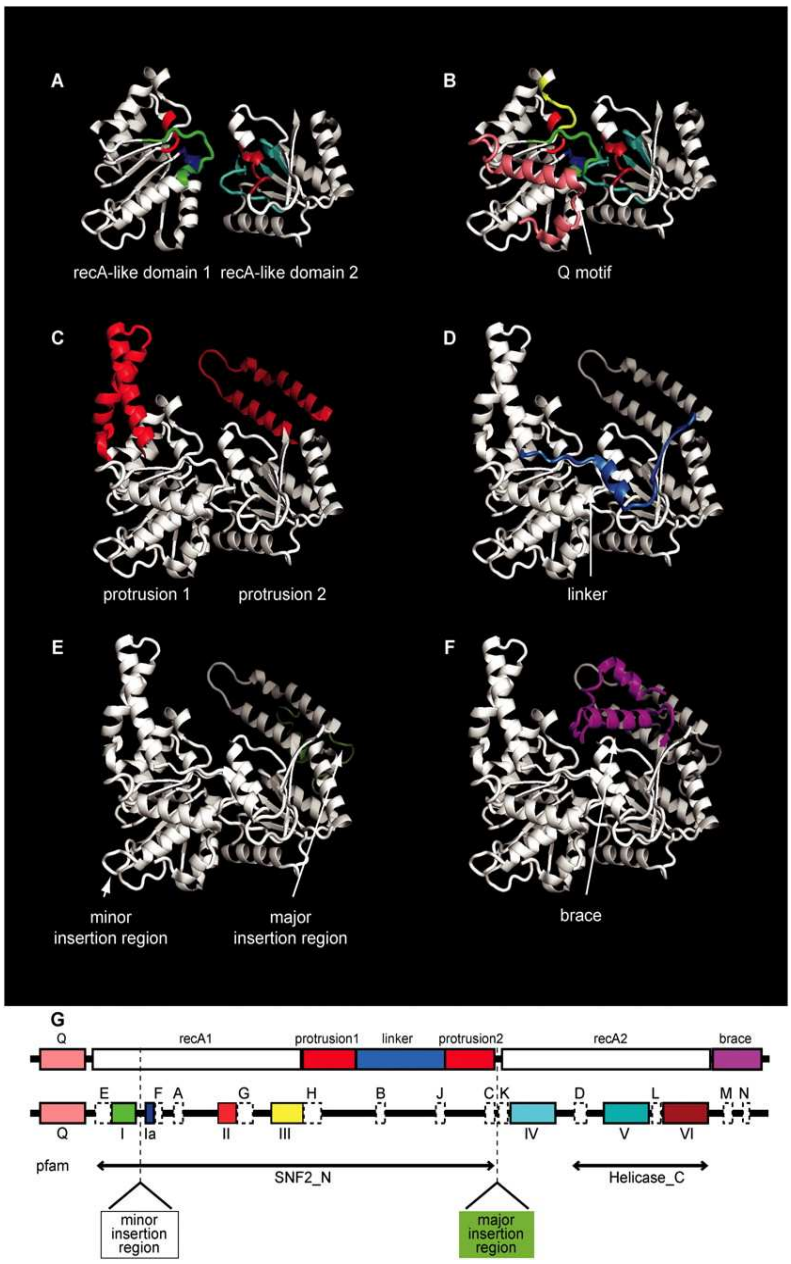

Figure 4. Conserved blocks contribute to distinctive structural features of Snf2 family proteins.

Structural components of Snf2 family proteins relevant to the conservation are illustrated on the zebrafish Rad54A structure [pdb 1Z3I (127)]. (A) Core RecA-like domains 1 and 2 including coloring of helicase motifs (I in green, Ia in blue, II in bright red, III in yellow, IV in cyan, V in teal and VI in dark red). (B) Q motif (pink). (C) Anti-parallel alpha helical protrusions 1 and 2 (red) projecting from RecA-like domains 1 and 2, respectively. (D) Linker spanning from protrusion 1 to protrusion 2 (middle blue). (E) Major insertion region behind protrusion 2 (light green). (F) Triangular brace (magenta). (G) Schematic diagram showing location of structural elements and helicase motifs colored as in A–F, with conserved blocks shown as white boxes. Spans identified by Pfam profiles SNF2_N and Helicase_C are shown flanking the major insertion site. Figure adapted form Flaus et al. (43)

Subfamilies in Snf2-like chromatin remodeling factors

Snf2-like remodeling enzymes can be further subdivided into four subfamilies on the basis of protein motifs and domains found outside of their RecA-like ATPase core domain. All four utilize ATP hydrolysis to alter histone-DNA contacts, and share a similar ATPase domain. However, all four family members are also specialized for a given biological purposes and contexts, imparted by unique accessory domains residing in the core Snf2-like ATPase subunit, and also by other accessory subunits.

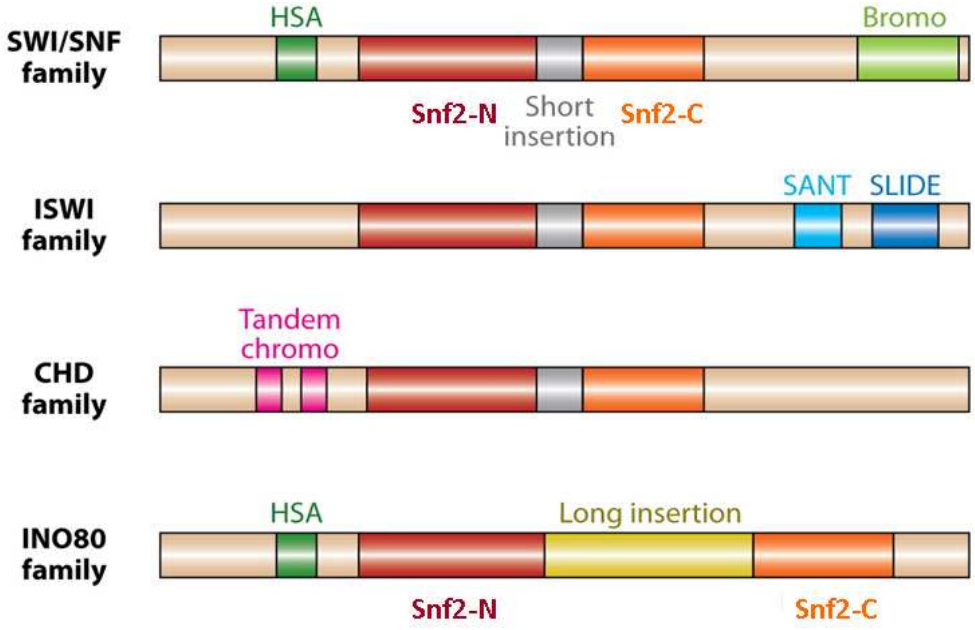

Figure 5. Remodeler Families, defined by their ATPase.

All remodeler families contain a SWI2/SNF2-family ATPase subunit characterized by an ATPase domain that is split in two parts: Snf2-N (*red*) and Snf2-C (*orange*). What distinguishes each family are the unique domains residing within, or adjacent to, the ATPase domain. Remodelers of the SWI/SNF, ISWI, and CHD families each have a distinctive short insertion (*gray*) within the ATPase domain, whereas remodelers of INO80 family contain a long insertion (*yellow*). Each family is further defined by distinct combinations of flanking domains: Bromodomain (*light green*) and HSA (helicase-SANT) domain (*dark green*) for SWI/SNF family, SANT-SLIDE module (*blue*) for ISWI family, tandem chromodomains (*magenta*) for the CHD family, and HSA domain (*dark green*) for the INO80 family. Figure adapted from Clapier *et al.* (25).

SWI/SNF family remodeling factors

As previously mentioned, the budding yeast Snf2 protein is the founding member of the SWI/SNF subfamily and indeed of all Snf2 family remodeling factors. Snf2 proteins of this subfamily contain HSA (helicase-SANT) and post-HSA domains and a C-terminal bromodomain. Like in many other Snf2-like remodeling factors, the Snf2 protein incorporates into a large multi-subunit protein complex, and serves as the catalytic subunit of the SWI/SNF remodeling complex. A pair of actin related proteins (ARP7 and ARP9) is present in yeast SWI/SNF complexes, whereas a dimer of actin and Arp4 (also known as Baf53a or b) are present in higher orthologs (86). Other conserved subunits contain additional conserved domains. For example, hBAF155/170 has SANT and SWIRM domains, hBAF60 has a SwiB domain, and human polybromo subunits have multiple bomodomains.

Close Snf2 homologues have been identified in many model organisms, and most eukaryotes build Snf2 chromatin remodeling complexes around related Snf2-like proteins, including paralogous Snf2 and Sth1 in yeast SWI/SNF and RSC (remodels the structure of chromatin), Brahma in *drosophila melanogaster*, and human BRM and BRG1. Many of these SWI/SNF family remodeling complexes have been shown to alter the structure of the nucleosome and to be involved in transcriptional regulation, presumably *via* disrupting histone-nucleosome contacts, thus leading to either nucleosome sliding or complete octamer removal (82).

Homologues in higher organisms such as BRG1 and BRM reside in multi-protein complexes with highly related components of the yeast SWI/SNF complex. However, SWI/SNF subfamily members have also been reported to associate with other nuclear proteins including histone deacetylases (HDACs), histone chaperones, methyl DNA-

binding proteins, histone methyl transferases, the retinoblastoma (RB) tumor suppressor protein, components of the basal transcription apparatus, and cohesin. These complexes can be recruited to specific regions of the genome through interaction with sequence-specific DNA-binding proteins or specific patterns of histone modifications (101).

ISWI family remodeling factors

The SNF2 family ATPase Iswi (Imitation of *SWI2*) was identified initially identified in *Drosophila melanogaster* based on its similarity to Snf2. Most eukaryotes assemble ISWI remodeling machineries (called NURF, CHARAC, and ACF complexes) of 2 to 4 subunits. These ISWI family remodelers share catalytic ISWI ATPases and include other specialized accessory subunits (29). ISWI family ATPases are characterized by the presence of C terminal regions that include a SANT domain with an adjacent SLIDE domain, which together form a nucleosome recognition module that is capable of recognizing unmodified histone tails and DNA (12). Specialized subunits carry unique domains, including a DNA-binding histone fold in hCHRAC, plant homeodomain (PHD) and bromodomain in hBPTF and hACF1, and the DNA-binding motif HMGI in dNURF301. Biochemical studies support the idea that ISWI complexes reposition rather than remove nucleosomes, thus modulating the spacing of a nucleosome array. Notably, all ISWI remodeling factors require a particular region of the histone H4 tail that is positioned near the DNA surface and presumably functions as an allosteric effector (27, 52). ISWI family members are reported to be involved in various functions, including activation or repression of transcription initiation and elongation, DNA replication and chromatin assembly (129).

CHD family remodeling factors

Mouse Chd1 (chromodomain, helicase, DNA binding, CHD) protein is the founding member of the chromodomain-containing subfamily of chromatin remodeling enzymes (33). The defining feature of CHD family members is the inclusion in their N-terminal regions of two tandemly arranged chromodomains, which have been demonstrated to recognize diverse binding partners, including proteins, DNA, and RNA (13). CHD family proteins have been purified as single subunit enzymes but in vertebrates can also assemble into multi-subunit complexes. For example, the Mi-2 ATPase is a component of NuRD (nucleosome remodeling and deacetylase) complexes, which also contain histone deacetylases (HDACs) and methyl CpG-binding domain (MBD) proteins (34), thus linking DNA methylation to chromatin remodeling and histone deacetylation. Certain CHD family remodeling factors can slide or eject nucleosomes in a way that is dependent on the presence of their chromodomains (10). CHD family remodeling factors have been reported to be involved in transcription elongation and termination, chromosome condensation, gene repression during developmental processes, and it has been suggested that CHD subfamily ATPases may assume these diverse and specific functions via combinatorial assembly with different homologous subunits (11).

INO80 family remodeling factors

The prototypical remodeler of the INO80 subfamily is the Ino80 ATPase from budding yeast, which was identified in a genetic screen for genes involved in transcriptional activation upon inositol starvation (40). The authors of this study also observed that Ino80 protein was present in a high molecular weight species in a yeast lysate, suggesting that it may reside in a multi-protein complex. Consistent with this possibility, Shen *et al*. (116) purified the INO80 containing complex from budding yeasts and identified 14

polypeptides other than Ino80 ATPase. Importantly, the study demonstrated that the yeast INO80 was able to catalyze ATP-dependent nucleosome sliding activity, DNA-stimulated ATPase activity, and to separate DNA strands in a primer-displacement assay, making the INO80 complex the only known Snf2 family remodeling complex so far to exhibit helicase activity *in vitro*.

Subsequently, the Conaway lab purified and defined the subunit composition of human INO80-like chromatin remodeling complexes from human cell lines. Together with reports on INO80 complexes identified in *Drosophila melanogaster* (71), it is apparent that INO80 complexes contain a subset of 9 subunits that is evolutionarily conserved in all eukaryotes. Among these are the snf2-like Ino80 ATPase, actin, actin-related proteins Arp4, Arp5, and Arp8, AAA^+ ATPases RvB1 and RvB2, Ies2, and Ies6. In addition to these conserved core subunits, yeast INO80 and human INO80 complexes each include a collection of species-specific subunits, including yeast specific subunits: TATA-binding-protein-associated factor 14 (Taf14), high mobility group (HMG) domain- containing non-histone protein 10 (Nhp10) and four additional Ies (INO Eighty Subunits) 1, 3, 4, and 5; and metazoan-specific subunits Gli-Kruppel zinc finger transcription factor Ying-Yang 1 (YY1), nuclear factor related to κB (NFRKB), ubiquitin protease UCH37, forkhead domain associated (FHA) domain-containing MCRS1, pre-B cell acute lymphoblastic leukemia fusion protein TFPT/Amida, and protein with unknown function FLJ20309 (INO80D), FLJ90652 (INO80E) (28).

The defining feature of Ino80 family remodeling ATPases is the inclusion of a large insertion region that is located at the major insertion site of Snf2-like ATPases between helicase motifs III and IV (Figure 4G), and that splits the conserved Snf2-like ATPase

domain. INO80 family remodeling complexes are also characterized by the inclusion of AAA^+ ATPases RvB1 and RvB2, which resemble the *E. coli* Holliday junction resolvase. It is suggested that the ATPase insertion region of the Ino80 ATPase is responsible for the assembly of RvB1 and RvB2 (Tip49a and Tip49b in human INO80 complexes) (140).

Functional analyses of the INO80 complex have suggested its involvement in multiple processes *in vivo*. INO80 directly occupies a large number of genomic targets in yeast, and mutant strains display transcriptional defects (40, 116). In human cells, INO80 also contributes to transcriptional regulation of at least some genes regulated by the transcription factor YY1, which is tightly associated with human INO80. Whether human INO80 has a more general function remains to be determined. In addition, mutations in INO80 complex subunits render yeast cells sensitive to DNA damaging agents and lead to defects in multiple repair pathways (18, 87, 132), and knocking down INO80 subunits lead to DNA repair defects in human cells as well (139). Mutation of genes encoding INO80 subunits also interferes with efficient progression of replication forks during DNA synthesis and with maintenance of telomere structure (96, 135, 146).

Mechanisms of chromatin remodeling

The electrostatic interactions underlying DNA-histone association collectively are strong and stable, energetically disfavoring spontaneous unwrapping. However, mechanistic studies of a variety of remodeling complexes have provided insight into how ATP-dependent chromatin remodeling complexes can catalyze disruption of these DNA-histone interactions in order to promote nucleosome sliding, and histone exchange *in vitro*. Initially, a twist diffusion model was proposed, in which DNA twists around nucleosomes to accommodate the gain of base pair due to the action of chromatin

remodelelers. The DNA twist is then propagated through the rest of DNA: histone contacts, leading to the relative movement of DNA around nucleosomes. However, this model was rejected on the basis that large impediments to DNA twisting, such as biotin crosslinks and DNA hairpins, produced no defect in nucleosome sliding (2, 122). The twist diffusion model was then replaced by a "loop recapture" model, which argues for the generation of a DNA loop created by an altered topological state of DNA induced upon engagement of ISWI family remodeling complexes to nucleosomal substrate (122). A subsequent release of the binding of nucleosomal DNA by the remodeler would then drive the movement of DNA loop over the histone octamer, thereby contributing to nucleosome movement on DNA.

The mechanistic basis for DNA loop/wave can be explained as a byproduct of the translocation process by chromatin remodeling complexes. In the case of budding yeast SWI/SNF, Saha *et al*. proposed that the Sth1 ATPase binds to a fixed position on the nucleosome, from which it utilizes its translocase activity to break histone-DNA contacts, and propagates a directional wave of the freed DNA around the octamer (107). In addition, DNA footprinting and crosslinking experiments have placed the Snf2-like ATPase at a site of weak DNA-histone contact, where torsional strain might be tolerated for propagation of the loop (113). Moreover, electron micrographic reconstitution of the full RSC and SWI/SNF complexes suggest that these remodeling machineries form a multi-lobed C-shaped structure that cradles the nucleosome in a central cavity with its DNA entry and exit points exposed (21, 32, 78). Arguing that neither DNA loop/bulging from the octamer surface nor DNA twisting could explain the basis of chromatin remodeling, Lorch *et al*.. (81) provided evidence that binding of the yeast RSC

remodeling complex to a nucleosome in the absence of ATP can release DNA from octamer surface, and initiate DNA translocation. Subsequently, ATP binding by the Snf2 ATPase kick starts the translocation, and the ATP hydrolysis completes and resets the cycle. Therefore, the authors proposed the model that the binding energy of the chromatin remodeling complexes to nucleosomes is sufficient to disrupt DNA-histone contacts, presumably by affecting histone octamer conformation and through extensive interaction with nucleosomal DNA.

In contrast to SWI/SNF, ISWI family chromatin remodeling complexes make fewer contacts with the nucleosome and extra-nucleosomal DNA, which is required for ISWI-nucleosome binding (31, 46, 68). These complexes bind a nucleosome as a dimer, and facilitate the bi-directional processive translocation of DNA (9, 103). This notion is consistent with the observations that ISWI remodeling complexes can measure the length of the linker DNAs and evenly position the nucleosome in the center of a piece of DNA of sufficient length; thereby, functioning as a spacing factor for nucleosome arrays (142). Mechanistically speaking, as a single remodeling ATPase Sth1 alone was reported to sufficiently catalyze nucleosome sliding, ISWI dimers may well employ a similar remodeling strategy as larger SWI/SNF complexes, destabilizing DNA-histone contacts via the substrate engagement, followed by ATP stimulated conformation change and translocation of one of the two ATP motors (47). The difference in the stoichiometry of ATPase motor over substrate, and the different subunit composition between SWI/SNF and ISWI family remodeling complexes may contribute to the functional specification *in vivo*. Taking the aforementioned cases as examples, nucleosome remodeling by SWI/SNF

complexes promotes DNA accessibility, whereas nucleosome spacing by ISWI facilitates chromatin assembly, and gene silencing.

Structural and functional analysis of the remodeling substrate also shed light on the biological activities of these different remodeling complexes *in vivo.* Mutagenesis analysis has uncovered that the catalytic activities of the ISWI remodeler are uniquely affected by a basic patch of residues ($R_{17}H_{18}R_{19}$) of the H4 tail (27, 52). Importantly, acetylation of the neighboring H4K12 and K16 residues impairs substrate recognition and chromatin remodeling by ISWI (118). These observations are consistent with the possibility that ISWI is targeted away from chromatin domains that carry H4K16 acetylation, which marks de-condensed and transcriptionally active chromatin regions. Based on the structural model, the extensive contacts and spatial converge between SWI/SNF family remodeling complexes and their nucleosome substrate would seem to exclude the binding of these complexes to a compacted chromatin structure. This agrees with reports suggesting that H1 incorporation would antagonize chromatin remodeling by remodelers of different families (61, 104, 106).

In summary, bioinformatic studies uncovered striking sequence similarity among all the Snf2-like chromatin remodeling complexes, suggesting these ATP motors may use similar mechanisms to participate in chromatin dynamics. Despite the sequence similarity, these remodeling ATPases are genetically non-redundant, suggesting specialized functions *in vivo.* Consistent with this idea, extensive structural and functional studies of different families of remodelers *in vitro* have uncovered differences in their subunit compositions, substrate specificities, differential ways in regulating basal enzymatic activity, and targeting remodeling activity of these complexes.

Combinatorial Assembly of chromatin remodeling complexes

Individual Snf2 family ATPase subunits, such as BRG1, BRM, Sth1, ISWI, SNF2h, and Mi-w, have been shown to catalyze ATP-dependent chromatin remodeling activity in the absence of other accessory subunits, suggesting these ATPase motors are intrinsically active and possess a sufficient toolkit to break DNA-histone contacts. However, these remodeling ATPases are genetically non-redundant, suggesting functional specialization *in vivo*. It is believed that combinatorial assembly of the remodeling ATPases with other accessory subunits confers biological specificity and functionality to these remodeling machineries.

Many chromatin remodeling complexes are evolutionarily conserved in term of their subunit composition and biological function, suggesting that the Snf2-ATPase and its particular accessory subunits may be collectively required for an essential biological function, thus the formation of a protein complex is retained through evolution. To form a multi-subunit protein complex, individual subunits of the complex form stable, protein-protein interactions, which are usually involved in structurally complementary surfaces comprised of two or more subunits, held together by various chemical attractions including hydrogen bonding, electrostatic interactions, Van der Waals forces, and hydrophobic interactions. The assembled complexes are more often found to be resistant to exchange with free unincorporated subunits, and can only be dissociated under denaturing conditions. In addition, the protein complexes usually remain intact during chromatographic separation. Lastly, genetic ablation of essential subunits of a given complex often leads to similar phenotypic changes to the cells and organisms. However,

different phenotypes can arise if the chosen subunit is shared with other complexes or is only essential for a subset of functions of the complex.

Why would Snf2-like ATPases be driven evolutionarily to function with other subunits in the context of a single structural entity, rather than simply use the activities of these other proteins in solution? One answer to this question lies in the ability of assembled complex to achieve rapid coupling of activities conferred by different subunits. The ATP-dependent nucleosome remodeling reaction can be envisioned as a multi-step process and requires orchestrated activities from different subunits, possibly including substrate recognition, activation of snf2 ATPase, regulation of enzyme processivity, and coupling to other enzymatic activities. However, the probability of related active subunits all to be within close proximity to the substrate is significantly lower than subunits co-associated in a complex. Thus, active subunits of chromatin remodeling complexes are selected to assemble during the course of evolution to provide proximity for efficient coupling of different activities.

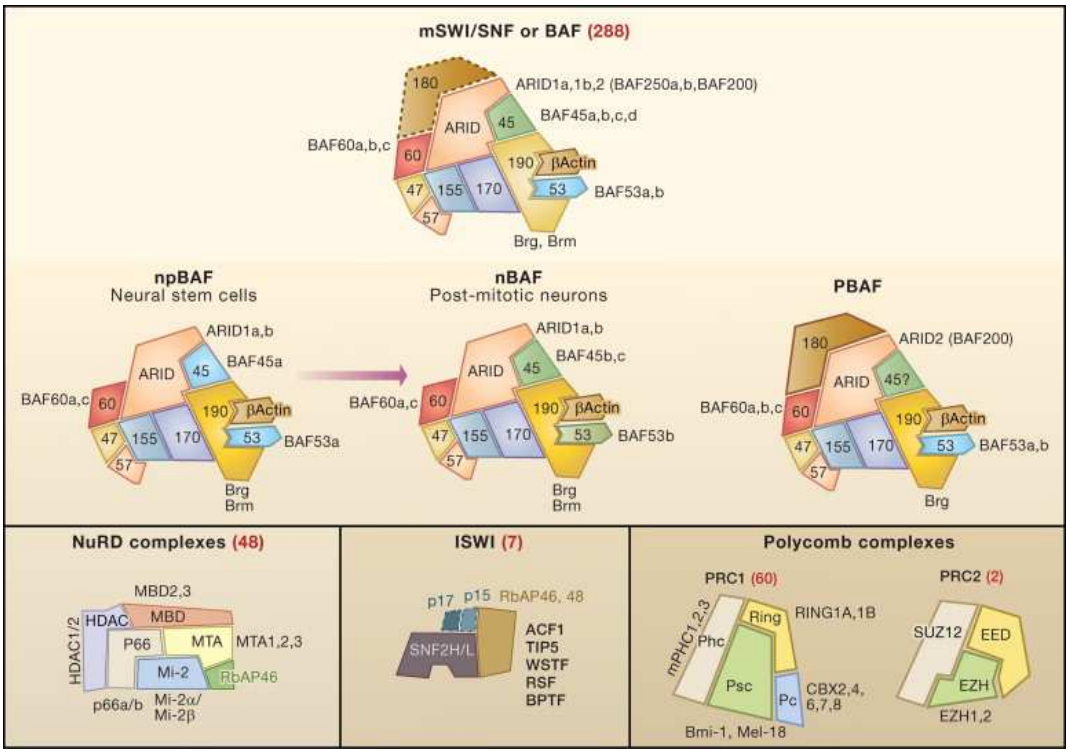

Figure 6. Combinatorial Assembly of Chromatin Regulatory Complexes

Shown is the predicted combinatorial diversity for the mammalian chromatin regulatory complexes: BAF (mSWI/SNF), NuRD, ISWI, and Polycomb (the number of possible combinations is shown in parentheses in red).(Top) Three examples of BAF complexes illustrate respelling of the chromatin remodeling word by switching subunit composition. The subunits are depicted as interlocking pieces in which a similar shape of the subunit denotes homology and thereby a specific position in the complex. Subunits shown in dashed outline are inconstant components of the complexes. The depicted area of each subunit is roughly proportional to its mass. Figure adapted from Wu et al. (138)

A second evolutionary force driving the formation of macromolecular complexes is the opportunity for functional diversification afforded through combinatorial assembly of protein complexes. In vertebrates, subunits of chromatin remodeling complexes are often encoded by gene families. For example, there are 20 genes that encode for the 11 subunits of the SWI/SNF subfamily remodeling complexes in vertebrates, giving a total of 288 predicted assemblies. Indeed, individual isoforms of gene families have been found to be expressed exclusively in specific developmental stages, or cell types, and to

play essential and non-redundant roles in organism development and maintenance of cellular identity (138). The expression variance of family members could provide mechanistic variation leading to the functional specialization of a specific chromatin remodeling complex, which can contribute to chromatin dynamics in a given cell type or developmental stage.

Chapter II. Methods to generate and characterize human INO80 chromatin remodeling complexes and subcomplexes

Abstract

INO80 chromatin remodeling complexes regulate nucleosome dynamics and DNA accessibility by catalyzing ATP-dependent nucleosome remodeling (28, 41). Human INO80 complexes consist of 14 protein subunits including Ino80, a SNF2-like ATPase, which serves both as the catalytic subunit and the scaffold for assembly of the complexes (28) (Figure 8A). Functions of the other subunits and the mechanisms by which they contribute to INO80's chromatin remodeling activity remain poorly understood, in part due to the challenge of generating INO80 subassemblies in human cells or heterologous expression systems. In the method chapter of this thesis, we present a procedure that allows purification and characterization of human INO80 chromatin remodeling subcomplexes that are lacking a subunit or a subset of subunits. We stably express N-terminal FLAG epitope tagged Ino80 cDNA in human embryonic kidney (HEK) 293 cell lines using Flp-In™ recombination technology. In the event that a subset of INO80 subunits is to be deleted, we express instead smaller Ino80s that lack the platform needed

for assembly of those subunits. In the event an individual subunit is to be depleted, we transfect siRNAs targeting this subunit into an Flp-In™ 293 cell line stably expressing FLAG tagged Ino80 ATPase. Nuclear extracts are prepared using the method of Dignam (37), and FLAG immunoprecipitation is performed to enrich protein fractions containing Ino80 derivatives. The compositions of purified INO80 subcomplexes can then be analyzed using methods such as immunoblotting, silver staining, and mass spectrometry. In addition, we measure activities of the purified INO80 subcomplexes using nucleosome binding and sliding assays and DNA- or nucleosome-stimulated ATPase assays. We examine the roles of given subsets of INO80 subunit(s) by comparing activities of smaller subcomplexes to those of the complete INO80 complex. The methods described in this chapter can be used to study the structural and functional properties of any mammalian multi-subunit chromatin remodeling and modifying complexes.

Introduction:

Evolutionarily conserved SNF2 family chromatin remodeling complexes are key regulators of chromatin organization and DNA accessibility (25). These remodeling complexes always include a central SNF2-like ATPase subunit, which, in some cases, assembles with various accessory proteins and forms multi-subunit macro-molecular assemblies. To study the molecular details of the ATP-dependent chromatin remodeling process, it is important to understand the contributions of given subsets of subunits and/or domain structures to activities of the complexes. Such analyses require (i) the generation of highly purified mutant complexes that lack particular protein subunits or domain structures, and (ii) the ability to analyze their nucleosome remodeling and other activities using defined molecular substrates in vitro.

Previous structure-function studies of ATP-dependent chromatin remodeling complexes have widely focused on the yeast model system due to the superior manipulatability of the yeast genome [see, for example, refs. (116, 117, 125)]. Given the conservation of subunit composition and functionality among orthologous remodeling complexes, studies of the structure and function of yeast remodeling complexes have provided important insights into their counterparts in higher eukaryotes. Nonetheless, appreciable species-specific differences among remodeling complexes do exist, resulting from gain or loss of species-specific subunits, gain or loss of species-specific domains of conserved subunits, and sequence variability within conserved domains of conserved subunits.

Differences between chromatin remodeling complexes in yeast and higher eukaryotes can in principle be driven by the need for higher eukaryotic cells to adapt to new molecular and cellular environments by acquiring new modes of regulating basal remodeling activities, new genomic targeting mechanisms, and coupling additional enzymatic activities to the ATP-dependent nucleosome remodeling process. Thus, understanding how subunits of higher eukaryotic remodeling complexes contribute to the nucleosome remodeling process is valuable, because it not only sheds light on basic mechanisms of the ATP-dependent chromatin remodeling process, but can also provide valuable insight into the mechanisms by which chromatin structure and gene expression in higher eukaryotes are regulated during speciation and development.

Thus far, there have been only limited structural and functional studies of multi-subunit mammalian chromatin remodeling complexes, due in part to the difficulties in obtaining biochemically defined chromatin remodeling complexes and subcomplexes. We have partially circumvented these difficulties with the procedures described below, in which we use immunoaffinity purification to prepare intact INO80 complexes or subcomplexes from human cells stably expressing N-terminally FLAG epitope tagged wild type or mutant versions of Ino80 (23) (Figure 7). To obtain intact INO80 complexes from human cells, we use Flp-In™ recombination technology to generate transgenic HEK293-Flp-in™ cell lines stably expressing FLAG epitope tagged cDNAs encoding subunits of the INO80 complex (65, 92, 109). Because we find that over-expression of INO80 subunits can be somewhat toxic, we find it necessary to isolate and maintain clonal cell lines under selective conditions to ensure stable transgene expression during the many passages

needed for expansion of large-scale cell cultures. To obtain smaller INO80 subcomplexes that contain only a subset of subunits, we have successfully used two approaches (Figure 8A and 8B). In the first, we generate HEK293 Flp-in™ cell lines stably expressing mutant versions of Ino80 that lack domains required for interaction with specific subunits (23). Alternatively, we use siRNA-mediated knockdown to deplete the desired subunit from cells expressing an appropriate FLAG-tagged INO80 subunit. Finally, to purify the human INO80 complexes, we use FLAG agarose based chromatography (16, 17, 23, 65) to enrich an INO80-containing fraction from nuclear extracts, thereby effectively reducing the presence of contaminating cytosolic proteins in the final fraction containing purified INO80 complexes or subcomplexes.

We conclude by describing biochemical assays that are used to measure INO80's ATP-dependent nucleosome sliding (Figure 9A) or binding (Figure 9B) activities and DNA- or nucleosome-stimulated ATP hydrolysis (Figure 10). The protocols described in this chapter can be applied more generally to structural and functional analyses of other mammalian multi-subunit chromatin remodeling and modifying complexes.

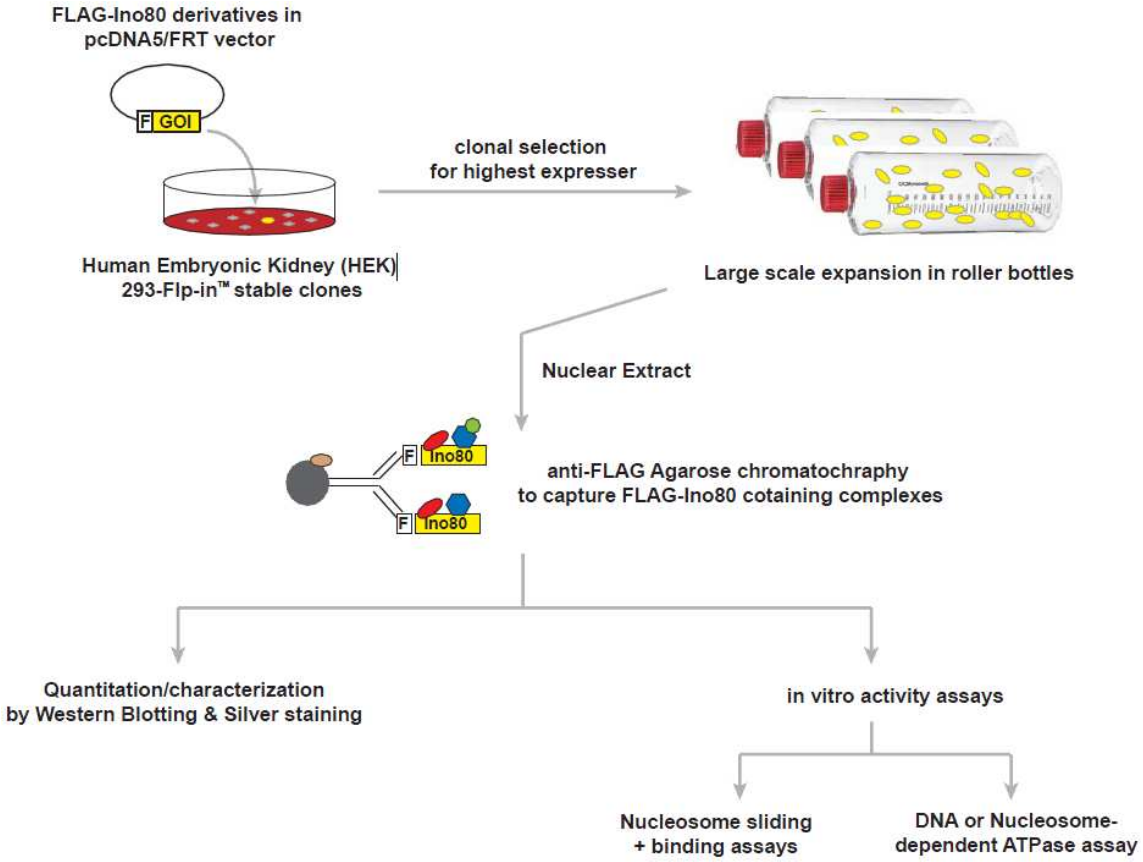

Figure 7. Flow chart of the method chapter

Overview of procedures used to generate, purify and characterize human INO80 ATP-dependent chromatin remodeling complexes. F, an N-terminal in-frame FLAG epitope tag; GOI, Gene-of-interest.

Procedure:

1) Generation and culture of HEK293 stable cell lines expressing full length or mutant versions of FLAG epitope-tagged Ino80 or other INO80 subunits

a. A cDNA encoding full length or mutant human Ino80 ATPase or another INO80 subunit is cloned into a mammalian expression vector (pcDNA5/FRT, Life Technologies™) with an in-frame, N terminal FLAG epitope tag. The sequence of the inserted cDNAs should be confirmed by DNA sequencing before proceeding.

pcDNA5/FRT, contains an FRT recombination site that allows Flp recombinase-mediated insertion of the cDNA into an FRT site stably integrated into a single transcriptionally active locus in the Flp-In™ HEK293 cells. Recombination between the FRT sites in the vector and the genome of Flp-In™ HEK293 cells allows rapid, targeted integration of cDNAs into the HEK293 cell genome and efficient generation of stable cell lines.

b. To perform the transfection, Flp-In™ HEK293 cells are grown in 10 cm tissue culture dishes in a medium containing DMEM (Dulbecco's Modified Eagle Medium, Cellgro), 5% GlutaMAX (Life Technologies™), and 10% FBS (Fetal Bovine Serum, SAFC®). When cells reach ~70% confluency, they are co-transfected, using 40 µl of FuGENE6 transfection reagent (Promega), with 0.5 µg of the appropriate pcDNA5/FRT expression vector plasmid and 9.5 µg of pOG44, which encodes Flp recombinase. 48 hours post-transfection, cells are split at a ratio of 1:10 into 10 cm dishes and grown in the presence of hygromycin B (100 µg/ml, AG Scientific) for 3-4 weeks. The culture medium should be changed whenever it begins to turn yellow (typically every 3-5 days).

c. To identify positive clones that express suitable levels of FLAG-tagged protein, individual hygromycin B-resistant colonies are selected and transferred to a single well of a 24-well plate. Once the cells reach 80% confluency, they are harvested in ~1 ml PBS and pelleted by centrifugation at 1000 x g for 5 min. After removal of the supernatant, the cell pellet is resuspended in 60 µl of SDS-PAGE sample buffer. Half of the resuspended cell pellet is subjected to SDS page and western blotting to monitor expression of the FLAG tagged bait protein; the other half is

saved for future analyses. Human Ino80 is typically expressed at only very low levels and hence can be difficult to detect in cell lysates. Accordingly, it is often necessary to expand clonal cell populations further by plating cells from a single well of a 24 well plate into a 15cm tissue culture dish. Once the cells have grown to near confluency, they are resuspended in ice cold PBS, transferred to a 50 ml conical tube, and brought to a final volume of 50 ml with PBS. Cells are pelleted at 1000 x g for 5 min, the supernatant removed and discarded, and cells are resuspended in 1 ml of Lys450 buffer (20 mM Hepes-NaOH pH7.9, 450 mM NaCl, 0.5% TritonX-100, 10 mM KCl, 4 mM $MgCl_2$, 0.2mM EDTA, 10% Glycerol, 1 mM DTT, 200 µM PMSF, and 1:1000 Sigma Protease Inhibitor Cocktail for use with mammalian cell and tissue extracts (cat. no. P8340). [Note: here and elsewhere, DTT, PMSF, and protease inhibitor cocktail should always be added to buffers immediately before beginning an experiment.] FLAG-tagged proteins can then be immuno-precipitated from the resulting whole cell lysate using 20 µl of EZview ™ Red ANTI-FLAG ® M2 Affinity Gel (Sigma) and analyzed by western blotting. [For details of immunoprecipitation procedure, see section 4).] Frozen stocks of clonal cell lines should be prepared and stored in liquid nitrogen until use.

d. For large scale preparation of INO80 complexes, cells are cultured in roller bottles, each seeded with cells from a single near confluent 15 cm dish and containing 200 ml DMEM, 5% GlutaMAX, and 10% calf serum (SAFC) without hygromycin B selection. Cells are grown in 10-20 roller bottles rotating at 0.2 rpm and are harvested once they reach ~70% confluency; we typically obtain ~1

ml of packed cells from each roller bottle. To harvest cells, medium is poured off and discarded. ~50 ml of ice cold PBS is added to each bottle. Bottles are manually rolled to loosen the cell monolayer. Reuspended cells are transferred to 250 ml plastic conical bottles and kept on ice. After cells have been removed, bottles are rinsed with an additional ~50 ml of PBS, which is then transferred sequentially to additional bottles. When rinse solution is no longer clear (typically after being used to rinse about 5 bottles), it is transferred to the 250 ml bottle. Cells are pelleted by centrifugation at 1300 rpm for 10 min in a JS-4.2 rotor in a J6 centrifuge (Beckman-Coulter) or similar high capacity rotor and centrifuge. Pelleted cells are gently resuspended in PBS, combined into a single 250 ml conical bottle, and kept on ice until further processing.

2) siRNA-mediated knockdown of INO80 subunits in cells expressing another FLAG-tagged INO80 subunit.

To obtain INO80 subcomplexes lacking a single subunit, we use FLAG-immunopurification to purify INO80 complexes from siRNA treated cells. Here, we describe a "reverse" siRNA (small interfering RNA) transfection protocol optimized for HEK293 cells growing in 15cm dishes. The protocol described below is for a single 15 cm dish of cells and should be scaled up accordingly depending on the number of cells needed. To prepare biochemically useful amounts of INO80 complex from siRNA-treated cells, we recommend scaling up to cultures grown in 40 15 cm dishes; these will yield approximately 2-4 ml of packed cell pellet.

a. Prepare siRNA stock solutions. siRNAs (TARGETplus SMARTpool, Dharmacon / Thermo Scientific) are reconstituted to 50 µM in 1x siRNA resuspension buffer (Thermo Scientific) according to the manufacturer's instructions.

b. Prepare a transfection cocktail containing siRNAs and transfection reagent. All reagents should be brought to room temperature before use. 10 µl of the 50 µM RNAi stock solution is mixed with 32 µl Lipofectamine™ RNAiMAX (Life Technologies™) and gently added into 4 ml of Opti-MEM® Reduced Serum Medium (Life Technologies™). The mixture is then incubated at room temperature for 30 min.

c. Prepare Flp-In™ HEK293 cells stably expressing the desired INO80 subunit for transfection. While incubating the transfection cocktail from step 2)-b, cells from a single 15 cm plate grown to near confluency are washed one time with room temperature PBS (Cellgro). After removal of PBS, cells are treated with 1 ml TrypLE (Life Technologies™) just until they begin to lift off the plate. Cells are immediately resuspended in 10 ml of complete medium (DMEM + 5% GlutaMAX + 10% FBS), collected by centrifugation at 1000 x g for 5 min at room temperature, resuspended in ~4 ml complete medium, and counted using a haemocytometer. Finally, cells are diluted with complete to a concentration of ~5.4 x 10^6 / ml.

d. To each 15 cm dish, add in order: 15 ml complete culture medium and 4 ml transfection cocktail. Swirl gently to ensure the medium and transfection cocktail are thoroughly mixed. Finally, add one ml of cell suspension and again swirl gently to disperse cells uniformly.

e. After 60 hours of culture in a 37^{o}C, 5% CO_2 incubator, gently remove medium, resuspend cells in ice cold PBS, and use immediately to prepare nuclear extracts.

3) Preparation of nuclear extracts.

Although it is possible to purify the INO80 complex from either whole cell or nuclear extracts, we have found that biochemical analyses of complexes purified from whole cell extracts are often confounded by the presence of contaminating activities. Accordingly, we prefer to start our purification with nuclear extracts even though they are somewhat more difficult to prepare. Here, we describe a procedure that we use routinely in the lab to make nuclear extracts from cell lines. It has been modified from the protocol of Dignam (37) and can be scaled up or down depending on the size of starting cell pellets. All buffers should be ice cold, and all steps should be performed in a cold room or on ice if a suitable cold room is not available.

a. **Isolation of nuclei**

   i. Gently transfer cells to a suitably sized (15 or 50 ml) graduated conical tube and spin at 1000 x g for 10 min at 4^{o}C. Remove the supernatant, and measure the size of the packed cell pellet. 1 ml of packed cells corresponds to ~ 3 x 10^8 HEK293 cells.

   ii. Add 5 packed cell volumes of Buffer A (10 mM Hepes, pH 7.9, 1.5 mM $MgCl_2$, 10 mM KCl and freshly added 1 mM DTT, 200 µM PMSF, and 1:1000 Sigma Protease Inhibitor Cocktail P8340). Resuspend the cell pellet by gentle pipetting, and incubate on ice for exactly 10 minutes. Pellet the cells at

1000 x g for 10 min at 4^{o}C, and remove the supernatant. If the cells are intact and healthy, the cell pellet is expected to swell up to two-fold following incubation in the hypotonic Buffer A. If cells do not swell and/or the supernatant becomes turbid at this step, the starting population of cells may have been unhealthy. Alternatively, cells may have been handled too roughly during harvest or resuspension steps, or they may have been incubated too long in Buffer A.

iii. Resuspend the cells in two packed cell volumes of buffer A, and transfer the cell suspension to an appropriately sized Dounce tissue homogenizer (Wheaton). For example, when starting with less than 2ml of packed cells, use a 7 ml homogenizer; for 2-4 ml packed cells, use a 15 ml homogenizer; and for 10 or more ml of packed cells, use a 40 ml homogenizer.

iv. Homogenize the cell suspension with the LOOSE glass pestle of the Dounce homogenizer until 90% of the cells stain positively with 1% trypan blue. For HEK293 cells, this can be expected to require 4-6 strokes of the homogenizer. To minimize potential disruption of nuclei and shearing of chromatin during this step, it is important to avoid introducing air bubbles while homogenizing and/or over-homogenizing. Thus, especially for the beginner, it is advisable to check the percentage of trypan blue-positive cells after each stroke of the homogenizer.

v. Transfer the suspension to a 45 ml Oak Ridge High-Speed centrifuge tube and spin at 25,000 x g for 20 min at 4 ^{o}C in a Beckman-Coulter JA-17 or similar

rotor. From the nuclear pellet, remove the supernatant, which contains cytosolic proteins or proteins that leak out of the nucleus during fractionation.

b. **Salt extraction of chromatin**

i. Add Buffer C (20mM Hepes, pH 7.9, 25% Glycerol, 1.5 mM $MgCl_2$, 0.2 mM EDTA, and freshly added 1 mM DTT, 200 µM PMSF, and 1:1000 Sigma Protease Inhibitor Cocktail P8340) to the nuclear pellet; use 2.5 ml Buffer C for every 3 ml of starting packed cell volume (~1 X 10^9 cells). Using a glass rod or a pipet, dislodge the nuclear pellet from the wall of the tube and transfer the entire mixture to a Dounce homogenizer of an appropriate size. Homogenize the mixture with two strokes of a LOOSE pestle to resuspend the nuclei. Do not over-homogenize as this will shear the chromatin and release DNA into the soluble fraction.

ii. Transfer the resuspended nuclear fraction into a chilled beaker. Choose a beaker such that the suspension will fill the beaker to at least 0.5 cm deep. To extract nuclear proteins from chromatin or other insoluble structures, the salt concentration of the suspension is gradually increased to 0.42 M NaCl by dropwise addition of 5 M NaCl while gently stirring the suspension with a pipet or glass rod; once all of the 5 M NaCl has been added, the solution should become very viscous or gel-like. The volume of 5 M NaCl needed to bring the solution to a final concentration of 0.42 M NaCl is calculated according to the following formula:

Volume 5 M NaCl = [initial packed cell volume + volume Buffer C added in step 3-b-i] / 10.9.

iii. Carefully transfer the viscous suspension into 10 ml polycarbonate tubes (Beckman cat. no. 355630) for a Beckman Type 70.1 Ti rotor or 70 ml polycarbonate bottles (Beckman cat. no. 355655) for a Beckman Type 45 Ti rotor. Seal tightly with parafilm if using 10 ml tubes or with cap assembly (Beckman cat. no. 355623) if using 70 ml bottles. Slowly rock the sealed tubes at 4^{o}C for 30min using a Nutator™.

iv. Spin the samples in a Type 45 Ti or 70.1 Ti rotor for 30 min. at 40,000 rpm at 4^{o}C.

v. Transfer the supernatant to a single plastic tube or bottle. This supernatant is the nuclear extract, and the pellet contains chromatin and other nuclear debris. The supernatant should be a clear, non-viscous solution, with only a very minimal amount of cloudy or viscous material near the chromatin pellet or floating on top. When collecting the supernatant, one should take care not to collect any of the cloudy or viscous material near the pellet.

vi. Divide the nuclear extract into conveniently sized aliquots, freeze it in liquid nitrogen, and store it at -80 ^{o}C. Typically, 1 ml of packed cell pellet yields 1 ml of final nuclear extract.

4) Immunoaffinity purification of the human INO80 complexes or subcomplexes.

We find that a single step immunopurification (14) using anti-FLAG agarose is sufficient for preparation of INO80 complexes or subcomplexes to a degree of purity adequate for reliable assays of their activities. The optimal ratio between the amount of starting extract and anti-FLAG agarose depends on the concentration of the FLAG bait protein present in the extracts and the accessibility of the FLAG epitope and needs to be determined empirically. We typically begin immunopurification with 100 µl bed volume of anti-FLAG agarose beads (EZview ™ Red ANTI-FLAG ® M2 Affinity Gel, Sigma) and 3-14 ml of nuclear extract; the amount of extract used depends on the goals of the experiment and availability of extract.

a. To thaw frozen nuclear extract, place tubes containing the extract on the benchtop or roll tubes between hands until the frozen material becomes a slurry. Then place the tubes on ice or in the cold room until the extract is completely thawed.
b. Transfer the thawed nuclear extract to 10 ml polycarbonate ultracentrifuge tubes, and spin at 40,000 rpm for 20 min at 4 ^{o}C in a Beckman Type 70.1 Ti rotor to remove any precipitate that may have formed during the freeze-thaw cycle. Transfer the supernatant to a 15 ml conical tube. Add fresh DTT, PMSF, and Sigma Protease Inhibitor Cocktail P8340 to final concentrations of 1 mM DTT, 200 µM PMSF, and 1:1000 Sigma Protease Inhibitor Cocktail P8340.
c. To prepare anti-FLAG agarose for the immunopurification, transfer 200 µl of 50% slurry of anti-FLAG agarose beads to a 1.5 ml microcentrifuge tube. Pellet the beads by centrifugation in a benchtop microcentrifuge at 8000 x g for 30 sec. Remove the supernatant, and wash the beads by resuspending the beads in 1 ml of

Lys450 buffer, and pellet the beads at 8000 x g for 30 sec. Wash the beads two more times.

d. Resuspend the washed anti-FLAG agarose beads in about 100 µl of the nuclear extract using a Gilson P200 or similar pipette with a tip from which the end has been cut off with a clean scalpel or razor blade and, using the same tip, transfer the resuspended beads to the 15 ml conical tube containing the extract. Repeat a few times until all of the beads have been transferred to the 15 ml tube. Incubate the extract / bead mixture for 4 hours at 4^{o}C with slow rotation on a laboratory rotator (such as a Glas-Col® Tube/Vial Rotator).

e. Collect the FLAG agarose by centrifugation at 1000 x g for 5 min at 4 ^{o}C. Resuspend in 10 ml Lys450, incubate 5 min at 4^{o}C with gentle rocking on a Nutator™. Pellet the beads at 1000 x g for 5 min at 4^{o}C.

f. Resuspend in a small volume of Lys450 and transfer beads to a 1.5 ml microcentrifuge tube. Continue to rinse the 15 ml conical tube with small volumes of Lys450 until all the beads have been transferred to the microcentrifuge tube. Spin down the beads at 8000 x g for 30 sec. at 4^{o}C in a microcentrifuge. Wash three times more with 1 ml Lys450 and once with 1ml EB100 buffer (10 mM Hepes pH 7.9, 10% glycerol, 100 mM NaCl, 1.5 mM $MgCl_2$, 0.05% TritonX-100, and freshly added 1 mM DTT, 200 µM PMSF, and 1:1000 Sigma Protease Inhibitor Cocktail P8340).

g. To elute bound proteins, add 200 µl EB100 buffer containing 0.25 mg/ml 1x FLAG® Peptide (Sigma cat. no. F3290). Incubate 30min at 4 ^{o}C each on a Nutator™. Pellet the beads at 8000 x g for 30 sec. at 4 ^{o}C in a microcentrifuge.

Transfer the supernatant, which contains the eluted INO80 complex, to a fresh microcentrifuge tube. Repeat the elution four more times, and pool all the supernatants into a single tube.

h. To remove any residual FLAG-agarose beads from the eluted protein fraction, pass the eluate through an empty Micro Bio-Spin® Chromatography Column. Concentrate the eluted protein fraction ~10-fold using an Amicon® Ultra Centrifugal Filter Device (50,000 molecular weight cutoff).

i. To remove the FLAG peptide, pass the concentrated protein fraction through two Zeba™ Desalting Columns (Thermo Scientific). The purified, desalted protein fraction should be divided into 20 µl aliquots, frozen in liquid nitrogen, and stored at -80 ^{o}C.

j. The subunit composition of INO80 or INO80 subcomplexes can be analyzed on silver-stained gels or by western blotting, and their concentrations can be estimated by semi-quantitative western blotting using preparations of recombinant INO80 subunits of known concentration as standards.

5) Biochemical assays for analyzing activities of INO80 or INO80 subcomplexes.

a. **ATP-dependent nucleosome remodeling assay**

To measure ATP-dependent nucleosome remodeling activities, we incubate the immunopurified INO80 or INO80 subcomplexes with ATP and a mononucleosomal substrate, which contains a single nucleosome positioned at one end of a 216-bp, ^{32}P-labeled DNA fragment. The reaction products are then

subjected to electrophoresis in native poly-acrylamide gels. The position of the nucleosome on the 216 bp DNA affects electrophoretic mobility; laterally positioned nucleosomes run faster in the gel than more centrally positioned nucleosomes. Since INO80 chromatin remodeling complexes preferentially move mononucleosomes toward the center of a piece of DNA (16, 23, 65, 130), remodeling activity can be readily monitored by the emergence of a population of nucleosomes that exhibit decreased electrophoretic mobility. At the end of the reaction, an excess of Hela oligonucleosomes and salmon sperm or other DNA is added to the reaction mix as competitors to remove any substrate-bound INO80 or INO80 subcomplexes, since bound remodeling enzyme will change the electrophoretic mobility of the nucleosome substrate (Figure 9A).

i. To generate the ^{32}P-labeled, "601" DNA fragment, a 216 bp DNA fragment containing an end-positioned 601 nucleosome positioning sequence is amplified in a PCR reaction from pGEM-3Z-601 (83) in the presence of 6000Ci/mmol [α-^{32}P] dCTP.
    1. The forward and reverse primers used are:
        a. 5′-ACAGGATGTATATATCTGACCGTGCCTGG
        b. 5′-AATACTCAAG CTTGGATGCCTGCAG.
    2. To amplify the “601” DNA sequence, 100 µl PCR reaction is set up as follows:
        i. Deionized H_2O, 67.5 µl
        ii. 10x PCR reaction buffer (Roche), 10 µl
        iii. pGEM-3Z-601 (10 ng/µl), 1 µl

iv. Forward primer (10 μm), 5 μl

v. Reverse primer (10 μm), 5 μl

vi. dNTP stock solution containing 10 mM each of the 4 dNTPs, 0.5 μl

vii. Roche Taq DNA Polymerase, 1 μl

viii. [α-^{32}P] dCTP (6000 Ci/mmol, 3.3 μM), 10 μl

3. The PCR reactions are performed in a thermal cycler (MJ Research, PTC 200) using the following program:

   i. 1 min @ 96 °C

   ii. 45 sec @ 94 °C

   iii. 30 sec @ 57 °C

   iv. 60 sec @ 72 °C

   v. Go to step ii. for another 29 cycles

   vi. 7 min @ 72 °C

   vii. Forever @ 4 °C

4. Reaction cleanup: to remove the unincorporated nucleotides, pass the PCR reaction product twice sequentially through NucAway™ spin columns (Ambion®, Cat. # AM10070) following the manufacturer's instructions. Following a successful PCR reaction, we typically detect over 15,000 k cpm read from the final eluate using a standard Geiger counter; otherwise the chance is high that the PCR reaction did not work.

5. To ensure that the PCR reaction generated the desired product, run 5 µl of the reaction product in an agarose gel. If a single ~216 bp DNA band is detected by ethidium staining, proceed to the next step; otherwise, the PCR reaction needs to be optimized.
6. Dilute 5 µl of the purified PCR product from step4 20-fold, and measure the DNA concentration using a UV spectrophotometer. The average yield is ~40 ng/µl.
7. Measure the radioactivity of 1 µl product in a Scintillation counter. The typical result is around 600,000 cpm/µl. Estimate the labeling efficiency by calculating the cpm/ng. A successful labeling reaction is expected to yield ~15 k cpm/ng of 601 DNA fragment.

ii. Nucleosomes are prepared from Hela cells and transferred onto the labeled 601 DNA by a serial dilution method essentially as described (95). 2 pmol of ^{32}P-labeled 601 DNA fragment are mixed with 6 µg of Hela nucleosomes in 50 µl of a buffer containing 1.0 M NaCl, 10 mM Tris-HCl, pH 8.0, 1 mM EDTA, 0.1 mM PMSF, and 1 mM DTT. After incubation at 30 °C for 30 minutes, the mixture is sequentially adjusted to 0.8, 0.6, and 0.4M NaCl by dilution with 12.5 µl, 20.8 µl, and 41.6 µl, respectively, of 10 mM Tris-HCl (pH 8.0), 1 mM EDTA, 0.1 mM PMSF, and 1 mM DTT, with a 30 min incubation at 30 °C after each dilution. Finally, the mixture is sequentially diluted to 0.2 and 0.1 M NaCl by addition of 125 µl and then 250 µl of the same buffer containing 0.1% Nonidet P-40, 20% glycerol, and 200 µg/ml

BSA. After reconstitution, the mononucleosome substrate can be stored at 4 °C for up to 3 months.

iii. ATP-dependent nucleosome sliding reactions are performed with ~20 nM INO80 or INO80 subcomplexes, a total of ~2.8 nM nucleosomes (consisting of a mixture of mononucleosomes on the ^{32}P-labeled 601 DNA fragment and Hela cell nucleosomes), and 1 mM ultrapure ATP (USB/Affymetrix) in buffer containing 20 mM Hepes-NaOH (pH 7.9), 50 mM NaCl, 5 mM $MgCl_2$, 1 mM dithiothreitol (DTT), 0.1 mM phenylmethanesulfonyl fluoride (PMSF), 0.1 mg/ml bovine serum albumin (BSA), 5% glycerol, 0.02% Nonidet P-40, 0.02% Triton X-100, in a final volume of 10 µl. The optimal NaCl concentration for INO80 nucleosome remodeling activity is ~50 mM NaCl (data not shown), so we adjust the concentration of NaCl in each reaction to 50 mM.

1. Before setting up assays, we cast native poly-acrylamide gels using the Hoefer® system. After pouring, gels should be allowed to solidify for at least 2 hours at room temperature. To prepare a single gel, mix the following ingredients to a total volume of 40 ml : (5% Acrylamide/Bis 37.5:1, 0.5x TBE (45mM Tris borate, 1mM EDTA), 0.01% ammonium persulfate (APS), and 0.001% N,N,N´,N´-tetramethylethylenediamine (TEMED))
    i. Deionized H2O, 32.6 ml
    ii. 40% Acrylamide/Bis 37.5:1, 5 ml
    iii. 10x TBE (900 mM Tris borate, 20 mM EDTA), 2 ml

iv. (add right before pouring the gel) 10% ammonium persulfate (APS), 0.4 ml

v. N,N,N´,N´-tetramethylethylenediamine (TE MED), 0.1 ml

2. Meanwhile, in pre-chilled lubricated 1.5ml microcentrifuge tubes (Costar®, Cat. No. 3207), combine ~20 nM INO80 or INO80 subcomplexes (estimated by comparing the amount of Arp5 in the purified complexes to recombinant Arp5 of known concentration by semi-quantitative western blotting) with an amount of EB100 buffer sufficient to give a volume of 4.75 µl (contains 100 mM NaCl). Immediately freeze down any remaining INO80-containing fractions using a bucket containing powdered dry ice.

3. Set up a master cocktail with the rest of the ingredients, scaling up by a factor of X (X = total number of reactions +3). The amount of each ingredient needed for a single reaction is as follows:

i. Deionized H_2O to a final volume of 5.25 µl

ii. 10x Remodeling Buffer (200 mM Hepes-NaOH (pH 7.9), 0.2 % NP-40, 0.2% Triton X-100, 50% Glycerol, 50 mM $MgCl_2$, 1 mg/ml BSA) , 1µl

iii. 100 mM ATP (USB/Affymetrix), 0.1 µl

iv. 1 M DTT, 0.01 µl

v. 100 mM PMSF, 0.01 µl

vi. Reconstituted mononucleosome substrate from Step 5)-a-ii., 0.25 µl

4. Mix well by tapping the tube or by pipetting up and down with a Pipetman, and briefly spin the tube in a benchtop hand spinner. Dispense 5.25 µl of the cocktail to each of the reaction tubes set up in the step 2. Mix well by pipetting up and down. Start the reactions by transferring reaction tubes to a 30 °C heat block and incubate for 2 hours.
5. Meanwhile, prepare "removing mix" cocktail containing competitor DNA and nucleosomes, scaling up by a factor of X (X = total number of reactions + 4). The amount of each ingredient needed to prepare 1.5µl removing mix for a single reaction is listed as follows:
    i. Hela nucleosomes (1.5µg/µl), 0.33µl ~400 nM
    ii. Sonicated salmon sperm DNAs (GE Healthcare), 0.75 µl ~ 100 nM
    iii. 1M DTT, 0.01 µl
    iv. 100 mM PMSF, 0.01 µl
6. Terminate the reactions by adding 1.5 µl of the removing mix. Mix well, spin down, and return the reaction tubes to the 30 °C heat block for 30 minutes.
7. Meanwhile, pre-run the native polyacrylamide gel at 100 V for 30 minute in cold room, using 0.5x TBE as running buffer. We use a Hoefer® vertical electrophoresis unit with a magnetic stir bar inside the lower chamber to maintain constant buffer circulation.

8. To load the sample, add 2.5 µl of loading dye containing 3x TBE, 30% glycerol, 0.25% Bromophenol Blue, and 0.25% Xylene Cyanol. Mix well, briefly spin the samples, and load onto the gel using loading tips.
9. Run the gel at 100 V, for 30 minute in a cold room with buffer circulation.
10. To detect the signal, transfer the gel to a stack of two sheets of Whatman 3MM filter paper. Wrap the filter paper with the gel on top using clear plastic wrap, and then expose them to a Storage Phosphor Screen (Molecular Dynamics) at 4 °C for the desired time. Scan the screen using a Typhoon PhosphorImager (GE Healthcare), and analyze the data using ImageQuant™ (GE Healthcare) software.

b. **Mononucleosome binding assay**

To assay the binding affinity of a given INO80 complex for mononucleosomes, we perform an Electrophoresis Mobility Shift Assay (EMSA) using the mononucleosomal substrates generated in Step 5)-a-ii. The reaction mixes for binding assays are set up similarly to nucleosome remodeling assays, except the ATP and removing mix are omitted from the reactions and samples are incubated at 30 °C for 30 minutes. At the conclusion of the binding reactions, add 2.5 µl of loading dye to each reaction mixture, and apply to a native polyacrylamide gel containing 3.5% Acrylamide/Bis 37.5:1, 1% Glycerol, 0.5x TBE (45mM Tris borate, 1mM EDTA), 0.01% ammonium persulfate (APS), and 0.001% N,N,N´,N´-tetramethylethylenediamine (TEMED). Using 0.5x TBE as running

buffer, run the gel at 200 V for 2.5 hours in a cold room with buffer circulation. (Figure 9B)

c. **DNA- and nucleosome- dependent ATPase Assay**

ATPase assays are performed in 5 μl reaction mixtures containing 20 mM Tris-HCl (pH 7.5), 60 mM NaCl, 6.6 mM $MgCl_2$, 0.8 mM EDTA, 0.015% Nonidet P-40, 2.5% glycerol, 0.1 mg/ml BSA, 1 mM DTT, 0.1 mM PMSF, 2 μM ATP, 2 μCi of [α-^{32}P] ATP (3000 Ci/mmol, PerkinElmer). For each INO80 complex or amount of INO80 complex to be assayed, we set up three parallel reactions, one containing EB100 buffer to measure DNA- or nucleosome-independent ATPase, one containing closed circular plasmid DNA (5000 bp, ~30 nM), and one containing Hela oligonucleosomes (~185 nM) (Figure 10). Reactions should be set up on ice.

1. For each reaction, combine the immunopurified INO80 or INO80 subcomplexes with an amount of EB100 buffer sufficient to give a volume of 2.2 μl in pre-chilled lubricated 1.5ml microcentrifuge tubes. (The optimal amount of INO80 complex needs to be determined by titration; we typically perform assays using 10-50 nM INO80.) Immediately re-freeze any INO80-containing fractions in powdered dry ice.
2. Set up a master cocktail, the amount of each ingredient needed for a single reaction is listed below. Scale up the recipe by scaling up by a factor of 3(X+2) +1, where X = the number of INO80 preparations to be assayed.
    i. Deionized H_2O to a final volume of 2.5 μl

ii. 20x ATPase Buffer (400 mM Tris-HCl (pH 7.5), 200 mM NaCl, 132 mM $MgCl_2$, 16 mM EDTA, 0.3 % Nonidet P-40, 50% glycerol, 2 mg/ml BSA, in deionized H2O), 0.25 µl

iii. 100 µM ATP (USB/Affymetrix), 0.1 µl

iv. 1 M DTT, 0.005 µl

v. 100 mM PMSF, 0.005 µl

vi. [α-^{32}P] ATP (3000 Ci/mmol, PerkinElmer), 0.1 µl

3. Mix well.
4. To prepare "sub-cocktails" containing buffer only, DNA, or nucleosomes, dispense 2.5(X+2) µl of the master cocktail into three separate tubes. Add 0.3(X+2) µl of either EB100, closed circular plasmid DNA (1.5 µg/µl), or Hela oligonucleosomes (1.5 µg/µl) and mix well.
5. Dispense 2.8 µl of the appropriate sub-cocktail to the enzyme-containing reaction tubes set up in step 5)-c-1. Gently pipette up and down to mix; avoid introducing bubbles.
6. To start reactions, transfer the reaction tubes to a 30 °C heat block.
7. After 5, 15, 30, and 60 min of incubation, spot 0.5 µl of each reaction mixture onto a cellulose polyethyleneimine thin layer chromatography (TLC) plate (EMD Millipore) in a straight line at least 1.5 cm away from the bottom edge. Reaction tubes should be returned immediately to the 30 °C heat block so multiple time points can be taken from a single tube. After spotting, dry the TLC plates using a blow dryer.

8. Develop plates in a glass chamber containing enough 0.375 M potassium phosphate (pH 3.5) to allow the bottom 0.5 cm of the TLC plate to be submerged in the solution. Cover the chamber, and develop until the front of the liquid phase reaches the top of the TLC plates. Immediate dry the plates thoroughly using the blow dryer.
9. Expose the dried TLC plates to a Storage Phosphor Screen (Molecular Dynamics) at room temperature. Scan the screen using a Typhoon PhosphorImager (GE Healthcare) to quantitate the amount radioactive ATP substrate and ADP product.
10. To calculate the amount of ATP hydrolyzed, multiply the % ATP hydrolyzed by the amount of ATP present in the starting reaction mixture using the following formula: pmol ATP hydrolyzed = 10 pmol ATP in starting reaction x [ADP/(ATP+ADP)]

REPRESENTATIVE RESULTS:

In Figure 7, we present a flow chart summarizing the procedures we use to generate, purify, and characterize human INO80 ATP-dependent chromatin remodeling complexes. Generating human cell lines stably expressing epitope tagged subunits of the INO80 complex is a key step in this procedure, as it enables the purification of well-defined chromatin remodeling complexes that can be tested using various biochemical assays. Although it is in principle more time consuming to generate stable cell lines than to use transient transfection to deliver engineered cDNAs into mammalian cell lines for the

production of recombinant protein, transient transfection suffers from several drawbacks. First, DNA—in the form of a transiently transfected extra-chromosomal vector—is short-lived and usually cannot self-propagate during the cell cycle. Second, transfection efficiency varies greatly depending on cell type and growth conditions. Heterogeneous transfection can cause a mosaic expression pattern that confers a selective growth advantage or disadvantage within the cell population. Thus, transiently introduced transgenes tend to get lost during the many cell passages required to generate the large amount of cells needed for purification of biochemically useful amounts of protein. Stable cell lines are most commonly generated using methods that result in random integration of cDNAs encoding a protein of interest. However, randomly integrated cDNAs can disrupt expression of endogenous genes and are subject to gene silencing with multiple cell passages. For these reasons, we typically introduce Ino80 cDNAs into cells using Flp-In™ recombination technology, in which the cDNA is stably incorporated into a specific chromosomal location via Flp recombinase-mediated insertion into a single FRT site stably integrated into the genome (92, 109). Also key to the success of our procedure is the use of nuclear extracts as the starting material for purification of INO80 complexes. We have found that immunopurified INO80 complexes from whole cell extracts are often contaminated with ATPase and/or nucleosome remodeling activities that are independent of the Ino80 ATPase; such contamination is largely avoided when complexes are purified from nuclear extracts.

As illustrated in Figure 8, our procedures enable the generation of both wild type INO80 and INO80 subcomplexes that lack various subunits, thereby enabling subsequent

biochemical analyses of the contribution of these missing subunits to INO80's enzymatic activities. This figure describes two strategies we have used to define the architecture of the INO80 complex and to generate INO80 subcomplexes. In the first, shown in Figure 8A, we purify intact INO80 complexes through FLAG-tagged versions of wild type subunits (Ies2 or INO80E). Subcomplexes can be purified through epitope-tagged versions of mutant Ino80 proteins that lack individual domains on which different sets of subunits assemble. Using this approach, we found that the subunits shown in red associate with the Ino80 NTD (N-terminal domain); subunits shown in blue associate with the Ino80 HSA (Helicase SANT Associated) domain; subunits shown in purple associate with the SNF2 ATPase domain, composed of SNF2N and HelicC regions (purple) separated by a long insertion region (white). Thus, INO80 subcomplexes (INO80ΔN.com or INO80ΔNΔHSA.com) that lack either the subunits shown in red or subunits shown in red and blue can be purified through FLAG-Ino80ΔN or FLAG-INO80ΔNΔHSA, respectively (23). Successful application of this approach to the analysis of other multi-protein complexes depends on (i) identification of an individual subunit or subunit(s) that serve as scaffold(s) on which other subunits assemble and (ii) definition of specific domains or regions with which specific subsets of subunits assemble. The definition of such domains can be facilitated by analyzing the primary sequence of the core scaffold subunit(s) for evolutionarily conserved regions or regions that correspond to known structural domains.

It is also possible to generate subcomplexes by depleting individual subunits from cells expressing an appropriate FLAG-tagged INO80 subunit. In the first example shown in

Figure 8B, siRNA-mediated knockdown of subunit X depletes only X from the INO80 complex, suggesting X is not required for assembly of any other subunits into INO80. In the second and third examples, siRNA knockdown of either Y or Z leads to co-depletion of both the Y and Z subunits, suggesting Y and Z assemble into the INO80 complex in a mutually dependent manner. The efficiency of siRNA-mediated knockdown is quite sensitive to cell density at the time of transfection; we find that knockdown efficiency decreased when transfections are performed with cells at densities other than that recommended in the protocol. The optimal length of time for siRNA transfection is variable and needs to be determined empirically for each target protein, as it depends on the stability of the target protein, the turnover rate of the targeted protein in protein complexes, and the degree to which the protein is essential for cell viability.

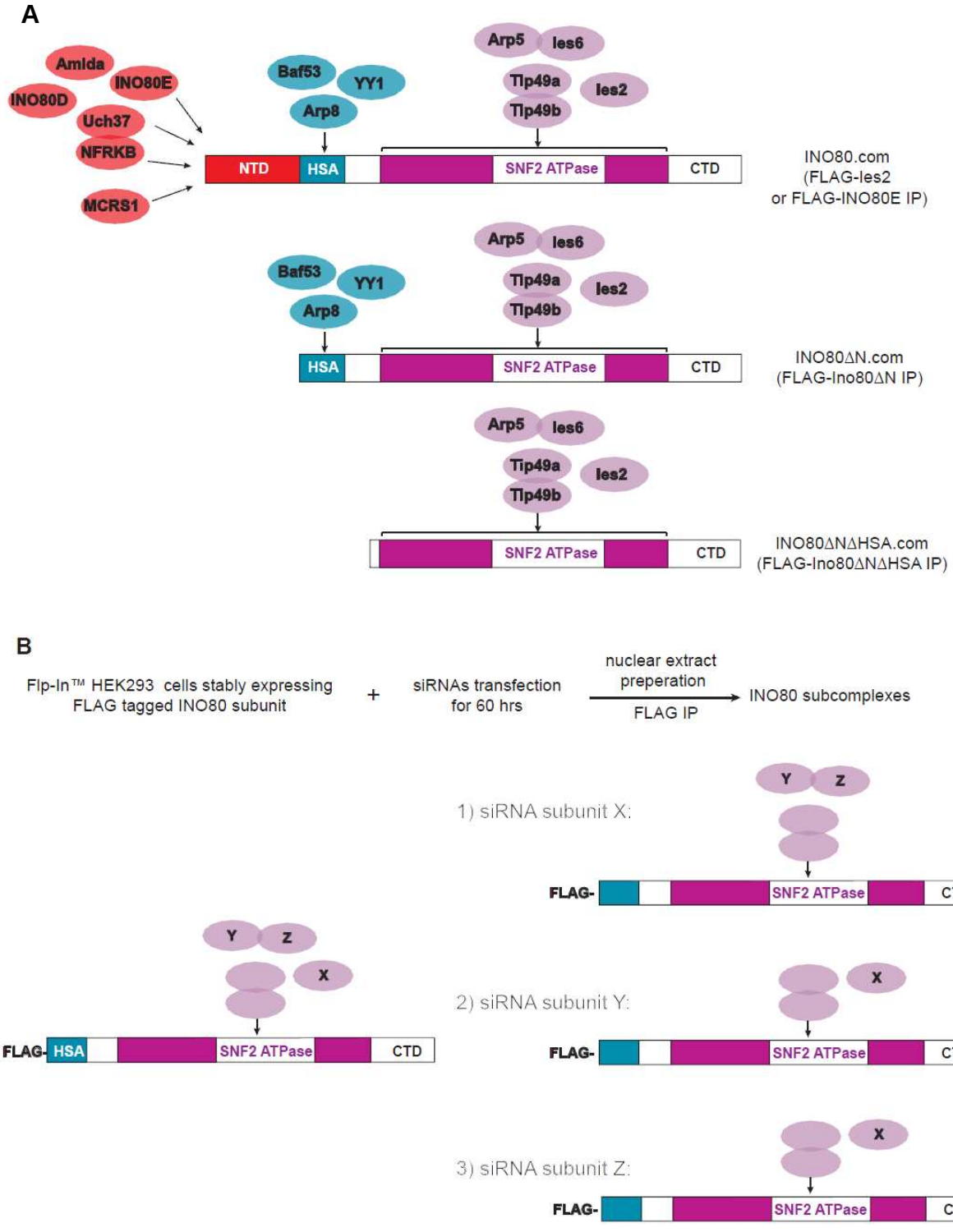
A
Amida
INO80E
INO80D
Uch37
NFRKB
MCRS1
Baf53
YY1
Arp8
Arp5
Ies6
Tip49a
Ies2
Tip49b
NTD
HSA
SNF2 ATPase
CTD
INO80.com
(FLAG-Ies2
or FLAG-INO80E IP)
INO80ΔN.com
(FLAG-Ino80ΔN IP)
INO80ΔNΔHSA.com
(FLAG-Ino80ΔNΔHSA IP)
B
Flp-In™ HEK293 cells stably expressing
FLAG tagged INO80 subunit
+
siRNAs transfection
for 60 hrs
nuclear extract
preperation
FLAG IP
INO80 subcomplexes
1) siRNA subunit X:
2) siRNA subunit Y:
3) siRNA subunit Z:
FLAG-
Y
Z
X

Figure 8. Diagram showing the two strategies used to generate INO80 subcomplexes that contain a subset of subunits.

(A) The Ino80 ATPase contains regions that function as modular scaffolds on which the other INO80 subunits assemble. Subunits shown in red associate with the Ino80 NTD (N-terminal domain); subunits shown in blue associate with the Ino80 HSA (Helicase SANT Associated) domain; subunits shown in purple associate with the SNF2 ATPase domain, composed of SNF2N and HelicC regions (purple) separated by a long insertion region (white). Intact INO80 complexes (INO80.com) can be purified through FLAG-tagged versions of any wild type INO80 subunit, such as FLAG-Ies2 or FLAG-INO80E. INO80 subcomplexes (INO80ΔN.com or INO80ΔNΔHSA.com) that lack either the subunits shown in red or subunits shown in red and blue can be purified through FLAG-Ino80ΔN or FLAG-INO80ΔNΔHSA, respectively (23). (B) siRNA-mediated knockdown can be used to deplete the desired subunit (X or Y or Z) from cells expressing an appropriate FLAG-tagged INO80 subunit (e.g. FLAG-Ino80ΔN). In the first example, siRNA knockdown of X depletes only the X subunit from the INO80 complexes, suggesting subunit X assembles independent of other subunit(s). In the the second and third examples, siRNA knockdown of either Y or Z leads to co-depletion of both the Y and Z subunits, suggesting Y and Z assemble into the INO80 complex in a mutually dependent manner.

In Figures 9 and 10, we show the representative results of biochemical assays used to characterize INO80 activities, including nucleosome sliding (Figure 9A) and binding assays (Figure 9B) and DNA- or nucleosome-dependent ATPase assays (Figure 10). In the experiment shown in Figure 9A, we compare the activity of the intact INO80 complex purified through FLAG-INO80E to that of INO80 subcomplexes purified through either FLAG-Ino80ΔN or Ino80ΔNΔHSA; nucleosome remodeling activity is indicated by conversion of more rapidly migrating, laterally positioned nucleosomes to more slowly migrating, centrally positioned nucleosomes. To calculate the number of nucleosomes remodeled during the reaction, we use the following formula:

$$\text{fmol nucleosomes remodeled} = \text{starting nucleosomes (in this protocol} \sim 30 \text{ fmol)} \; X \left[\frac{\text{radioactivity in upper band}}{(\text{radioactivity in upper band} + \text{radioactivity in lower band})} \right]$$

In the experiment shown in Figure 9B, we use electrophoretic mobility shift assays to detect nucleosome binding. When nucleosomes are incubated with increasing amounts of intact INO80 complexes purified through the INO80E subunit, we see a dose-dependent disappearance of the band corresponding to free mononucleosomes and appearance of a new "shifted" species that migrates near the top of the gel. In contrast, when nucleosomes are incubated with smaller complexes that had been purified through Ino80ΔN and that lack a subset of INO80 subunits, the shifted species migrates more rapidly (lanes 2-5 and 9-11).

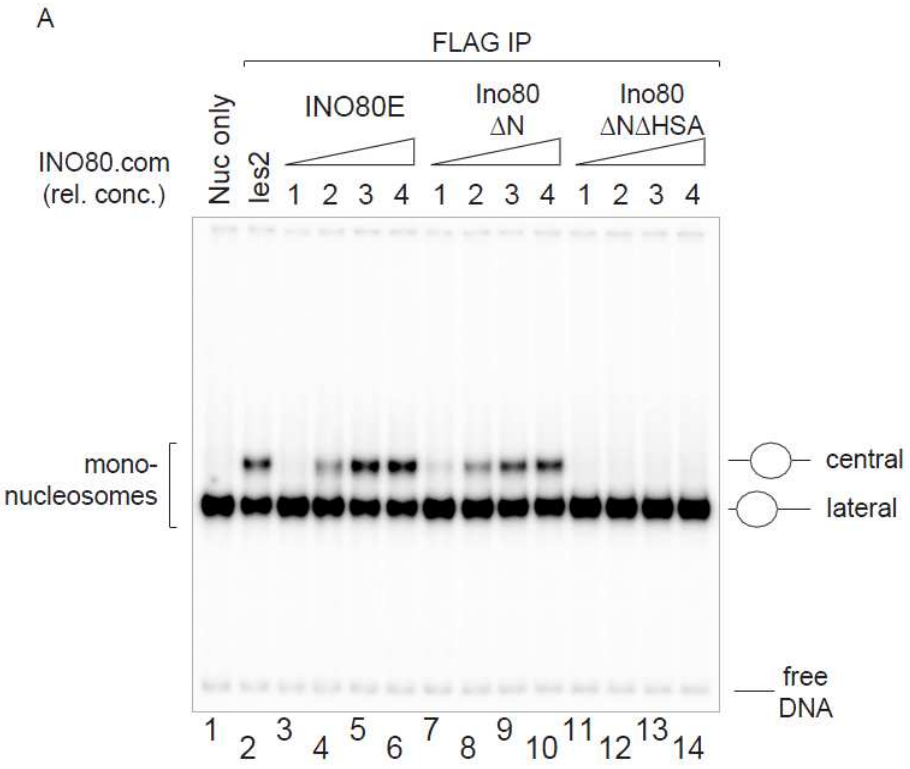

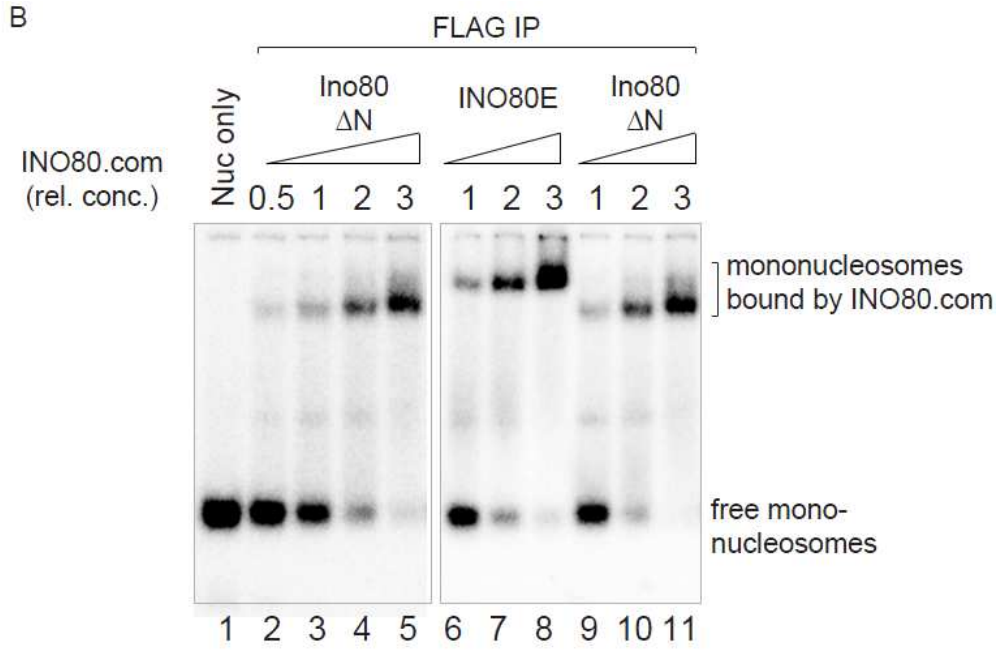

Figure 9. Nucleosome remodeling and binding activities of INO80 and INO80 subcomplexes.

(A) INO80 nucleosome remodeling activity depends on the Ino80 HSA domain and/or associated subunits but is independent of the Ino80 NTD and associated subunits. Nucleosome remodeling assays were performed with FLAG-immunopurified complexes from nuclear extracts prepared from cell lines expressing FLAG-tagged versions of wild type or mutant INO80 subunits. Intact INO80 complexes were purified from cell lines expressing FLAG-Ies2 or FLAG-INO80E; INO80 subcomplexes were purified from cell lines expressing.FLAG-Ino80ΔN or FLAG-Ino80ΔNΔHSA. The subunit composition of each INO80 complex tested is shown in Figure 8A. A relative concentration (rel. conc.) of 1 corresponds to ~10 nM INO80 complex. (B) Nucleosome binding by the INO80 complex is independent of the Ino80 NTD and associated subunits. Nucleosome binding assays were performed in the presence of varying amounts of the indicated FLAG-immunopurified INO80 complex. Binding of INO80 or INO80 subcomplexes to mononucleosomes results in the emergence of slow-migrating "super-shifted" bands corresponding to mononucleosomes stably bound by INO80 or INO80 subcomplexes. Note that the relative mobility of the super-shifted band is determined by the size of the complexes tested: mononucleosomes bound by intact INO80 complexes purified through FLAG-INO80E migrate more slowly than those bound by the smaller FLAG-INO80ΔN-containing subcomplexes.

Nucleosome remodeling and binding assays should always include a control in which nucleosomes are incubated in buffer alone to assess nucleosome integrity and electrophoretic mobility / positioning without remodeling enzyme (e.g. Figures 9A and 9B, lanes 1). To confirm that nucleosome remodeling is ATP-dependent, we perform remodeling reactions in which ATP has been omitted or replaced with the nucleotide

analog adenosine 5'-O-(3-thio) triphosphate (ATPγS), which is bound by ATPases but cannot be hydrolyzed; we expect to observe no change in nucleosome position in reactions lacking ATP or containing the non-hydrolyzable analog ATPγS. In addition, to confirm that ATP-dependent nucleosome remodeling depends on the catalytic activity of the INO80 complex and not on a contaminating remodeling activity, we perform assays in the presence of INO80 complexes purified through a catalytically inactive version of the Ino80 ATPase containing a glutamic acid to glutamine (E653Q) mutation that prevents nucleotide hydrolysis (54). INO80 complexes or subcomplexes containing an Ino80 EQ mutant should exhibit no nucleosome remodeling activity even in the presence of ATP. Any activity that is independent of ATP hydrolysis or is detected in reactions containing Ino80 EQ mutants is likely due to contaminating activity(s) and suggests that further purification of the INO80 complex is needed.

Figure 10 shows results of an assay comparing the DNA- and nucleosome-activated ATPase activities of two different INO80 subcomplexes. One, INO80ΔN, includes an Ino80 ATPase subunit that extends to the proteins normal C-terminus, while the other, INO80ΔNC, lacks the Ino80 C-terminal region (see diagram in Figure 8). Although these complexes are otherwise identical, the rate of ATP hydrolysis (measured by conversion of radio-labeled ATP to ADP) is greater in the presence of INO80ΔNC, suggesting the C-terminus of the Ino80 ATPase may negatively regulate its activity (23). When measuring the rate of ATP hydrolysis, it is advisable to perform assays for varying lengths of time and with more than one concentration of enzyme to ensure measurements are being taken when product-time and dose-response curves are linear. To calculate the amount of ATP

hydrolyzed in any given reaction, multiply the % ATP hydrolyzed by the amount of ATP present in the starting reaction mixture using the following formula:

$$\text{pmol ATP hydrolyzed} = \text{pmol ATP in starting reaction } X \frac{\text{radioactivity in ADP}}{\text{radioactivity in (ATP + ADP)}}$$

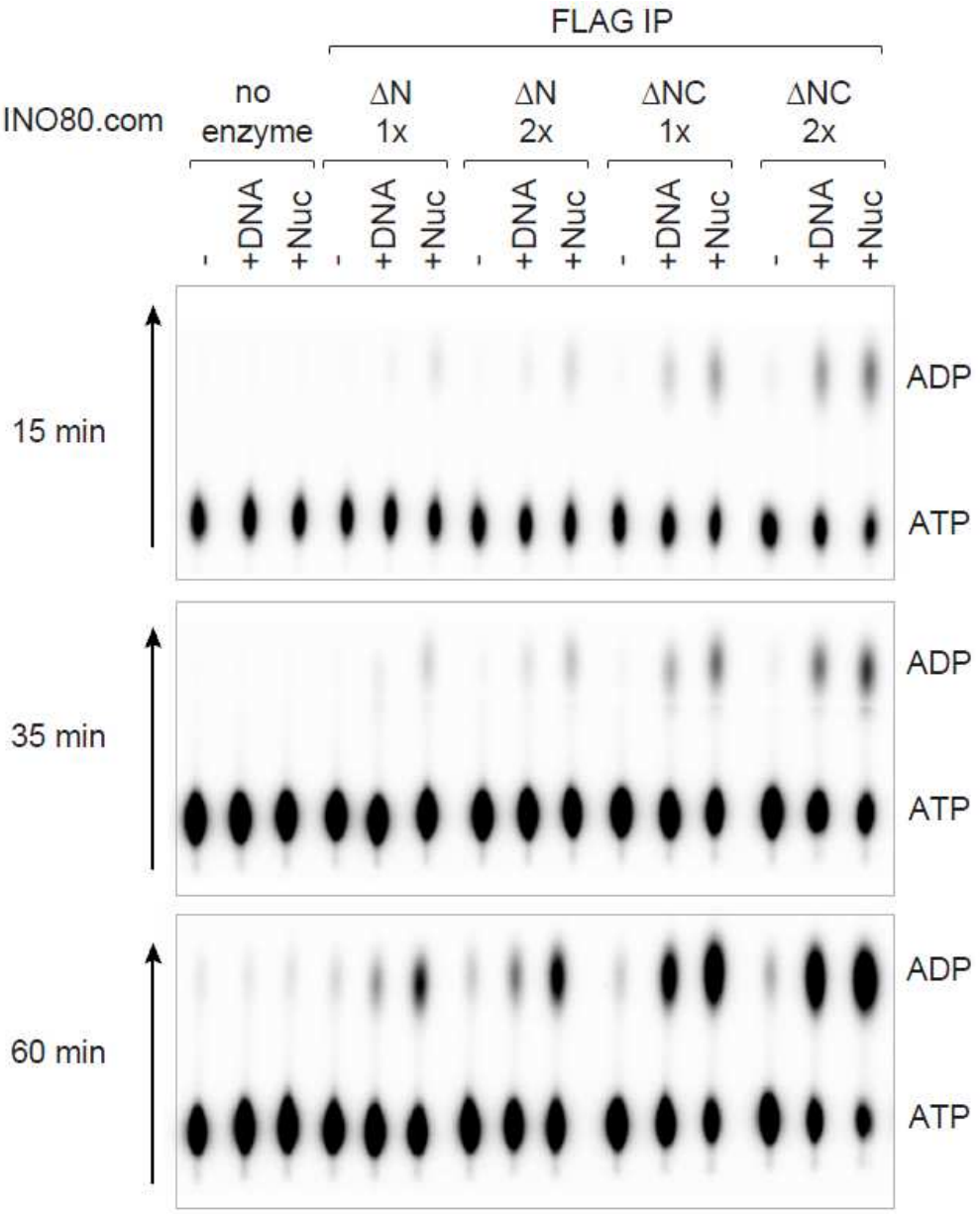

Figure 10. DNA- and nucleosome-dependent ATPase assays.

TLC (thin layer chromatography) -based ATPase assays were performed to measure the rate of ATP hydrolysis by INO80 subcomplexes purified through FLAG-Ino80ΔN (ΔN) or FLAG-Ino80ΔNC (ΔNC) in the presence of saturating amounts of DNA or nucleosomes. Assays were performed using two different amounts of each complex and for three different reaction times. The more slowly migrating spots correspond to the starting α-^{32}P labeled ATP, and the more rapidly migrating species are the ADP reaction products; arrows indicate the direction of solvent migration. Note there is minimal ATP hydrolysis by either complex in the absence of either DNA or nucleosome cofactors, suggesting there is little contamination by other ATPases or by DNA and/or nucleosomes in these preparations of purified INO80 complexes. In addition, the rate of ATP hydrolysis by both complexes is greater in the presence of nucleosomes than DNA, suggesting the INO80 nucleosome remodeling complexes prefer nucleosomal substrates for ATP hydrolysis.

The interpretation of ATPase assays could, in principle, be complicated by the fact that INO80 chromatin remodeling complexes contain several potential ATPases, including the SNF2-like core ATPase Ino80, actin-like proteins Arp5, Arp8, Baf53a, actin, and the AAA+ ATPases Tip49a and Tip49b. Despite the physical presence of multiple ATPases, however, only complexes containing catalytically active Ino80 can support DNA- or nucleosome-activated ATP hydrolysis; complexes containing the catalytically inactive E653Q (54) form of Ino80 ATPase fail to exhibit any detectable ATPase activity under any conditions tested (23). Thus, DNA- and/or nucleosome- stimulated INO80 ATPase activity is mainly contributed by the Ino80 ATPase subunit. The presence of DNA- and nucleosome-independent ATPase activity in the purified preparations of the INO80 complex suggests the presence of contaminating cellular DNA, or alternatively, contaminating non-INO80 ATPases that were not successfully removed during purification. Several steps can be taken to minimize introducing unwanted DNA and/or ATPase during the purification.

i. Increase the salt concentration (NaCl) in the binding and washing steps during the purification;

ii. Decrease the ratio of FLAG agarose to cell lysate during immunopurification; the optimal amount of FLAG-agarose should be determined by titration;

iii. ATP-dependent chaperones may remain bound to FLAG-tagged proteins during immunopurification. These can often be removed by including 1 mM ATP in the washing buffer during immunopurification;

iv. We have successfully removed contaminating DNA by including benzonase (1:1000, Novagen®, Cat. No. 70664) during incubation of extract with FLAG-agarose beads. CAUTION: It is essential to make sure benzonase is removed during the subsequent washing steps, as residual DNase will degrade substrate DNA or nucleosomes during assays for INO80 activity.

DISCUSSION:

Structural and functional studies of multi-subunit mammalian chromatin remodeling complexes from higher eukaryotes have been hampered by the difficulty of preparing biochemically useful amounts of such complexes containing mutant subunits or lacking certain subunits altogether. There are a number of technical hurdles: First, genetic manipulation in mammalian cells has been technically challenging and time-consuming. Unlike yeast cells, whose genome can be readily edited and targeted using recombineering techniques, the mammalian genome is more structurally complex and less susceptible to recombineering interventions. Thus, deletion or modification of mammalian genes in cultured cells or animals is more time consuming and requires more specialized expertise. As a consequence, the generation of mutant mammalian complexes carrying structural mutations or lacking subsets of subunit(s) has been rate-limiting. Second, biochemical reconstitution approaches using heterologous protein expression systems are often used to generate defined multi-protein assemblies. However, such approaches become technically challenging for very large complexes, whose subunits may need to be simultaneously expressed in proper stoichiometry and/or to be assembled

in a particular order, with help from specific chaperones or cofactors. These problems are especially severe in the case of the INO80 complex, because its Ino80 ATPase subunit is particularly difficult to express in insect or *E. coli* cells in biochemically useful amounts. In our studies of the INO80 chromatin remodeling complex, we have been able to circumvent some of these challenges using the strategies described in this chapter, and we anticipate these approaches should be more generally useful for studies of other chromatin remodeling enzymes as well as other large multiprotein complexes.

Chapter III. Subunit organization of the human INO80 chromatin remodeling complex

ABSTRACT

We previously identified and purified a human ATP-dependent chromatin remodeling complex with similarity to the *Saccharomyces cerevisiae* INO80 complex (65) and demonstrated that it is composed of (i) a Snf2 family ATPase (hIno80) related in sequence to the *S. cerevisiae* Ino80 ATPase, (ii) 7 additional evolutionarily conserved subunits orthologous to yeast INO80 complex subunits, and (iii) 6 apparently metazoan-specific subunits. In this chapter, we present evidence that the human INO80 complex is composed of three modules that assemble with three distinct domains of the hIno80 ATPase. These modules include (i) one that is composed of the N-terminus of the hIno80 protein and all of the metazoan-specific subunits and is not required for ATP-dependent nucleosome remodeling, (ii) a second that is composed of the hIno80 HSA/PTH domain,

the actin-related proteins Arp4 and Arp8, and the GLI-Kruppel family transcription factor YY1, and (iii) a third that is composed of the hIno80 Snf2 ATPase domain, the Ies2 and Ies6 proteins, the AAA+ ATPases Tip49a and Tip49b, and the actin-related protein Arp5. Through purification and characterization of hINO80 complex subassemblies, we demonstrate that ATP-dependent nucleosome remodeling by the hINO80 complex is catalyzed by a core complex comprised of the hIno80 protein HSA/PTH and Snf2 ATPase domains acting in concert with YY1 and the complete set of its evolutionarily conserved subunits. Taken together, our findings shed new light on the structure and function of the INO80 chromatin remodeling complex.

INTRODUCTION

The Ino80 protein is a Snf2 family ATPase evolutionarily conserved from yeast to man (4, 5, 28). The Ino80 protein was initially identified in the yeast Saccharomyces cerevisiae, where it was found to function as an integral component of a multisubunit ATP-dependent chromatin remodeling complex with roles in transcription, DNA replication, and DNA repair (4, 28, 40, 116). We subsequently purified the human Ino80 ATPase (hIno80) and found that it is also a component of a multisubunit ATP-dependent chromatin remodeling complex possessing both similarities and intriguing differences with the *S. cerevisiae* INO80 complex (17, 65, 143). Evidence suggests that, similar to its yeast counterpart, the human INO80 complex regulates transcription as well as DNA repair and replication processes (17, 62, 64, 98, 139).

The hINO80 complex shares with the *S. cerevisiae* INO80 complex a set of 8 evolutionarily conserved subunits, including the hIno80 Snf2-family ATPase, the AAA+

ATPases Tip49a and Tip49b (also called RuvBL1 and RuvBL2), actin-related proteins Arp4 (also called Baf53a), Arp5, and Arp8, and the Ies2 and Ies6 proteins; however, it lacks obvious orthologs of the remaining *S. cerevisiae* INO80 complex subunits Nhp10, Taf9, Ies1, Ies3, Ies4, and Ies5 (65). In their place, it contains several apparently metazoan-specific subunits, including the deubiquitinating enzyme Uch37 and the less well characterized Amida, INO80D (FLJ20309), INO80E (CCDC95 or FLJ90652), forkhead-associated (FHA) domain containing MCRS1, and nuclear factor related to κB (NFRKB) proteins (65, 143). A *Drosophila melanogaster* INO80 complex with a collection of subunits similar to those of the hINO80 complex was recently described by Muller and coworkers (71). Both human and Drosophila INO80 complexes were found to include the GLI-Kruppel family zinc finger transcription factor YY1 (17, 71, 139) (referred to as Pleiohomeotic (PHO) in flies.) Although YY1 and PHO were initially thought to be metazoan-specific subunits of the INO80 complex, the recently characterized *Schizosaccharomyces pombe* INO80 complex contains a GLI-Kruppel family zinc finger protein referred to as Iec1 (60), which may be orthologous to YY1 and PHO.

As part of our effort to understand the mechanism(s) by which the hINO80 complex regulates chromatin structure, we wish to define the architecture of the hINO80 complex and to learn how its individual subunits contribute to its ATP-dependent nucleosome remodeling activity. Ino80 proteins from yeast to humans share conserved Snf2-like ATPase/helicase and Helicase-SANT-Associated/Post-HSA (HSA/PTH) domains flanked by non-conserved amino- and carboxy-terminal regions (43). Previous studies

have established that the catalytic activity of the Ino80 Snf2-like ATPase domain is required for ATP-dependent nucleosome remodeling by the *S. cerevisiae* INO80 complex (116). The Ino80 ATPase/helicase domain has also been proposed to provide a binding site for the AAA+ ATPases and Arp5, based on evidence: (i) that the corresponding domain of a related Snf2-like ATPase, Swr1, binds the AAA+ ATPases and (ii) that binding of Arp5 to *S. cerevisiae* Ino80 depends on the AAA+ ATPases (67, 140). The HSA/PTH domain of *S. cerevisiae* Ino80 is also required for ATP-dependent nucleosome remodeling and serves as a docking site for actin and actin-related proteins Arp4 and Arp8 (117, 125). *S. cerevisiae* INO80 complexes lacking one or more of the actin-related proteins or the AAA+ ATPases exhibit greatly reduced nucleosome remodeling activities, suggesting these proteins either participate directly in nucleosome remodeling or are required for proper assembly of active complexes (67, 117). We note that we have not yet determined whether actin is a bona fide subunit of the hINO80 complex. Our current evidence suggests that actin is present in our most highly purified preparations of the hINO80 complex in significantly smaller amounts than the actin-related proteins Arp4, Arp5, and Arp8.

Although the information described above has provided useful preliminary insights into the organization of the INO80 complex and the functions of some of its subunits, major questions remain. In particular, the architecture of the conserved portion of INO80 complexes has not been fully defined, there is no information about which domain(s) of the hIno80 protein govern assembly of the metazoan-specific subunits into the hINO80 complex, and, importantly, there is no information about the potential contributions of the

metazoan-specific subunits to the ATP-dependent nucleosome remodeling activity of the hINO80 complex.

To define further the organization of the hINO80 complex and to explore the contributions of various domains of the hIno80 protein and of the evolutionarily conserved and metazoan-specific subunits to its ATP-dependent nucleosome remodeling activity, we have carried out a systematic structure-function analysis of the hIno80 ATPase. Our findings reveal that ATP-dependent nucleosome remodeling *in vitro* can be carried out by a hINO80 complex subassembly composed of the hIno80 HSA/PTH and Snf2 ATPase domains acting in concert with YY1 and the 7 evolutionarily conserved subunits of the complex. Furthermore, we observe that all 6 metazoan-specific subunits of the hINO80 complex assemble together with an N-terminal hIno80 region to form a module that is not essential for ATP-dependent nucleosome remodeling. Taken together, our findings shed new light on the roles of the hIno80 ATPase and its associated subunits in chromatin remodeling.

RESULTS

Defining the architecture of the human INO80 chromatin remodeling complex

To begin to investigate the role of the hIno80 ATPase and individual subunits of the hINO80 complex in reconstitution of ATP-dependent nucleosome remodeling, we generated a series of human embryonic kidney (HEK) 293 cell lines stably expressing the N-terminally FLAG-tagged hIno80 mutants shown in Figure 11.

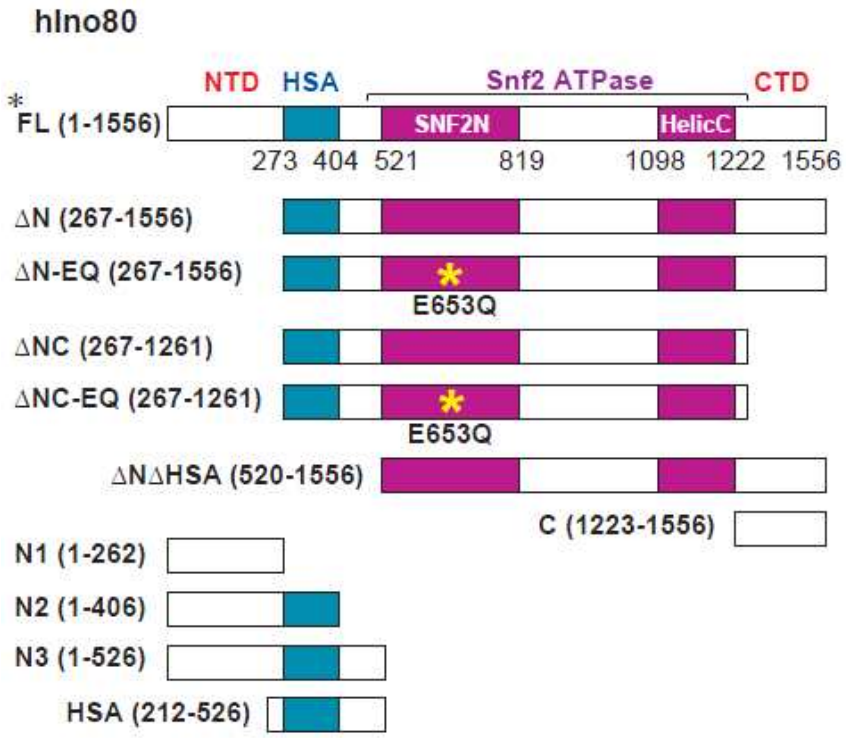

Figure 11. Schematic diagram showing the domain organization of the hIno80 ATPase and hIno80 mutants used in this chapter.

NTD, N-terminal domain; HSA, HSA/PTH domain; Snf2N (Snf2 family amino-terminal) and HelicC (helicase superfamily carboxy-terminal), conserved domains in the Snf2 ATPase domain of hIno80. CTD, carboxy-terminal domain. Numbers refer to positions in the amino acid sequence of the hIno80 protein (accession number NP_060023.1); boundaries of conserved HSA domain is from(125), and boundaries of SNF2N and HelicC are from conserved domain database entries 201060 and 28960, respectively. Yellow asterisk shows the position of the E653Q mutation used to inactivate the hIno80 ATPase.

These mutants include deletion mutants lacking the N-terminal domain (NTD), the HSA/PTH domain, and/or the C-terminal domain (CTD), with or without a DEAD/H box point mutation (E653Q) predicted to interfere with hIno80 ATPase activity (54). In addition, we generated 293 cell lines expressing hIno80 fragments that contain the NTD alone, the NTD and HSA/PTH domain, and the CTD alone. Because we observed that neither full-length FLAG-hIno80 nor FLAG-hIno80 mutants containing both the N-terminus and Snf2 ATPase domains could be stably expressed in HEK293 cells at levels sufficient for subsequent analyses, we purified intact hINO80 complexes for this study

from an HEK293 cell line stably expressing FLAG-tagged INO80 subunit INO80E (16, 65). Nuclear extracts prepared from HEK293 cells expressing FLAG-INO80E or the FLAG-hIno80 mutants were subjected to anti-FLAG agarose immunoaffinity chromatography, and proteins present in anti-FLAG agarose eluates were identified by MudPIT mass spectrometry (44, 136) (Figure 12A) and analyzed by SDS-polyacrylamide gel electrophoresis (Figure 12B) and Western blotting (Figure 12C).

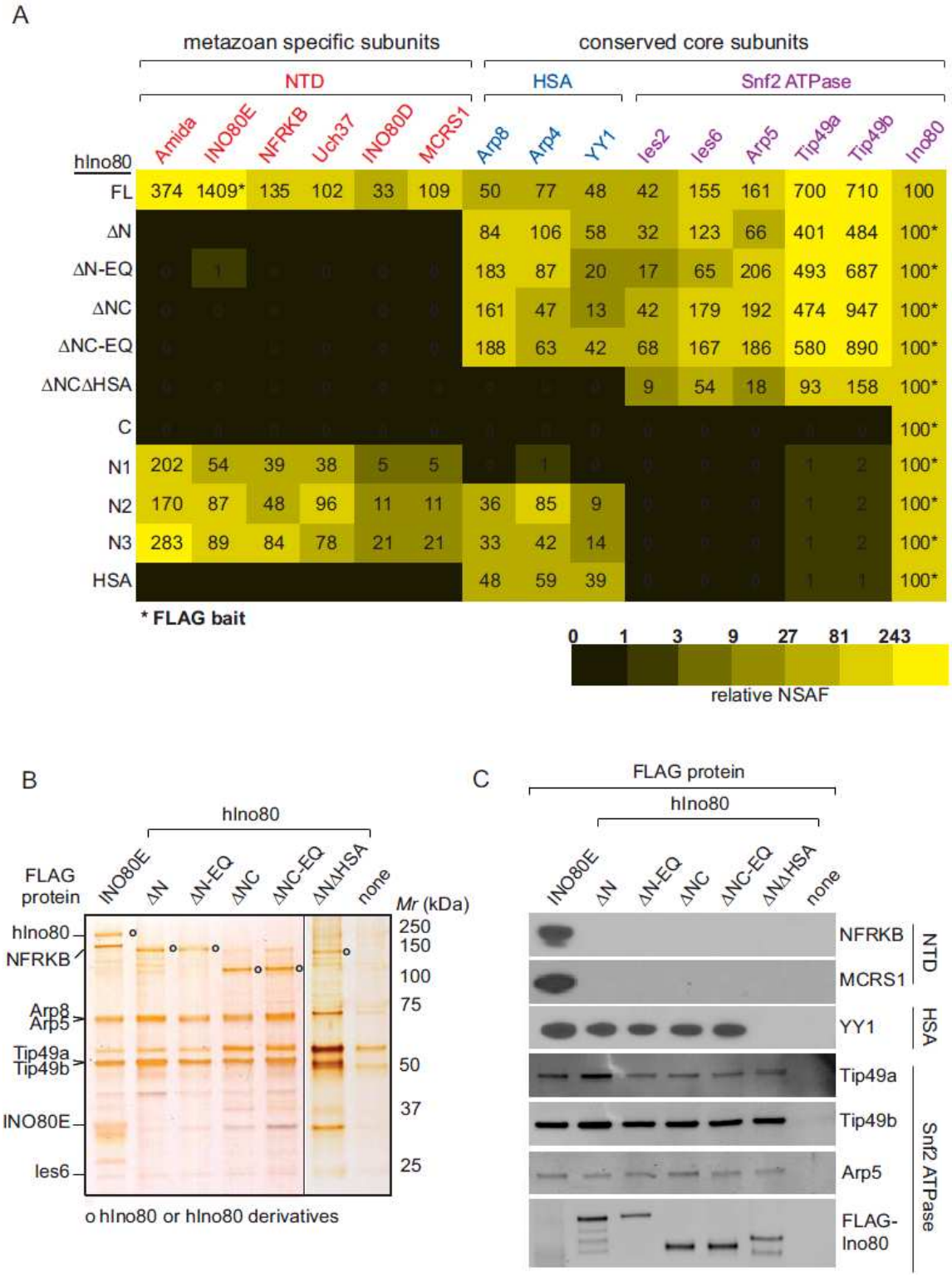

Figure 12. Modular organization of the hINO80 complex.

(A) MudPIT analysis of intact hINO80 complex and hINO80 complex subassemblies. The table shows hINO80 subunits detected by MudPIT mass spectrometry in complexes containing full-length hIno80 or the indicated hIno80 mutants. Red, subunits associating with the hIno80 NTD; blue, subunits associating with the hIno80 HSA/PTH domain; purple, subunits associating with the Snf2 ATPase domain. The subunit used as FLAG-bait for purification of each complex is indicated with an asterisk. Normalized spectral abundance factors (NSAFs) provide a rough estimate of the relative amounts of each protein detected in a MudPIT dataset (26-29); relative NSAFs shown in the table were calculated by normalizing the NSAF for each subunit to the NSAF for hIno80 or hIno80 derivative in each complex. (B) hINO80 complex and hINO80 subassemblies analyzed by SDS-polyacrylamide gel electrophoresis and silver staining. Open circles indicate the position of hIno80 and hIno80 derivatives. Lanes separated by black line are from separate gels. (C) hINO80 complex and hINO80 subassemblies analyzed by Western blotting with anti-FLAG antibodies to detect FLAG-hIno80 fragments or with antibodies against the indicated subunits.

The results of these experiments argue that the hINO80 complex is composed of at least three modules and can be summarized as follows. The metazoan-specific subunits Amida, INO80E, INO80D, NFRKB, Uch37, and MCRS1 were lost from INO80 complexes containing hIno80ΔN, which lacks the first 266 amino acids of hIno80, but retains the HSA/PTH, Snf2 ATPase, and C-terminal domains. Arguing that the hIno80 NTD is both necessary and sufficient to nucleate a hINO80 complex subassembly containing all of the metazoan-specific subunits, complexes containing just the hIno80 NTD (fragment N1) included each of the 6 metazoan-specific subunits (Figure 12A). In contrast, the 295 amino acid non-conserved CTD fragment of hIno80 did not copurify with any of the INO80 subunits. In addition, deletion of the CTD from hIno80 did not result in the loss of any subunits from the complex. Complexes with either hIno80ΔN or a hIno80 fragment lacking both the NTD and the CTD (hIno80ΔNC) contained all of the conserved subunits, including actin-related proteins Arp4, Arp5, Arp8, the AAA+ATPases Tip49a and Tip49b, Ies2, Ies6, and YY1, as did complexes containing the catalytically inactive hIno80ΔN EQ or hIno80ΔNC EQ mutants.

Arguing that the HSA/PTH domain nucleates assembly of a module containing YY1 and actin-related proteins Arp4 and Arp8, deletion of the HSA/PTH domain from hIno80 ΔNTD led to loss of YY1, Arp4, and Arp8, whereas all hINO80 fragments that include the HSA/PTH domain copurified with YY1, Arp4, and Arp8. These findings are consistent with previous results indicating that in the S. cerevisiae INO80 complex, the Ino80 HSA/PTH domain serves as a docking site for actin and actin-related proteins Arp4 and Arp8 (117, 125).

Finally, we observed that the remaining evolutionarily conserved subunits Ies2, Ies6, Arp5, and the AAA+ ATPases Tip49a and Tip49b, are all capable of assembling into a module that includes just the hIno80 Snf2 ATPase domain. While none of these subunits had previously been shown to assemble with a specific Ino80 domain, our observation that Arp5, Tip49a, and Tip49b are among the subunits associated with the hIno80 Snf2 ATPase domain is consistent with previous data suggesting that, in the yeast SWR1 remodeling complex, binding of the actin-related protein Arp6 and the yeast orthologs of Tip49a and Tip49b to Swr1 depends on the presence of an intact Swr1 Snf2-like ATPase domain (140, 141).

Evolutionarily conserved INO80 core complexes catalyze ATP-dependent chromatin remodeling activity

In a previous study, we observed that, like the *S. cerevisiae* INO80 complex, the hINO80 complex is capable of catalyzing both ATP-dependent nucleosome sliding and DNA-dependent ATPase in vitro (65, 116). To begin to investigate the potential roles of individual subunits of the hINO80 complex in these activities, we tested the purified

hINO80 complex subassemblies generated above for their abilities to catalyze ATP-dependent nucleosome remodeling and DNA-stimulated ATP hydrolysis.

To assay ATP-dependent nucleosome remodeling, the FLAG-immunopurified hINO80 complex or hINO80 complex subassemblies shown in Figure 12 were incubated in the presence of ATP with mononucleosomes assembled on a 216 base pair, ^{32}P-labeled DNA fragment with a 601 nucleosome positioning sequence near one end of the DNA. Following reactions, HeLa oligonucleosomes and free DNA were added to reaction mixtures as competitor to remove nucleosome- or DNA-binding proteins that might alter mononucleosome electrophoretic mobility, and reaction products were analyzed on native polyacrylamide gels.

The electrophoretic mobility in a native gel of a DNA fragment containing a nucleosome at one end is greater than that of the same DNA fragment containing a more centrally located nucleosome. The majority of nucleosomes used in our assays are initially located on the laterally positioned nucleosome positioning sequence; thus, nucleosome sliding toward the middle of the DNA can be readily detected by a decrease in electrophoretic mobility of the labeled nucleosome.

As shown in Figure 13, lanes 1-4, the intact hINO80 complex is capable of sliding laterally positioned nucleosomes to a more central position in a dose dependent manner. In addition, subassemblies containing hIno80ΔN (lanes 5-8) or hIno80ΔNC (lanes 9-12) and all of the conserved subunits exhibited nucleosome sliding activities very similar to that of the intact hINO80 complex, indicating that neither the NTD and CTD of hIno80 nor any of the metazoan-specific subunits are essential for nucleosome remodeling.

Nucleosome sliding was strictly dependent on the presence of a catalytically active hIno80 Snf2 ATPase, since complexes containing hIno80ΔN EQ or hIno80ΔNC EQ were inactive (compare lanes 16-19 to 20-23 and 24-25 to 26-27). Arguing that the hIno80 HSA/PTH domain and/or Arp4, Arp8, and YY1 are required for nucleosome sliding, subassemblies containing the hIno80 ΔNΔHSA and Ies2, Ies6, Arp5, Tip49a, and Tip49b, but lacking the HSA/PTH domain and Arp4, Arp8, and YY1 were not active (lanes 13,14).

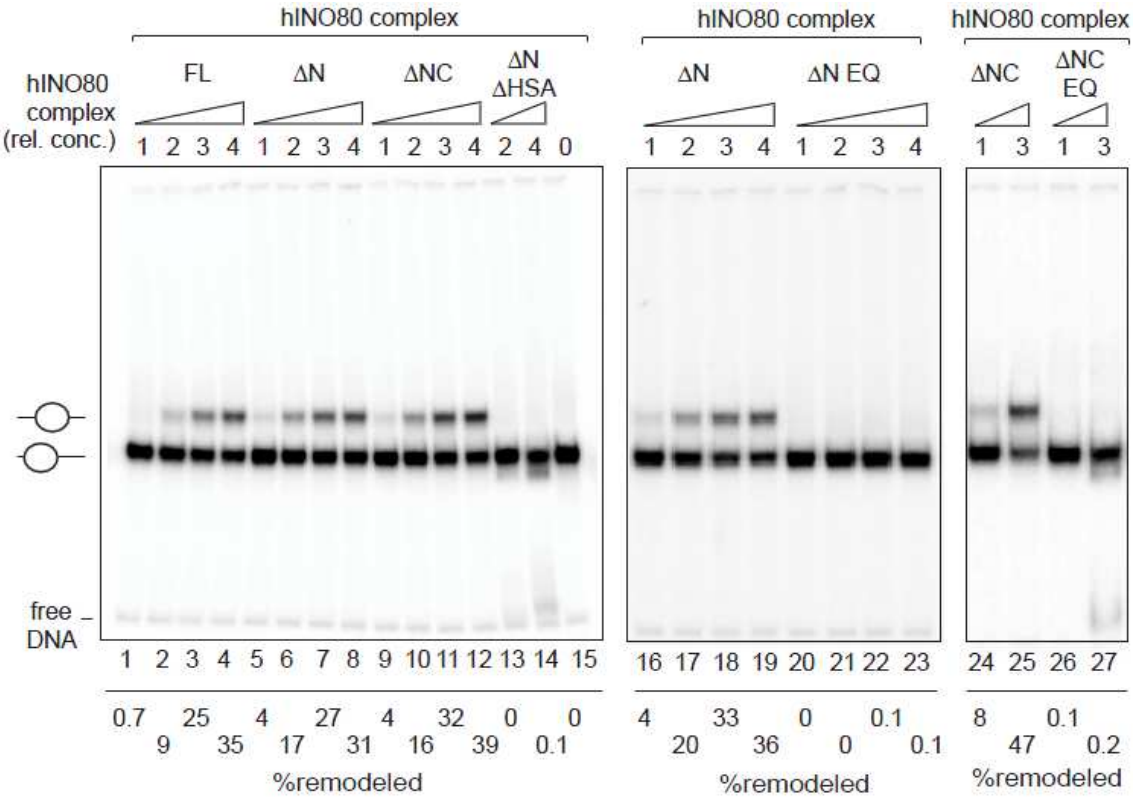

Figure 13. Nucleosome remodeling activities of hINO80 complex and hINO80 complex subassemblies.

Nucleosome sliding assays were performed with the indicated complexes as described in the method chapter. hINO80 complexes at a relative concentration (rel. conc.) of 4 contain ~400 fmol of Arp5, equivalent to the amount of material loaded onto the gels shown in Figure 12, panels B and C. % remodeled nucleosomes is equivalent to the amount of radioactivity in the upper band, corresponding to the centrally positioned remodeled nucleosome, divided by the total amount of radioactivity in the

remodeled nucleosome and the prominent lower band, which corresponds to the laterally positioned, starting nucleosome (see lane 15). The faint band at the bottom of the gels is due to a small amount of free DNA in the nucleosome preparation. The data in lanes 1-15, 16-23, and 24-27 are from three separate experiments; quantitative comparisons should be made only within an individual experiment.

In parallel experiments, the intact hINO80 complex and hINO80 complex subassemblies were assayed for their abilities to catalyze DNA-dependent ATP hydrolysis in the presence of closed circular plasmid DNA. As shown in Figures 14 and 15, the relative DNA-dependent ATPase activities of the intact hINO80 complex and complexes containing hIno80ΔN, hIno80ΔN EQ, hIno80ΔNC EQ, and hIno80ΔNΔHSA mirrored their relative activities in nucleosome sliding. Surprisingly, however, complexes containing hIno80ΔNC exhibited substantially higher DNA-dependent ATPase activity than intact complexes or hINO80ΔN complexes. Similarly, complexes containing hIno80ΔNC exhibit higher nucleosome-stimulated ATPase than the other complexes (data not shown; see also Figures 18). Because complexes containing hIno80ΔNC EQ did not exhibit significant DNA-dependent ATPase, this activity depends on a catalytically active hIno80 Snf2-like ATPase. Although future studies will be required to define the underlying mechanisms, these observations suggest that the hIno80 CTD might function in some contexts as a negative regulator of ATP hydrolysis by the hINO80 complex. In addition, while our findings argue that the ATPase activity of hIno80 is required for nucleosome remodeling activity, they also suggest that ATPase activity may not be strictly coupled to nucleosome remodeling.

INO80 complex	DNA-dependent ATP hydrolysis (pmol/min per 1× complex)
Wild type	0.007 ± 0.001
Ino80ΔN	0.007 ± 0.003
Ino80ΔN EQ	<0.001
Ino80ΔNC	0.095 ± 0.021
Ino80ΔNC EQ	<0.001
Ino80 ΔNΔHSA	<0.001

Figure 14. DNA-dependent ATPase activity associated with wild type hINO80 complexes and hINO80 complex subassemblies.

Reactions were performed with or without DNA as described in the method chapter and contained 1x, 2x, 3x, or 4x wild type hINO80, hINO80ΔN, hINO80ΔN EQ or hINO80ΔNC complexes or 4x hINO80ΔNC EQ or hINO80ΔNΔHSA complexes, where 1x contains ~100 fmol Arp5. Aliquots of each reaction were removed at various time points between 15 and 120 min for measurement of ATP hydrolysis. Values shown for the hINO80ΔNC and hINO80ΔNΔHSA complexes are based on data from two independent reactions. Values for wild type hINO80, hINO80ΔN, hINO80ΔN EQ, or hINO80ΔNC complexes are based on measurements from at least three independent reactions and include only data points in which less than ~25% of the starting ATP was hydrolyzed.

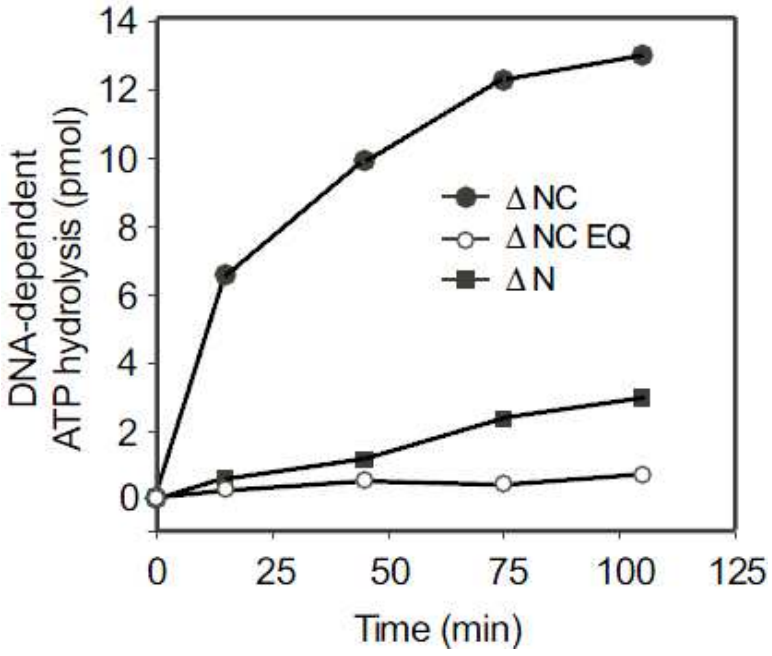

Figure 15. Modulation of DNA-dependent ATPase activity by the hIno80 CTD.

Representative DNA-dependent ATPase assays performed as described in the method chapter. Each reaction included ~400 fmol of Arp5, equivalent to the amount of material loaded onto the gels shown in Figure 12, panels B and C.

Phosphorylation and regulation of the human Ino80 CTD

The experiments described above provide evidence that hIno80 CTD (residues 1261-1556) can negatively regulate the DNA- or nucleosome-dependent ATPase activity of the hINO80 complex, even though this region of hIno80 does not bind stably to any of the known INO80 subunits or affect ATP-dependent nucleosome remodeling in our assays. Within this region, residues 1261-1287 are conserved in metazoa and, as noted in the Introduction, may adopt a triangular brace-like structure that sits on top of the Snf2 ATPase domain (See Figure 4F). Sequences C-terminal to residue 1287 are conserved only in mammals and, based on analyses performed with the PSIPRED program (66),

may be largely unstructured. In thinking about mechanisms by which the CTD might affect INO80 activity, we considered the possibility that the unstructured CTD domain might fold back onto and interact with the conserved Snf2-like ATPase domain and block access to key structural motifs within the Snf2 ATPase core, potentially interfering with essential steps in the ATP hydrolysis cycle, such as remodeler engagement with DNA or ATP binding, hydrolysis, and release. Agreeing with this possibility, the linker region that connects the Ino80 CTD and the Snf2-C domain corresponds to a region in the zebrafish Rad54 that was poorly ordered in the crystal structure, suggesting the potential of adopting alternative conformations (127). In addition, this model predicts that addition of an excess of Ino80 CTD to INO80 ΔNC complexes might inhibit ATPase activity *in trans.*

To begin to address this possibility, we immunopurified FLAG epitope tagged Ino80 CTD fragments from nuclear extracts of 293-FRT cell lines stably expressing the Ino80 CTD. INO80ΔNC complexes were assayed for DNA-stimulated ATPase in the presence of various concentrations of CTD fragment, all in excess. In control reactions, we tested the effect of adding excess CTD fragment to reactions containing INO80ΔN complexes, which contain covalently linked CTD domains. As shown in Figure 16 (black bars), we observed a gradual reduction of DNA-stimulated ATPase activity in INO80ΔNC reactions as more CTD fragments were included. Arguing against the possibility that contaminating activity(s) in the purified fraction containing the CTD fragment might inhibit DNA-dependent ATPase activity by mechanisms independent of INO80 complexes, addition of the fragment had no effect on reactions containing INO80ΔN.

Thus, the purified INO80 CTD fragments specifically inhibit the DNA-stimulated ATPase of INO80 complexes lacking CTD tails, but not those with covalently linked CTD tails (INO80ΔN complexes). Notably, in the presence of the highest dosage of Ino80 CTDs, INO80ΔNC complexes exhibited a decreased level of ATPase activity that is comparable to INO80ΔN complexes (Figure 16). This observation is consistent with the possibility that free CTD fragments in the reaction can interact with INO80ΔNC and transform it into an INO80ΔN-like complex, thus recapitulating the *cis* inhibitory regulation posed on INO80ΔN complexes *in trans*.

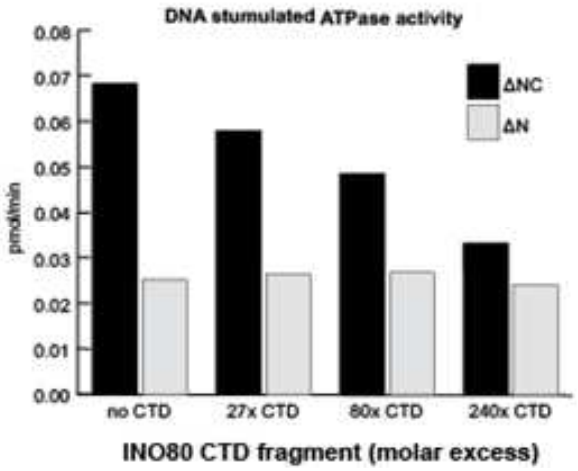

Figure 16. Ino80 CTD region negatively regulates ATPase activity of INO80 complexes

DNA-stimulated ATPase activity of INO80 ΔN and ΔNC were measured in the presence of increasing amounts of FLAG-tagged Ino80 CTD fragment, which was purified from a nuclear extract of HEK293 cells. The relative molar concentrations of the CTD and the Ino80 ATPase were estimated by comparing the intensity of bands in silver-stained gels; INO80 CTD fragment was included in assays in excess over INO80 as indicated in the graph.

The Ino80 CTD has been shown to be a target for cell-cycle-dependent, phosphorylation on serine residues 1490, 1512, and 1516 and threonine residue 1550 during mitosis (35); thus it was of interest to determine whether phosphorylation of this domain might regulate activity(s) of the hINO80 complex.

To determine whether the hIno80 CTD is phosphorylated in human cells, we used a phosphorylation specific staining method (121). To do so, FLAG-Ino80 CTD purified from HEK293 cells and HIS-Ino80 CTD purified from *E. coli* were fractionated by SDS-PAGE, and the gel was stained with SyproRuby, which fluoresces at 457 nm to detect total protein (Figure 17, lanes 1-3) and with the phospho-specific stain Pro-Q Diamond, which fluoresces at 550 nm (Figure 17, lanes 4-6). Comparison of total protein and phosphorylation-specific staining indicates that Ino80 CTD fragments purified from nuclear extracts from 293-FRT cells stably expressing FLAG epitope tagged CTD fragment were phosphorylated. In contrast, a strong phosphorylation signal was not detected on a histidine tagged version of the same Ino80 CTD fragment purified from *E. coli* cell extracts.

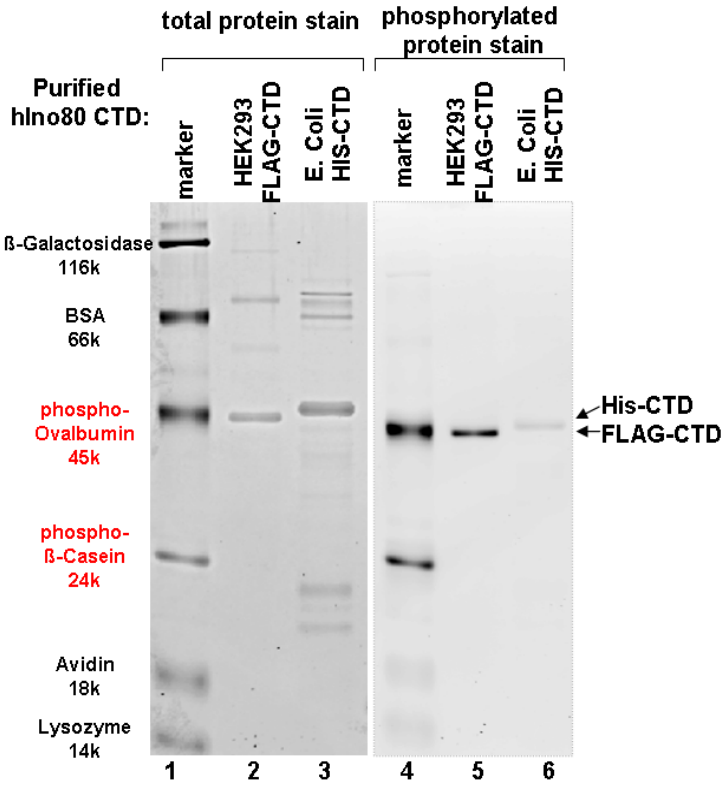

Figure 17. Human Ino80 CTD can be phosphorylated when purified from nuclear extracts of HEK293 cells.

Ino80 CTD fragment (1223-1556) cDNA was fused with either FLAG epitope tag or 10x Histidine tag, and expressed in HEK293 cells and E. coli cells, respectively. Purified FLAG-Ino80 CTD (lanes 2 and 5) and His-Ino80 CTD (lanes 3 and 6) were applied to SDS-PAGE. The same gel were stained by Sypro-Ruby to visualize total protein (lanes 1-3), and Pro-Q Diamond phospho-stain to visualize phosphorylated polypeptide (lanes 4-6). Markers (lanes 1 and 4) include two phosphorylated protein Ovalbumin and ß-Casein, and additional un-phosphorylated proteins ß-galactosidase, bovine serum albumine (BSA), Avidin, and Lysozyme.

To confirm the presence of phosphoryl group(s) on the Ino80 CTD fragment, we treated the purified FLAG Ino80 CTD with two amounts of alkaline phosphatase *in vitro*. As shown in Figure 18A, alkaline phosphatase treatment resulted in a dosage-dependent reduction of the phosphorylation signal on the Ino80 CTD fragment. This reduction could be inhibited completely by the addition of 50 mM EDTA, which chelates

magnesium and consequently inhibits the enzymatic activity of the alkaline phosphatase CIP (calf intestinal phosphatase).

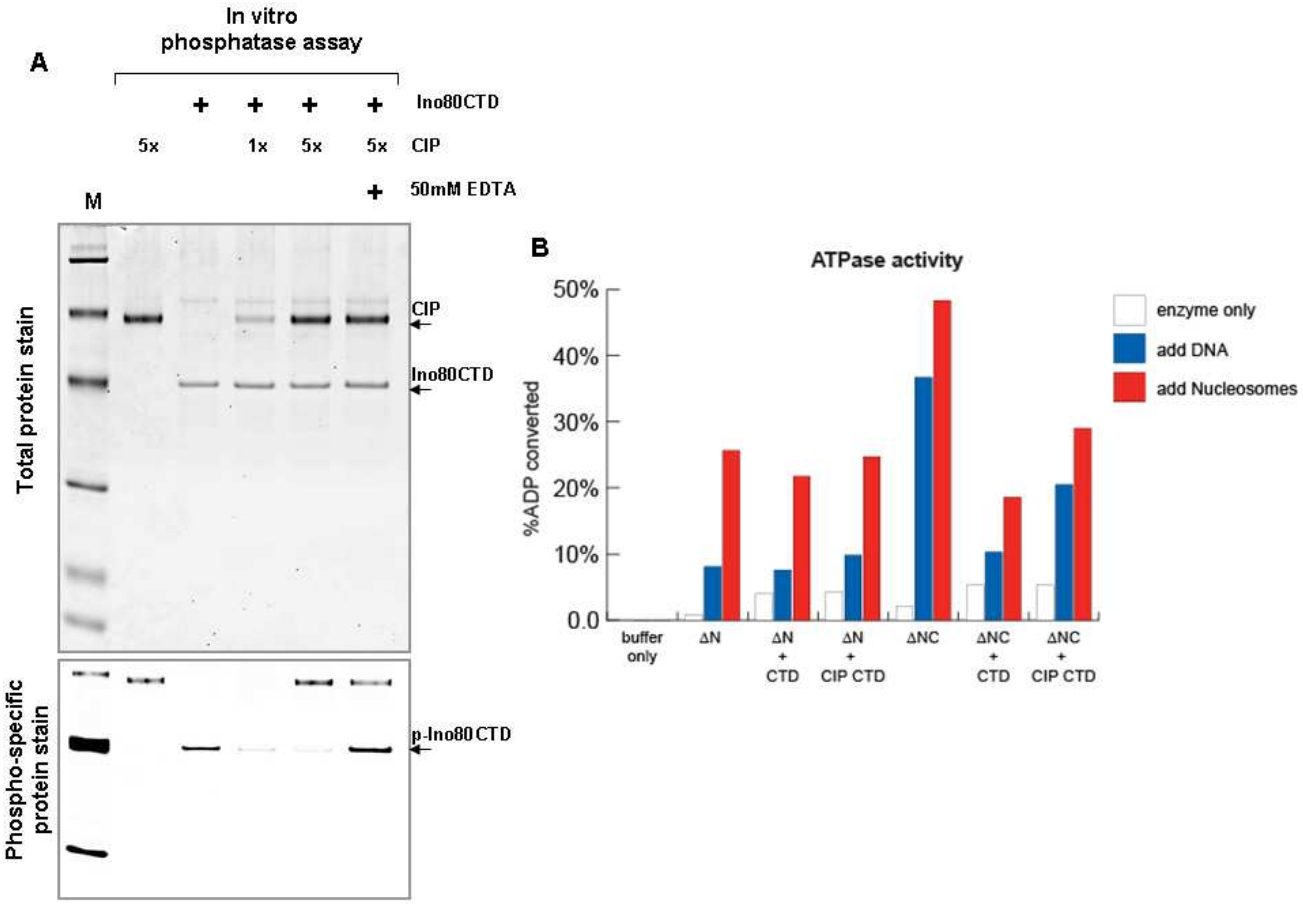

Figure 18. The hypo-phosphorylated Ino80 CTD is less of a potent ATPase inhibitor

(A) *In vitro* phosphatase treatment can reduce Ino80 CTD phosphorylation. Ino80 CTD purified from nuclear extracts of 293 cells was incubated with varying amount of alkaline phosphatase CIP (calf intestinal phosphatase) in vitro. 50mM EDTA was applied to inhibit the activity of CIP. The reaction products were subjected to SDS-PAGE, and the same gel were stained either with Sypro-Ruby to visualize total protein (upper panel), and Pro-Q Diamond phospho-stain to visualize phorphorylated polypeptide (lower panel). (B) CIP-treated Ino80 CTD exerted less inhibitory effect on the ATPase activity of INO80ΔNC complexes. Same amount of mock treated and CIP-treated Ino80 CTD were incubated with INO80 complexes ΔN or ΔNC, and DNA- and nucleosome-stimulated ATPase hydrolysis were measured as the ratio of hydrolyzed ATP (ADP) over the overall input ATP.

To determine whether phosphorylation of the CTD fragment affects its ability to inhibit *in trans* the DNA-dependent ATPase activity associated with INO80ΔNC complexes, we generated Ino80 CTD fragments that were either hyper- or hypo-phosphorylated. FLAG tagged Ino80 CTD fragments were immobilized on anti-FLAG antibody agarose beads and incubated with or without CIP at 37 ^{o}C for 1 hour, followed by extensive washing to remove CIP. The hyper- and hypo- phosphorylated status of the CTD fragments was then confirmed using Pro-Q Diamond phosphoproteins-specific staining (data not shown). To compare the inhibitory potential of hyper- or hypo-phosphorylated CTD fragments on the ATPase activity of INO80ΔNC complexes, we compared the DNA- and nucleosome-stimulated ATPase activity of INO80ΔNC complexes in the presence of an excess of either mock- or CIP-treated CTD fragment. As shown in Figure 18A, addition of hyper-phosphorylated CTDs (mock treated) led to a significant decrease of both DNA- and nucleosome- stimulated ATPase activities of INO80ΔNC complexes; whereas such activities were down-regulated to a lesser extent with the addition of hypo-phosphorylated CTDs (CIP treated) (Figure 18B). Consequently, both DNA- and nucleosome-stimulated ATPase activities were higher in the presence of CTDs treated by CIP than mock treated. We did not observe any noticeable inhibitory effect of both CTD groups on the ATPase activity of INO80ΔN complexes. We note that the Ino80 CTD preparations in these experiments likely contain a mixture of un-phosphorylated and phosphorylated CTDs with heterogeneous phosphorylation, and that the removal of phosphoryl group by CIP treatment was by no means complete. Whether the inhibitory activity in CIP-treated CTD fragments reflects the presence of residual phosphorylated CTDs remains to be determined. Nevertheless, the greater inhibitory potential of hyper-

phosphorylated preparation of CTD fragments is consistent with the model that the presence of phosphoryl groups on Ino80 CTD may contribute to negative regulation of INO80 ATPase activity.

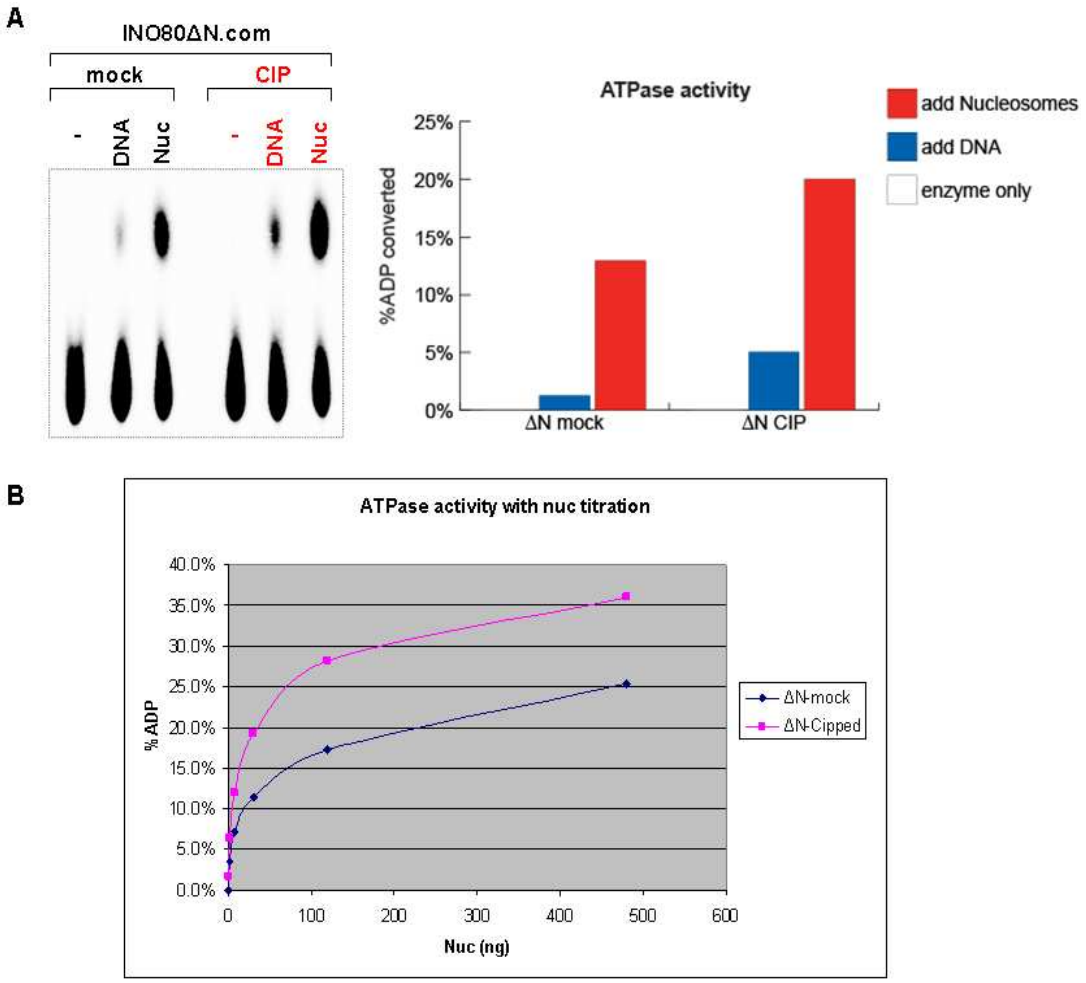

Figure 19. De-phosphorylated INO80 complexes are more active in DNA- and nucleosome-stimulated ATPase assays.

(A) Equal amount of INO80ΔN complexes, either mock treated or CIP treated, were subject to DNA and nucleosome-stimulated ATPase assays. (left) p^{32} radiograph of the assay done with saturating amount of DNA and nucleosomes; (right) quantification of the result to the left; (B) ATPase activity measurement with nucleosome titration to compare the rate of ATP hydrolysis by mock treated or CIP treated INO80ΔN complexes.

To test this model in the context of INO80 complexes, in which the CTD is present *in cis*, we sought to remove the phosphoryl groups from the Ino80 CTD by treating INO80ΔN complexes with CIP. We compared the ATPase activity of either hyper- or hypo-phosphorylated INO80ΔN complexes in DNA- and nucleosome-stimulated ATPase assays. Consistent with the observation that CIP treated CTD fragments were less inhibitory when added *in trans*, CIP treated INO80ΔN reproducibly exhibited higher ATPase activities stimulated by both DNA and nucleosomes compared with mock treated complexes (Figure 19A). The increase in DNA stimulated ATPase activity following CIP treatment was more pronounced, but the increase in nucleosome-stimulated ATPase activity was also consistently observed over a wide range of nucleosome concentration (Figure 19B). This observation is consistent with the possibility that phosphorylation of CTD regulates INO80 ATPase activity, but we can not rule out the possibility that potential phosphorylation event(s) on subunits other than Ino80 ATPase may also contribute to negative regulation of INO80 ATPase activity. Notably, we do find that the Ino80 ATPase may be the most heavily phosphorylated subunit in INO80 complexes (see Figure 21B). We concluded from these data that the phosphorylation of INO80 complexes may negatively regulate ATPase activities of the complex.

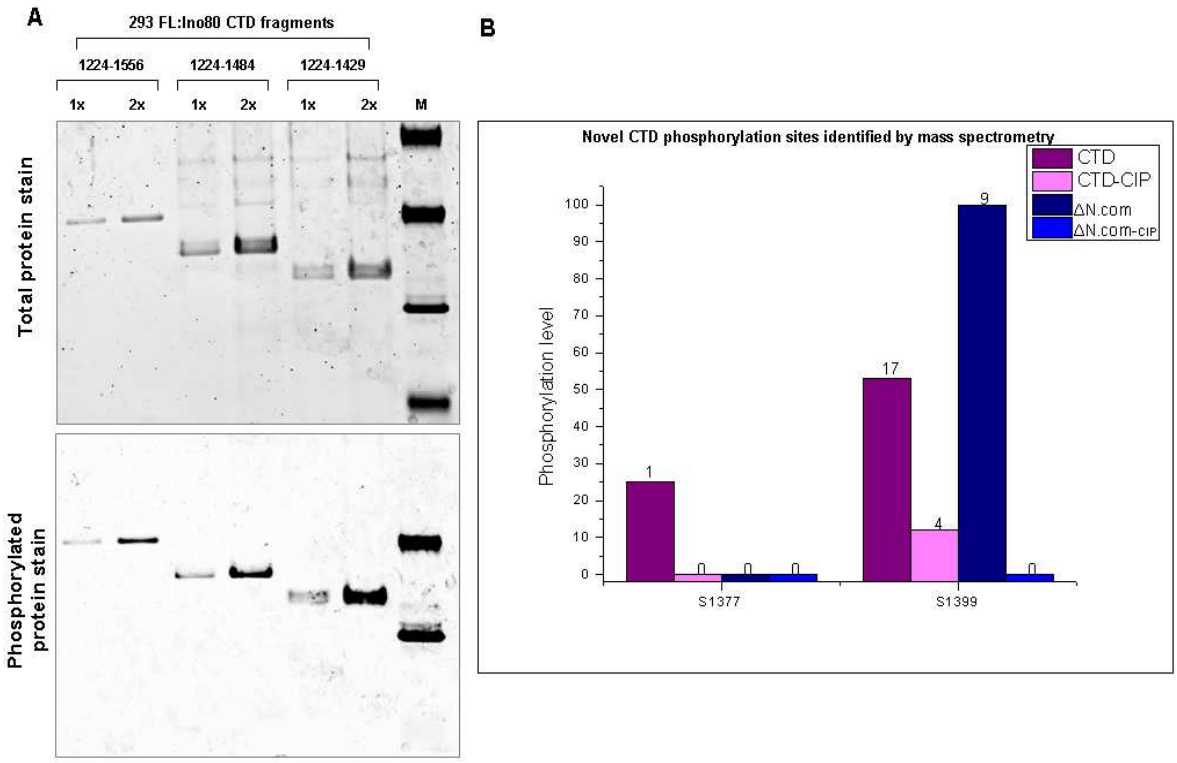

Figure 20. Identification of novel phosphorylation sites on Ino80 CTD

(A) Various Ino80 CTD fragments that contain either residues 1224-1556, 1224-1484, or 1224-1429 were purified from nuclear extracts of 293 cells, and subjected to SDS-PAGE. The same gel were stained either with Sypro-Ruby to visualize total protein (top panel), or Pro-Q Diamond phospho-stain to visualize phosphorylated polypeptide (bottom panel). (B) Purified Ino80 CTD and INO80ΔN complexes, either mock treated or CIP treated, were subject to MUDPIT mass spectrometry analysis to identify phosphorylated peptide. Each sample was divided to half, digested by protease. One half of the material was subjected to phospho-peptide enrichment by TiO2 and IMAC columns, and analyzed by mass spectrometry for phosphor spectrum; the other half was used to quantitate the overall spectrum abundance of a given peptide. Phosphorylation level represents the spectrum percentage of phosphorylated peptide vs. overall peptide counts. The number of spectrum identified in the phosphor enriched group was listed above each bar.

Our observations that INO80ΔN complexes appear to be regulated by phosphorylation, potentially of Ino80 CTD, suggest that the INO80 complex could be targeted by cellular signaling pathways that culminate in the phosphorylation of INO80. In light of previous evidence that specific residues of the Ino80 CTD, including serine 1490, 1512, 1516, and threonine 1550, are phosphorylated in mitotic, but not G1 cells, we considered the

possibility that catalytic activities of INO80 complexes might become repressed by phosphorylation of the Ino80 CTD during the mitotic phase of the cell cycle.

To determine whether our preperations of Ino80 CTD are phosphorylated at sites that were reported, we subjected the purified Ino80 CTD and INO80ΔN complexes to MUDPIT mass spectrometry analysis for phosphorylation site mapping, in collaboration with the Washburn lab. As a control for false positive signal, we also included CIP-treated hypo-phosphorylated Ino80 CTD and INO80ΔN complexes for the analysis. The results identified multiple peptides containing phosphoryl groups at serine 1399 position in both Ino80 CTDs (17 spectra) and INO80ΔN complexes (9 spectra). Supporting the validity of the identified phosphorylation sites, the ratio of phosphorylated vs. non-phosphorylated peptide (phosphorylation level) went down when the samples were treated with CIP. We identified only one phosphorylated spectrum at the serine 1377 position, and none in CIP treated sample, suggesting serine 1377 of Ino80 can be phosphorylated. The low phosphorylated spectrum count of this site could be explained by the possibility that the serine 1377 is not a major phosphorylated residue compared with serine 1399; or alternatively, the spectrum of the phosphorylated peptide may be intrinsically difficult to detect. In summary, we identified two previously unrecognized phosphorylation residues serine 1377 and 1399 in the Ino80 CTD. Surprisingly, we did not identify any phosphorylated spectrum corresponding to the previously identified (35) Ino80 CTD phospho sites (serine 1490, 1512, 1516, and threonine 1550).

As an initial attempt to locate the phosphorylation site on the Ino80 CTD, we sought to validate the phosphorylation sites identified by our mass spectrometry analysis, and

confirm the absence of reported phospho sites in our system. We generated C-terminally truncated Ino80 CTD fragments containing residues 1224-1484 or 1224-1429. Both of these fragments lack the reported CTD phosphorylation sites, but retain the sites identified in our analysis. When these shorter fragments were compared with Ino80 CTD (1224-1556), we observed comparable amount of phosphorylation signal by the gel staining method, again suggesting that the previously reported residues did not contribute to the phosphorylation signal we detected on the purified Ino80 CTD. Instead, the phosphorylation specific staining is evidently due to modifications occurring in a region that contains the phosphorylated residues (serine 1377 and 1399) we identified by mass spectrometry. Further mutagenesis study on these two phospho-sites is needed to unambiguously validate the bona fide phosphorylation sites of the Ino80 ATPase.

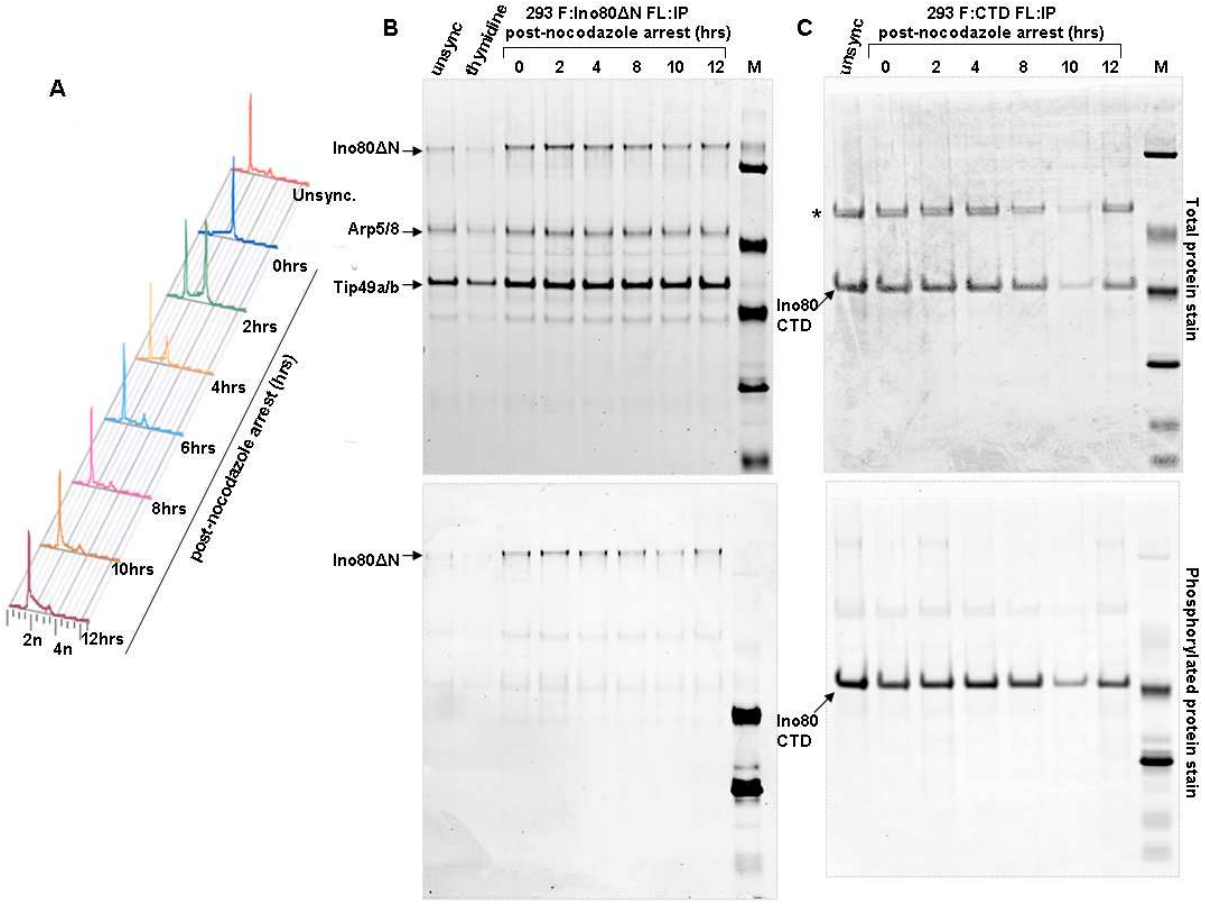

Figure 21. Cell cycle specific phosphorylation profile of purified INO80 complexes or Ino80 CTD

(A) Flow cytometry analysis of DNA content in 293 F: Ino80ΔN cells released from mitotic arrest over a twelve hour time course. Cells were released from nocodazole block and harvested at two hour intervals, and a portion of cells were fixed and stained with propidium iodide to monitor synchrony. The zero hour time point corresponds to unreleased cells. (B and C) INO80ΔN complexes (B) and F: Ino80 CTD (C) were purified from cells released from mitotic arrest over a twelve hour time course. FLAG eluates were subjected to SDS-PAGE, and same gels were stained either with Sypro-Ruby to visualize total protein (upper), and Pro-Q Diamond phospho-stain to visualize phosphorylated polypeptide (lower). The association of Arp5/8 and Tip49a/b with F: Ino80ΔN is constant across the cell cycle. The asterisk (upper, C) denotes contaminated proteins during FLAG immunoprecipitation from a whole cell extract, which are hypo-phosphorylated.

Despite the fact that our mass spectrometry analyses did not identify any of the previously identified mitosis-specific phosphorylation sites, we wished to test the possibility that phosphorylation at the sides we found might be regulated in a cell-cycle

dependent manner. In these experiments, 293-FRT cell lines stably expressing either FLAG tagged Ino80 CTDs or Ino80ΔN were synchronized and arrested in mitosis by a microtubule depolymerization drug nocodazole. Cells were released from mitotic arrest, and were harvested at two hour intervals over the next 12 hours. Propidium iodide stained cells were analyzed by FACS (fluorescence activated cell sorting) to confirm the efficacy of mitotic arrest and release (Figure 21, A). Results of this analysis suggested that the majority of the cell population had gone through mitosis and entered G1 phase 6 hours after release from mitotic arrest. We subsequently purified the Ino80 CTD and INO80ΔN complexes from whole cell extracts from each cell line at each time point. Purified complexes were subjected to SDS PAGE, and subjected to total and phosphorylation-specific protein stainings. The results suggested that the fraction of Ino80 ATPase that is phosphorylated remains rather constant from M phase to G1 phase, though the obtained protein level of Ino80 CTDs or Ino80ΔN ATPases did fluctuate mildly (Figure 21B). We did not detect mitotic-specific enrichment of Ino80 phosphorylation per reported study (35). But we indeed observed 1) that the association of conserved INO80 subunits Arp5, Arp8, Tip49a and Tip49b with the Ino80ΔN ATPase stayed rather constant throughout the M-G1 cell cycle transition (Figure 21B); 2) that the Ino80 ATPase is the most heavily phosphorylated INO80 subunit under the condition examined in our system (Figure 21B). Noticeably, our Ino80 CTDs and INO80ΔN complexes were purified from nuclear extracts of HEK293-FRT cells; whereas the reported data were obtained from cell extracts containing the whole proteome of Hela cells without enrichment of INO80.

Our observation is consistent with the possibility that the phosphorylation of the Ino80 CTD is limited to cells in mitotic phase. Instead, INO80 appears to be phosphorylated throughout multiple stages of cell cycle. Hence INO80 phosphorylation could contribute to regulation by cell-cycle independent processes.

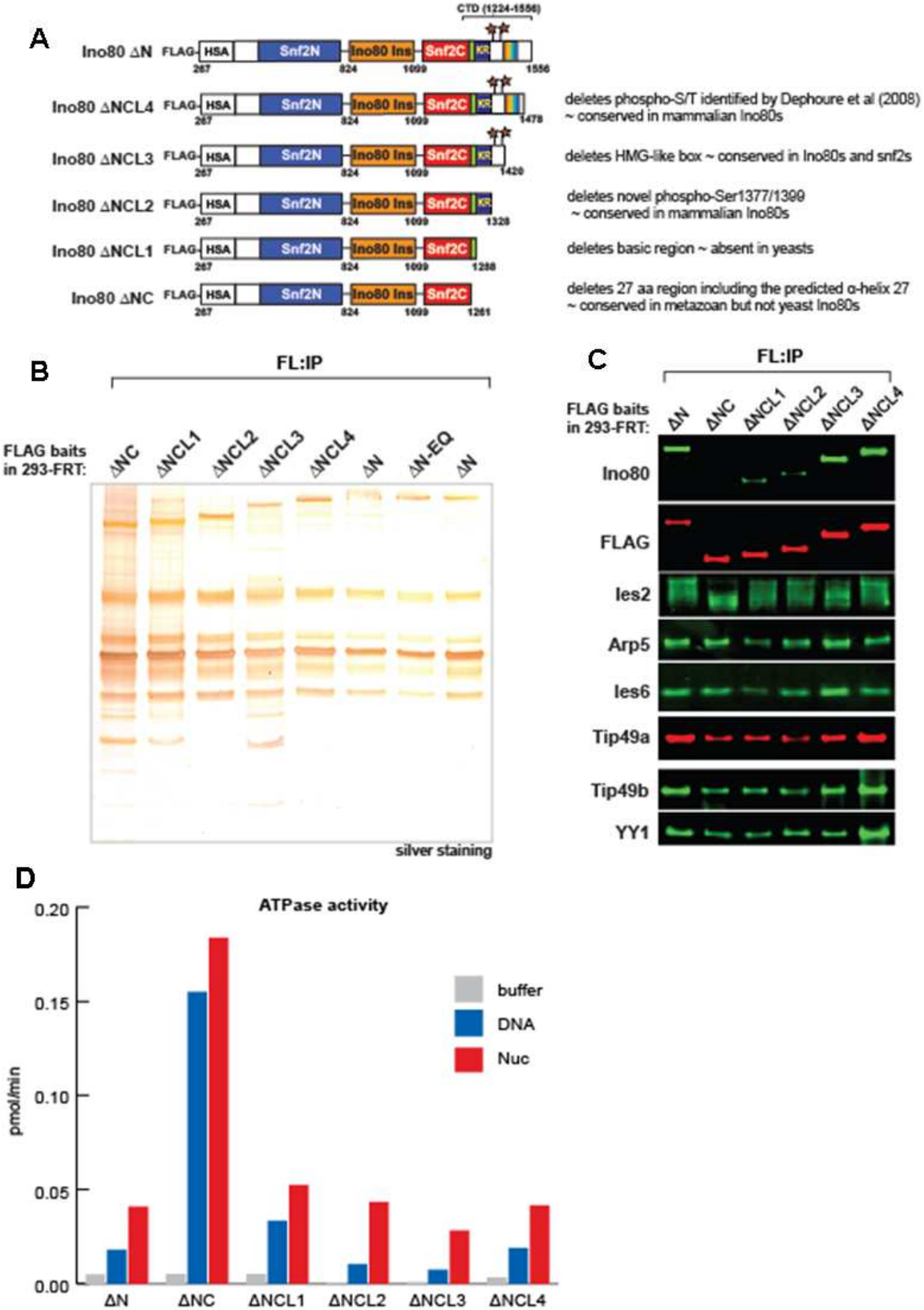
A
CTD (1224-1556)
Ino80 ΔN
Ino80 ΔNCL4
Ino80 ΔNCL3
Ino80 ΔNCL2
Ino80 ΔNCL1
Ino80 ΔNC
FLAG
HSA
Snf2N
Ino80 Ins
Snf2C
KR
deletes phospho-S/T identified by Dephoure et al (2008)
~ conserved in mammalian Ino80s
deletes HMG-like box ~ conserved in Ino80s and snf2s
deletes novel phospho-Ser1377/1399
~ conserved in mammalian Ino80s
deletes basic region ~ absent in yeasts
deletes 27 aa region including the predicted α-helix 27
~ conserved in metazoan but not yeast Ino80s
B
FL:IP
FLAG baits
in 293-FRT:
ΔNC
ΔNCL1
ΔNCL2
ΔNCL3
ΔNCL4
ΔN
ΔN-EQ
ΔN
silver staining
C
FL:IP
FLAG baits
in 293-FRT:
ΔN
ΔNC
ΔNCL1
ΔNCL2
ΔNCL3
ΔNCL4
Ino80
FLAG
Ies2
Arp5
Ies6
Tip49a
Tip49b
YY1
D
ATPase activity
pmol/min
0.20
0.15
0.10
0.05
0.00
buffer
DNA
Nuc
ΔN
ΔNC
ΔNCL1
ΔNCL2
ΔNCL3
ΔNCL4

Figure 22. A predicted triangle brace region of Ino80 accounts for majority of the inhibitory effect on INO80 ATPase activities

(A) Schematic representation of the smaller C-terminal truncated INO80Δ constructs used to generate INO80ΔNCL complexes. ΔNCL4 (267-1478) lacks the predicted phosphorylation sites in Dephoure *et al*. (35); ΔNCL3(267-1420) further lacks a predicted HMG-like sequence; ΔNCL2 (267-1328) lacks the phosphorylation sites (serine 1377/1399) we identified by MUDPIT mass spectrometry analysis; ΔNCL1 (267-1288) lacks a region that is rich in basic residues; ΔNC (267-1261) lacks 27 amino acid corresponding to the α-27 helix of the zebrafish Rad54 structure (Thoma *et al.* (127)), which is predicted to adopt a triangular brace-like structure. Purified INO80ΔNCL complexes were analyzed by silver staining (B), and western blotting (C) using INO80 subunit-specific antibodies; (D) ATPase activity of Purified INO80ΔN and INO80ΔNCL complexes were analyzed by TLC-based ATPase assay. The bar graph represents the rate of ATP hydrolysis in each reaction. The rate for each INO80 complex was measured in the presence of buffer only (grey), DNA (blue), and nucleosomes (red).

In a final set of experiments addressing the contribution of the CTD to INO80 regulation, we wished to define in more detail the region of the CTD that is the most critical for CTD-dependent regulation of Ino80 ATPases. To do so, we made systematic deletion constructs (Ino80ΔNCLs) that lack the region of predicted significance (Figure 22A). INO80 complexes associated with Ino80ΔNCLs mutants were purified, and subjected to SDS PAGE, followed by silver staining (Figure 22B) and western blotting with various INO80 antibodies (Figure 22C). We found that the subunit composition and stoichiometry of these INO80ΔNCLs are very similar to INO80ΔN and INO80ΔNC complexes. We compared the DNA- and nucleosome-stimulated ATPase activities of these ΔNCLs complexes with ΔN and ΔNC complexes (Figure 22D). The result revealed that ΔNCL complexes exhibited ATPase activity that is very similar to the ΔN complex, but significantly lower than hyper-activated INO80ΔNC complexes, suggesting that INO80ΔNC is the only complex tested so far that contains a potent inhibitory motif. When compared with other INO80 complexes tested, the unique region that INO80ΔNC

complexes lack is a 27 amino acid region (1261-1288**)**. This sequence region corresponds to the α-27 helix of the zebrafish Rad54 structure (127), which is modeled to adopt a triangular brace-like structure (43). The deletion of our identified phosphorylation sites on the Ino80 CTD did not lead to detectable increase in INO80ATPase activity, whereas the loss of a 27 amino acid motif (1261-1288) seems to be largely account for the hyper-activated ATPase activity observed with INO80ΔNC complexes, suggesting the inhibitory effect observed earlier with the phosphorylated CTD fragment may only occur when added *in trans*. We will further discuss this inhibitory motif in the Ino80 CTD in the discussion chapter.

Chapter IV. Characterization of the organization and functions of core subunits of the human INO80 chromatin remodeling complex

Abstract

Ino80, a member of the Snf2 family of ATPases, functions as an integral component of the multi-subunit ATP dependent INO80 chromatin remodeling complex. The defining feature of Ino80 family ATPases is the presence of a long insertion domain that splits the conserved Snf2-like ATPase. INO80 complexes from yeast to human share a common core of conserved subunits, including Ies2, Ies6, Arp5, the AAA+ ATPases Tip49a and Tip49b, Arp8, Arp4/Baf53a, and YY1. Previous studies have demonstrated that a human INO80 subcomplex containing all of these conserved subunits and the conserved region of the Ino80 ATPase can reconstitute the full catalytic activities of INO80 *in vitro*.

In this chapter, we seek to define the requirement for assembling core subunits Ies2, Ies6, Arp5, Tip49a and Tip49b, and to distinguish their functional contribution to INO80 chromatin remodeling process. We obtained evidence that the ATPase insertion regions of INO80 family ATPases are necessary and sufficient for assembling all of the five ATPase-associating subunits Ies2, Ies6, Arp5, Tip49a and Tip49b. The loss or inclusion of this insertion module correlates with loss or gain of nucleosome binding capacity of the INO80 subcomplexes, suggesting they contribute to nucleosome binding. Consistent with this hypothesis, the subcomplexes missing the insertion module were not able to bind to nucleosome, thus were deficient in nucleosome-stimulated ATPase, and ATP dependent nucleosome remodeling activities. Within the insertion module, Ies6 and Arp5 form a heterodimer, and are mutually dependent for assembly into INO80. The heterodimer is dispensable for INO80's ATPase activity, but is required for the optimal nucleosome remodeling, presumably via its contribution to nucleosome binding. To the contrary, Ies2 assembles independently of the Arp5-Ies6 heterodimer, and is absolutely required for the catalytic activities of the INO80 complex, while dispensable for its binding affinity to nucleosomes. Our studies shed light on the structure and function of the human INO80 chromatin remodeling complex.

Introduction

ATP-dependent nucleosome remodeling machineries always contain a central Snf2-like ATPase subunit that is responsible for fueling the nucleosome remodeling process, and additional accessory protein subunit(s) that contribute to the specialized activities of diverse remodeling complexes. Based on the domain structure of the core Snf2-like

ATPase, these complexes can be categorized into subfamilies, such as SWI/SNF (switching defective/sucrose non-fermenting) family remodelers, including Snf2 ATPases in yeast, Brg1 ATPases in human; INO80 (Inositol requiring 80) family remodelers, including Swr1 (Swi2-related ATPase 1) ATPases in yeast SWR1 complexes, SRCAP (Snf2-related CREB-binding protein activator protein) ATPases in human SRCAP complexes, and Ino80 ATPases in INO80 complexes.

INO80 subfamily of chromatin remodeling complexes share structural and functional similarities. Functionally speaking, INO80 complex can catalyze ATP-dependent nucleosome sliding *in cis*, whereas SWR1 complex catalyze an ATP-dependent histone dimer exchange reaction, replacing H2A-H2B dimer in nucleosomes with variant H2AZ-H2B. Recent reported evidence indicates INO80 complex can catalyze the "reverse" dimer exchange reaction, putting the H2A-H2B dimer back into a H2AZ containing nucleosome. Consistent with this possibility, both SRCAP and INO80 complexes are essential for the proper genome-wide distribution of H2AZ, and play important roles in transcription, replication and DNA damage repair processes. Structurally speaking, among Snf2-like remodeling ATPases, Ino80 ATPase and SRCAP ATPase include unusually long insertion regions (250 amino acids and 1000 amino acids respectively, see Figure 23) that split the two conserved ATPase domains SNF2-N and SNF2-C. In addition, both multisubunit complexes share similar subunit composition: 1) AAA+ ATPases Tip49a and Tip49b (Rvb1/2 in yeast) as shared subunits in both complexes; 2) actin-related protein (Arp) Arp5 in INO80 complexes, and Arp6 in SRCAP complexes. Both complexes are unique among other Snf2-like remodelers in harboring an Arp

subunit that assembles independently with the HSA (helicase SANT Associated) domain of the Snf2-like ATPases; 3) Zn-HIT (Zinc and histidine triad) domain containing subunits Ies2 of INO80 complexes, and ZnHIT1 of SRCAP complexes (Swc6 in yeast SWR1 complexes); 4) YL1_C domain containing subunit Ies6 of INO80 complexes, and YL1 of SRCAP complexes (Swc2 in yeast SWR1 complexes).

Consistent with the possibility that the Ino80 family insertion region is needed for structural integrity of the complex, deletion of the Swr1 ATPase insertion resulted in loss of subunits from the yeast Swr1.com, including Swc2, Swc3, Swc6, Arp6, and Rvb1/2. We reported previously that the intact Ino80 ATPase domain including the insertion region can assemble an INO80 subcomplex containing conserved subunits Ies2, Ies6, Arp5, and Tip49a/b (INO80ΔNΔHSA complex). Given the aforementioned similarity between INO80 and SRCAP complexes, it is not known yet whether the insertion of the Ino80 ATPase also plays an important role in maintaining structural integrity of the INO80 complexes, nor it is the mechanism known that directs the specific association of these highly related subunits with their corresponding complex.

In the previous report, we present evidence that the human INO80 complex is composed of three modules that assemble with three distinct domains of the Ino80 ATPase. These modules include (i) NTD module is composed of the N terminus of the Ino80 ATPase and all of the metazoan-specific subunits; (ii) HSA module is composed of the HSA domain of the Ino80 ATPase, conserved subunits Arp4/Baf53a and Arp8, and YY1; and (iii) a third ATPase module is composed of the hIno80 Snf2-like ATPase domain, conserved core subunits Ies2, Ies6, Arp5, Tip49a and Tip49b. Through purification and

characterization of hINO80 complex subcomplexes, we demonstrate that ATP-dependent nucleosome remodeling by the INO80 complex is catalyzed by a core complex comprising the hIno80 HSA and Snf2-like ATPase domains acting in concert with the complete set of its evolutionarily conserved subunits. We do not know how Ies2, Ies6, Arp5, Tip49a/b assemble with the snf2-like ATPase domain of human Ino80, nor do we know whether any or all of these subunits of the core complex are required for ATP-dependent nucleosome remodeling by human INO80 complexes.

Arp5 is a member of the conserved actin-related protein family, those of which share similar ATP binding fold with conventional actin, namely the actin fold. Unlike the conventional actin, several Arps reside solely in the nucleus, and are bona fide components of multi-protein nuclear complexes, including Arp5 in INO80.com and Arp6 in SWR1/SRCAP.com. INO80.com purified from Arp5Δ yeast cells exhibited no defect in integrity of the rest of the complex, but failed to induce nucleosome mobilization, nucleosome-stimulated ATP hydrolysis, and binds half as efficient to DNA as the wildtype INO80.com, suggesting Arp5 is important for the chromatin remodeling activities of INO80.com (117). Analysis of the yeast strain with Arp6 deleted has revealed that the chromatin deposition of histone variant H2AZ is dependent on Arp6; the deletion of Arp6 from the SWR1.com results in the co-depletion of Swc2 from the complex, which is an essential subunit required for the basal H2AZ replacement activity, indicating Arp6 is important for the structural integrity and functional activities of the yeast SWR1.com (140).

Tip49a and Tip49b are evolutionarily conserved AAA ATPases that show sequence similarity with bacterial Holliday junction enzymes RuvB1/2. They have ATP binding and hydrolysis motifs, and the integrity of which is required for viability of the organism. In yeast, Tip49a and Tip49b are bona fide components of both INO80.com, and SWR1.com; while, in human cells, they are subunits of the INO80.com, SWR-like SRCAP.com, and the transformation/transcription domain-associated protein (TRRAP) - Tip60 histone acetyltransferase (HAT).com. Arguing Tip49a and Tip49b are required for the assembly and function of the yeast INO80.com, transient depletion of the Tip49a or Tip49b led to a co-depletion of Arp5 from the INO80 complex, the purified INO80.com failed to exhibit chromatin remodeling activity (63, 67). In addition, Tip49a and Tip49b associate with Arp5 in an ATP and Ino80 ATPase -dependent manner. These observations are consistent with the possibility that Tip49a/b play a chaperone-like role by actively recruiting Arp5 subunit, and are required for the assembly and functions of the INO80.com. Consistent with this hypothesis, Tip49a and Tip49b have also been implicated in the assembly of ribonulceolar protein complexes (RNPs), such as snoRNPs and telomerase (63, 89, 134). Tip49a and Tip49b associate directly with components of the RNPs, and are required for the assembly, stability, and enzymatic activities of the RNP complexes.

Ies2 and Ies6 (Ino Eighty subunits 2 and 6) reportedly associate with INO80.com from yeast *Saccharomyces cerevisiae*, *S. pombe*, and human cells. Notably, Ies2 and Ies6 are absent from budding yeast INO80.com under high salt washes (0.5 M KCl), but remain associated with the complex under low salt washes (0.2 M KCl) (85). In the case of

INO80.com in *S. pombe*, both subunits stay stably associating with an INO80.com when purified using buffers containing 0.5 M KCl (60). In the case of human complexes, we have shown that Ies2 and Ies6 both remain stably associated with the human INO80.com when immunoprecipitated from human cells under stringent washing condition (23, 65) (0.45 M NaCl, 0.1% Triton X-100 in Lys450 buffer, see the method chapter). Importantly, the estimated stoichiometry of Ies2 and Ies6 to most of the INO80 subunits is roughly 1:1, except 1:6 for Tip49a or Tip49b; the stoichiometry of Ies2 and Ies6 relative to other INO80 subunits in immunopurified INO80.com is reproducibly observed and not dependent on the tagged subunit from which the INO80.com is immuno-purified. Additionally, we routinely immunoprecipitate enzymatically active human INO80.com from human cell lines stably expressing N-terminal FLAG epitope tagged version of Ies2 and Ies6, suggesting these two subunits do stably associate with a fraction of INO80.com that is enzymatically active. In addition, siRNA knockdown of Ies2 and Ies6 in human cells led to compromised INO80 ChIP signal to at least two gene promoters, and reduced transcriptional activation of these two target genes. It has also been reported in the budding and fission yeast that Ies2 and Ies6 are required for the normal cellular response upon DNA damage and replication stress (22, 60). Moreover, loss of Ies6 leads to polyploidy and chromosome mis-segragation. However, it is not yet known whether Ies2 and Ies6 play any mechanistic role in the chromatin remodeling process.

In the presented study, we seek to define the requirement for assembling core subunits Ies2, Ies6, Arp5, Tip49a and Tip49b, and distinguish their functional contribution to the

ATP-dependent chromatin remodeling activities of the INO80 complex. We obtain evidence to support the possibility that:

1) Ino80 family specific insertion region can dictate assembly of all the subunits that associate with the snf2-like ATPase domain. The integrity of the Ino80 insertion is required for assembly of these core subunits.

2) Ies6 and Arp5 can interact, and are mutually dependent for their association with Ino80; whereas, Ies2 assembles with Ino80 independently of the Ies6-Arp5 heterodimer.

3) The intact Ino80 insertion in concert with Ies2, Ies6, Arp5, and Tip49a/b are together required for the nucleosome binding, remodeling and ATPase activities of the INO80 complexes. Individually speaking, Ies2 is required for the catalytic activities of the INO80 complex, but dispensable for its nucleosome binding capacity; while, Ies6 and Arp5 are required for the optimal nucleosome binding and remodeling activities, but are dispensable for the ATP hydrolysis by the complex.

RESULT

The Ino80 family specific insertion region can dictate assembly of all the subunits that associate with the snf2-like ATPase domain.

In an effort to understand the role played by the insertion region of the Ino80 family remodeling ATPase, we start our investigation by generating INO80 complexes that lack the Ino80 insertion.

Crystal studies demonstrate the core of the Snf2-like remodeler enzyme consists of two flexible RecA-like protein folds that encompass a central ATP binding/hydrolysis pocket. ATP binding status regulates the relative position of the two RecA lobes, which have to adopt a close conformation for the catalysis to occur (42).

Thus, instead of blunt deletion of the whole Ino80 insertion (257 a.a.) from the Ino80 ATPase domain, we exchange it for the analogous region (24 a.a.) of the human Brg1 ATPase. The resulting chimeric protein (Ino80ΔN BRGIns) essentially carries an N-terminal Ino80 HSA domain, and a hybrid ATPase domain similar to the one in the Brg1 ATPase, but missing the Brg1-specific C-terminal Bromo domain.

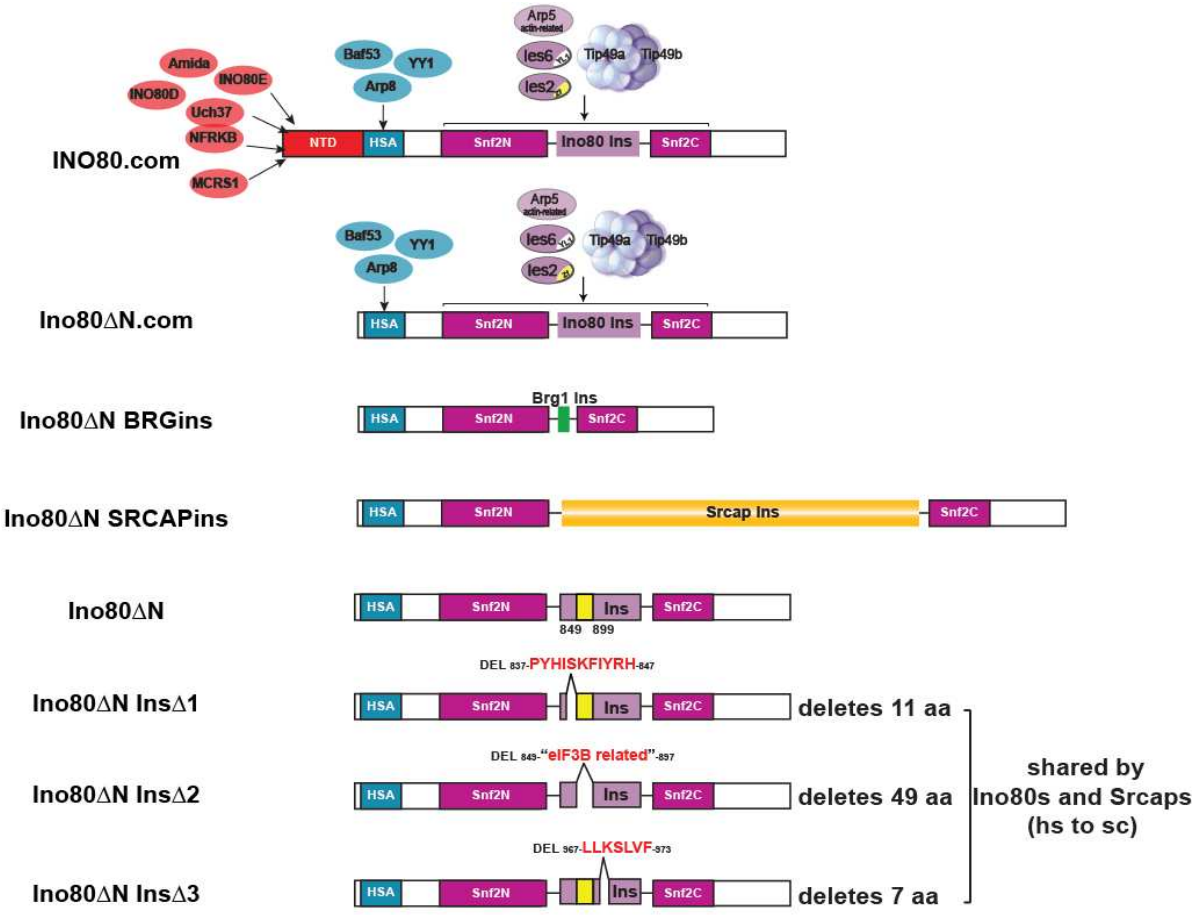

Figure 23. Schematic representation of the Ino80ΔN ATPase derivatives carrying insertion mutations

(upper) INO80.com and Ino80ΔN.com illustrates the modular organization (red, metazoan NTD module; blue, HSA module; pink, ATPase module) and subunit composition of INO80 complexes, and INO80ΔN subcomplexes. YL1 (YL1_C like domain), the name of the domain shared by Ies6 and YL1. Zn-HIT (Zinc and histidine triad), the name of the domain shared by Ies2 and ZnHIT1. The double hexameric ring-like structure is depicted for Tip49a and Tip49b, and their 6:1 stoichiometry to the rest of INO80 subunits. (lower) Ino80ΔN ATPase derivatives used to generate INO80ΔN subcomplexes carrying mutations in the ATPase insertion region, including Insertion-swapping constructs, Ino80ΔN BRGins and Ino80ΔN SRCAPins; and insertion deletion constructs, Ino80ΔN InsΔ1/2/3. The yellow box denotes for the "eIF3B-related" sequence. The basis of design will be explained in Figure 25.

We engineered the insertion swapping in an Ino80 mutant that lacks the N terminal domain (FLAG-Ino80ΔN), since the Ino80 NTD module is dispensable for the assembly and the activities of the complex, and we can readily obtain active, stoichiometric INO80

core complexes through immunoprecipitation of Ino80ΔN proteins. We stably expressed an N terminal FLAG epitope tagged version of Ino80ΔN BRGins in HEK293 cells, and performed anti-FLAG agarose immunoaffinity chromatography from the nuclear extracts. The proteins present in the FLAG eluates were identified by mass spectrometry (data now shown), and analyzed by SDS PAGE and western blotting. (Figure 24) When stably expressed in 293 cells, Ino80ΔN BRGins ATPases (wildtype or ATPase inactive version) assemble subcomplexes containing only YY1, Baf53a, and Arp8 proteins. (Lane 7 and 8, Figure 24)

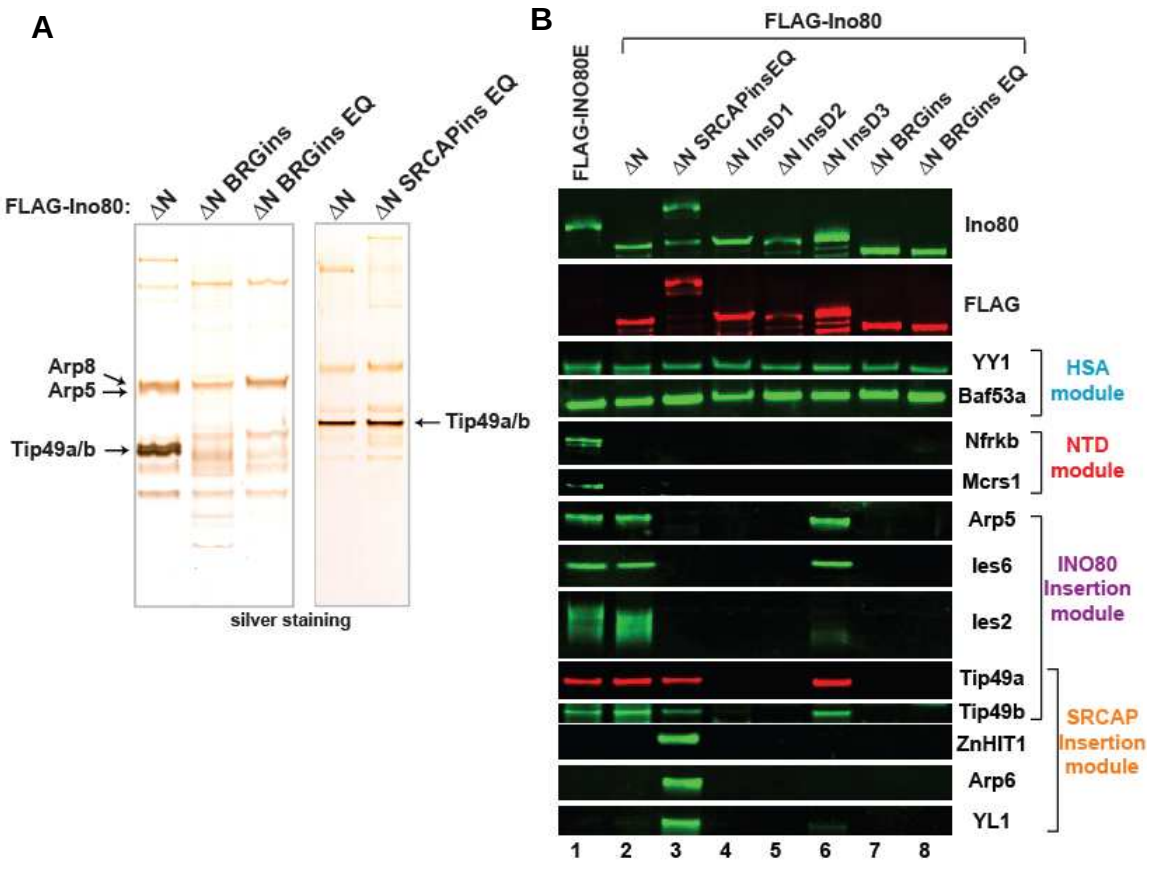

Figure 24. Subunit composition of INO80 complexes and INO80ΔN subcomplexes carrying insertion mutations

(A) silver staining analysis of purified INO80ΔN and insertion swapping mutant complexes. The recognizable bands were annotated based on previous results and predicted molecular weight of INO80 subunits. (B) western blotting analysis of purified INO80ΔN and insertion mutant complexes; each stripe was probed by a subunit-specific antibody, which was grouped based on modularity of INO80 complexes. Tip49a and Tip49b are shared components between INO80 and SRCAP complexes.

This observation is consistent with the possibility that Ies2, Ies6, Arp5, and Tip49a/b associate with the Ino80 ATPase in a way that is dependent on the insertion region, which agrees with the reported role of Swr1 insertion in maintaining the integrity of the yeast SWR1 complex.

To test whether Ino80 family insertions are sufficient to direct assembly of ATPase domain binding subunits, we exchanged the insertion region of Ino80ΔN with the longer insertion (1162 a.a.) within the hSrcap ATPase domain. Analysis of the composition of the proteins copurified with this Ino80ΔN SRCAPins identified INO80 HSA module subunits Baf53a, YY1, and Arp8; SRCAP ATPase-binding subunits ZnHIT1, Arp6, YL1, Tip49a/b. No detectable amount of Ies2, Ies6, and Arp5 is present in the Ino80ΔN SRCAPins complexes, though the conserved Snf2-N and Snf-C domains of Ino80 are intact. Our result argues the possibility that the insertion regions of Ino80 family ATPases carry specificity that determines assembly of ATPase domain-binding subunits.

In addition, the amount of YY1 and Baf53a that associate with the Ino80ΔN BRGins and Ino80ΔN SRCAPins is comparable with those presented in the wildtype INO80 complexes, suggesting the absence of Ies2, Ies6, Tip49a/b, actin-like protein Arp5 does not affect the optimal assembly of the HSA module of INO80 complexes.

Structural integrity of the Ino80 insertion is required for assembly of ATPase-binding subunits Ies2, Ies6, Arp5, and Tip49a/b.

We have narrowed down the binding requirement of Ies2, Ies6, Arp5, and Tip49a/b to the Ino80 insertion region. To further characterize the binding requirement of these subunits, we sought to identify key region/motif within the Ino80 insertion that may be involved in assembly of a single or a set of subunits.

Blast search of the whole human Ino80 insertion identifies eIF3B protein, which share sequence similarity with a region (849-897) within the Ino80 insertion, namely eIF3B related sequence (Figure 25A). eIF3B is a core component of the evolutionarily conserved translation initiation complex eIF3. Orthologs of Tip49a/b have been found to associate with the eIF3B containing complex in fission yeast (115). Though the molecular detail of the Tip49a/b and eIF3B interaction is not known, it is tempting to hypothesize that the shared eIF3B-related sequence may be responsible for the association of AAA+ ATPase Tip49a/b, the shared feature between INO80 and eIF3 complexes. Therefore, we generated a deletion mutant (Ino80ΔN InsΔ2) that lacks the eIF3B related sequence.

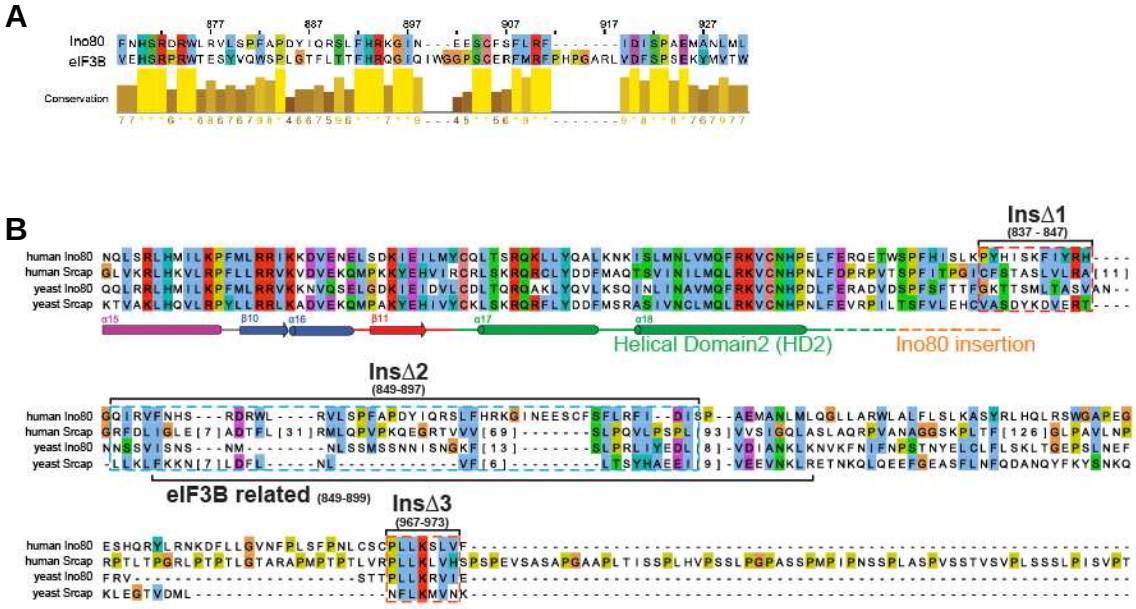

Figure 25. Basis of design for Ino80ΔN insertion deletion mutants

(A) A motif in the Ino80 ATPase insertion (849-899) shares sequence similarity with an eIF3B protein. The yellow bar chart represents the score of similarity. (B) A sequence alignment contains Ino80 and Srcap ATPases from both human and budding yeast. Structural motifs were annotated according to the homology with the zebrafish Rad54. The highlighted sequences, InsΔ1 (837-847), InsΔ2 (849-897), and InsΔ3 (967-973), show sequence similarity and were deleted in INO80ΔN InsΔ1, InsΔ2, and InsΔ3 subcomplexes, respectively.

Since the SRCAP and INO80 complexes are both evolutionarily conserved from yeast to human, and both share similar subunit composition, we hypothesize that any conserved Ino80 sequence that is similar with Srcap and Swr1 may have a higher chance to be structurally and/or functionally significant. Multiple sequence alignment of yIno80, hIno80, ySwr1, and hSrcap have identified two homology blocks within the insertion regions, with a 11 amino acid box (InsΔ1, 837-847) immediately upstream of the eIF3B-related sequence, and a 7 amino acid box (InsΔ3, 967-973) downstream. We deleted these sequence motifs (InsΔD1/2/3) within the FLAG-Ino80ΔN construct, and generated

subcomplexes purified through these mutants, namely INO80ΔN InsΔ1/2/3 subcomplexes. We analyzed the subunit composition of the three complexes by MudPIT mass spectrometry, sliver staining, and western blotting analysis. Arguing that the eIF3B-related sequence is required for the association of Tip49a/b with Ino80, Tip49a and Tip49b are indeed missing in both INO80ΔN InsΔ1 and InsΔ2 complexes. Additionally, we failed to detect Ies2, Ies6, and Arp5, whereas the HSA module binding subunits are present in a comparable level to the wild-type complex (lane 4, 5, Figure 24B), indicating the association of Ies2, Ies6, and Arp5 is dependent on the presence of the eIF3B-related sequence and/or Tip49a/b.

This observation is consistent with the previous report that a transient depletion of Rvb1/2 (orthologs of Tip49a/b) resulted in loss of Arp5 from yeast INO80 complexes (67). Notably, no additional subunit was reportedly missing from this study. This can be explained by the possibility that Ies2 and Ies6 were not associating with the yeast INO80 complexes as discussed in the introduction, or an additional change could happen in a way that was not reflected in the silver staining method used in the study.

On the contrary, arguing against the possibility that loss of Ies2, Ies6, Arp5, and Tip49a/b is due to the non-specific effect caused by deletion mutation in the Ino80 insertion, the subcomplexes containing Ino80ΔN InsΔ3 still assemble a comparable amount of Ies6, Arp5, and Tip49a/b with the wildtype INO80. Surprisingly, the amount of Ies2 that associates with the complex is reduced to ~ 15% of the wild type INO80 (Lane 6, Figure24B), suggesting the optimal association of Ies2 with the Ino80 insertion is dependent on the presence of both the eIF3B-related and InsΔ3 sequences. While the

assembly of Ies6, Arp5, and Tip49a/b does not require the InsΔ3 sequence, the differential requirement of Ies2 may suggest that Ies2 assembles with INO80 complexes in a manner that differs from Ies6, Arp5, and Tip49a/b.

Ies6 and Arp5 can interact, and are mutually dependent for their association with Ino80; whereas, Ies2 assembles with Ino80 independently of the Ies6-Arp5 heterodimer.

To define the role played by Ies2, Ies6, and Arp5 in maintaining the structural integrity of the INO80 complex, we knock-down individual subunits from HEK293 cells stably expressing FLAG tagged Ino80ΔN, and examined the subunit composition of affinity-purified INO80ΔN complexes from nuclear extracts made from these cells. As revealed by western blotting (Figure 26), Ino80ΔN complexes from cells treated with Ies2 siRNA were depleted for Ies2, as expected, and retained the normal association of Ies6, Arp5, and Tip49a/b, and YY1, suggesting Ies2 is not obligatory for the overall integrity of the INO80 complex. Neither depletion of Ies6 or Arp5 resulted in the loss of Ies2, indicating Ies2 assembles with Ino80 independent of Ies6 and Arp5. Notably, depletion of either Ies6 or Arp5 in a single knockdown resulted in the reciprocal loss of the other subunit from the INO80 complex, suggesting Ies6 and Arp5 are mutually dependent on each other to assemble into the INO80 complex. No detectable change has been observed for the association of Tip49a and Tip49b upon the knockdown of Ies2, Ies6, or Arp5, suggesting Tip49a and Tip49b may assemble with Ino80 or Srcap insertion independent of other ATPase-bound subunits.

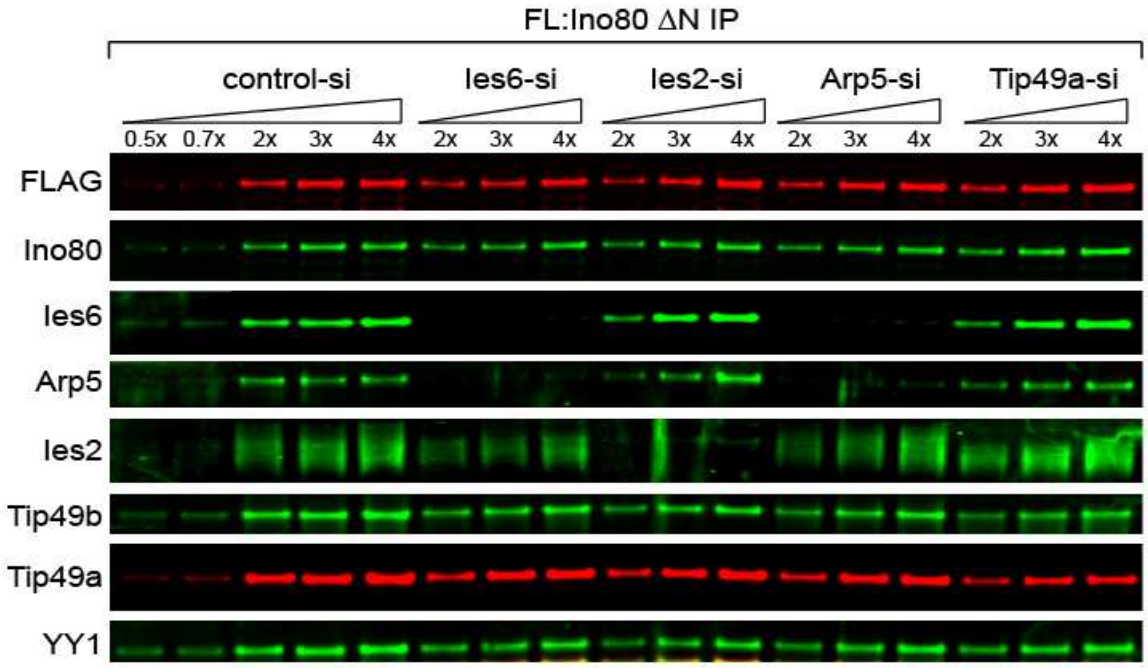

Figure 26. Subunit composition INO80ΔN subcomplexs with depleted INO80 core subunits targeted by siRNAs

INO80ΔN subcomplexes were purified from nuclear extracts of 293 FRT cells transfected with siRNA targeting Ino80 insertion-binding subunits. Each siRNA targeted subcomplex was titrated, and subjected to SDS-PAGE, and western blotting using INO80 subunit-specific antibodies to evaluate the effect of siRNA treatment.

It has been proposed that AAA ATPases Rvb1/2 (Tip49a/b) recruits Arp5 subunit into yeast INO80 complexes in a way depends on ATP and Ino80 (67). It is tempting to hypothesize that Tip49a/b recruits Arp5 into the complex via direct interaction. In an effort to identify the subunit(s) that may directly interact with human Arp5 protein, we carried out systematic pairwise screen using a baculovirus over-expression system. The baculovirus containing HA epitope tagged human Arp5 cDNA and one of the viruses encoding FLAG epitope tagged INO80 subunits, including Ino80, Arp8, Arp5, YY1, Tip49a, Tip49b, Tip49a and Tip49b, Baf53a, β-actin, Ies6, and Ies2, were coexpressed in pairwise fashion in sf9 cells. The whole cell extracts of these infected cells were

subjected to reciprocal immunoprecipitation either with anti-FLAG or HA antibody conjugated agarose under stringent washing condition (Lys450, see the method chapter), precipitated proteins were then eluted by SDS, and analyzed by SDS PAGE and western blotting (Figure 27).

Notably, neither Tip49a, or Tip49b, or coexpressed Tip49a and Tip49b were able to co-purify with Arp5 under condition that allows ample association of Ies6 and Arp5. We also tried to repeat the same experiment with the supplement of ATP, arguing that the recruitment of Arp5 into INO80 may not be simply explained by direct interactions between Arp5 and Tip49a and Tip49b. Among all the INO80 subunits (except Ino80, which expressed at much lower level), Ies6 is the only subunit that copurified with significant amount of Arp5, and in a reciprocal fashion. We did observe small, but detectable amount of Arp5 associated with other actin-related proteins, including Arp8, Arp5, and Baf53a (data not shown).

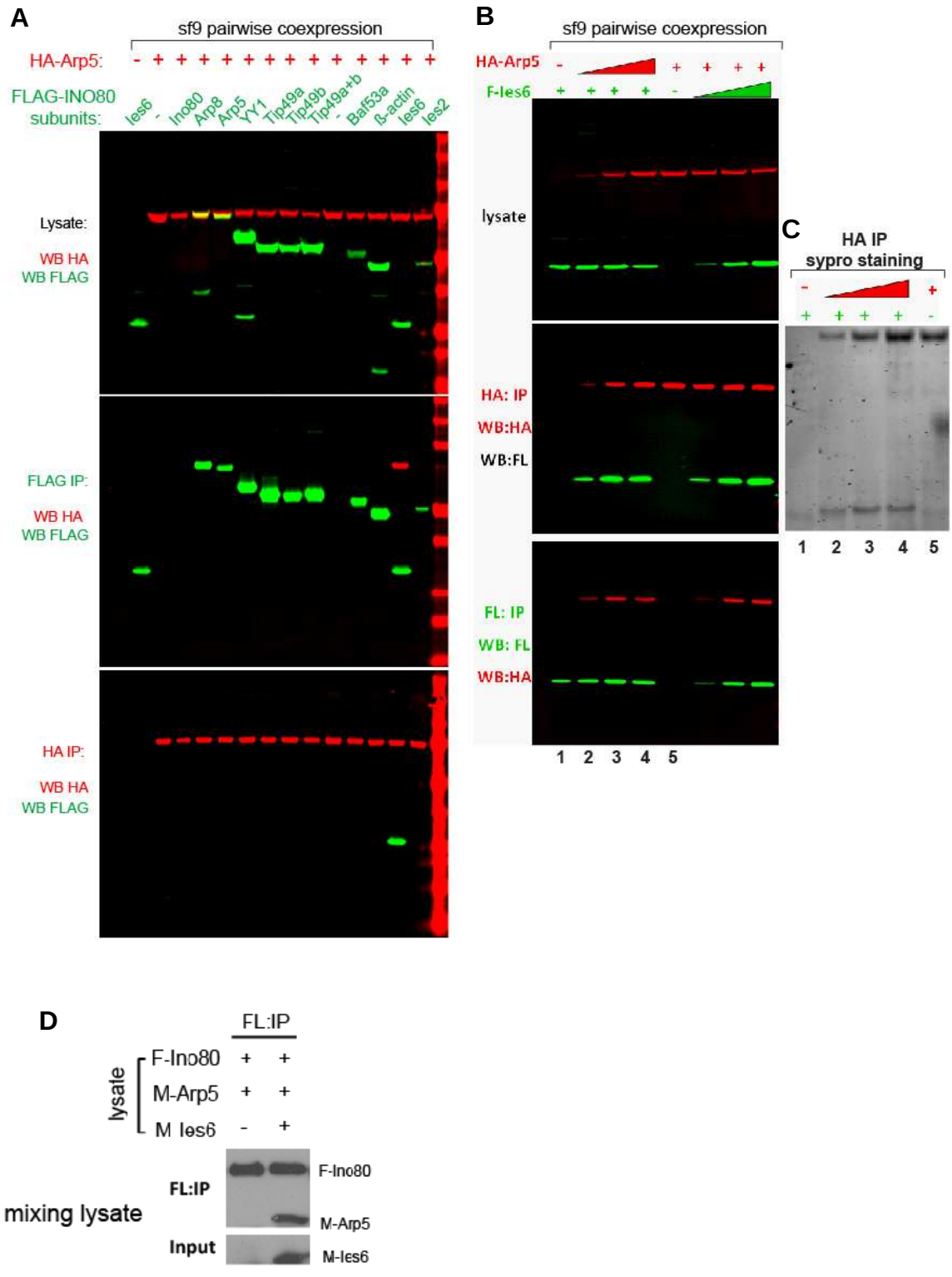

Figure 27. Ies6, but not Tip49a and/or Tip49b, interacts with Arp5 in a heterologous insect cell expression system

(A) Arp5 interacts with Ies6. Pairwise interaction screen between HA tagged Arp5 (red colored), and FLAG tagged (green colored) INO80 subunits by co-infecting insect sf9 cells with indicated combinations of baculoviruses encoding a single INO80 subunit. The co-infected cells were harvested for making whole cell extracts (top panel, A), from which anti-FLAG and anti-HA affinity purifications were performed. Input lysates, FLAG (middle panel, A) and HA bait (lower panel, A) immunoprecipitated proteins were subjected to SDS PAGE, and visualized by anti-FLAG and anti-HA antibodies. (B) Confirming the Arp5-Ies6 dimeric interaction; pairwise coexpression of varying amount of HA-Arp5 and FLAG-Ies6 to confirm the Arp5 and Ies6 interaction using the same reciprocal immunoprecipitation methods. (C) The HA peptide eluates from sample 1-5 in B were subjected to SDS page and Sypro Staining. (D) Ies6 is required for the association of Arp5 with the Ino80 ATPase. Whole cell extracts made from insect cells infected with FLAG tagged human Ino80, Myc tagged human Arp5 and Ies6 were mixed and incubated *in vitro*, and followed by anti-FLAG immunoprecipitation to test the association between Arp5 and Ino80.

We further confirmed the interactions between Arp5 and Ies6, and demonstrated they form a heterodimer shown in a SDS PAGE gel stained by SYPRO ruby protein stain (Figure 27D). Consistent with the mutual dependency of Arp5 and Ies6 for the assembly into INO80, we observed that abundant Arp5 can be immunoprecipitated by Ino80 only when Ies6 was also coexpressed. The association between Ino80 and Arp5 had also been recapitulated by supplementing a lysate expressing Ies6 or purified recombinant Ies6 proteins into lysates containing Arp5 and Ino80 (Figure 27D and data not shown). Hence, using a heterologous expression system, we demonstrated that Arp5 interacts with Ies6 among other INO80 subunits, which is also required for the association of Arp5 with Ino80. Thus, we provided complementary evidence to support the model that the assembly of Arp5 and Ies6 into INO80 complexes is interdependent, and presumably as a heterodimeric module; whereas Ies2 assembles with INO80 complexes independently.

The intact Ino80 insertion in concert with Ies2, Ies6, Arp5, and Tip49a/b are collectively required for the nucleosome binding, remodeling and ATPase activities of the INO80 complexes.

Thus far, we have generated a series of human INO80 subcomplexes with defined subunit composition, including Ino80ΔN BRGins, InsΔ1, InsΔ2 complexes that lack Ino80 ATPase-associating subunits Ies2, Ies6, Arp5, and Tip49a/b; Ino80ΔN SRCAPins complexes that contain Srcap ATPase-associating subunits ZnHIT1, Yl1, Arp6, and Tip49a/b; Ino80ΔN InsΔ3 and Ino80ΔN:: si-Ies2 complexes that contain depleted Ies2; Ino80ΔN:: si-Ies6 and si-Arp5 complexes depleted of the Ies6 and Arp5 heterodimer. These subcomplexes enabled us to further explore the functional contribution of the subunits that bound to the insertion region and the insertion region itself to the ATP-dependent nucleosome remodeling process by INO80.

When subjected to mononucleosome sliding assay, in which Ino80ΔN complexes can reposition a lateral “601” mononucleosome (83) to a more central position (23, 130), INO80ΔN BRGins complexes failed to exhibit robust sliding activity, suggesting the ATP-dependent nucleosome remodeling activity is dependent on the Ino80 insertion and/or insertion binding subunits. (Figure 28)

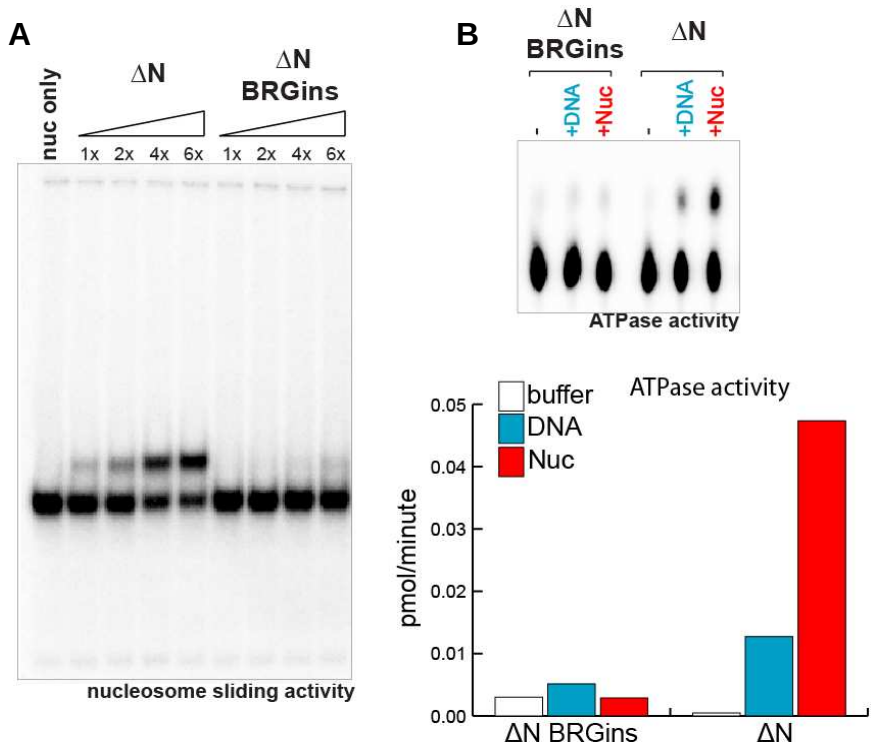

Figure 28. INO80ΔN BRGins subcomplexes exhibited compromised nucleosome remodeling activities

(A) INO80ΔN BRGins complexes failed to slide nucleosome efficiently compared with INO80ΔN complexes. Same concentration of complexes were titrated and compared. (Upper, B) INO80ΔN BRGins complexes exhibited defective ATPase activity. DNA and nucleosome-dependent ATPase assays were performed to measure the rate of ATP hydrolysis in INO80ΔN BRGins, and INO80ΔN complexes. (Lower, B) the rate of ATP hydrolysis was calculated based on the data obtained in the ATPase assay.

Consistent with the possibility that Ino80 insertion binding subunits are important for INO80 remodeling activity, two mutant INO80 complexes carrying mutated insertions that have eIF3B-related sequence deleted (INO80ΔN InsΔ1/2) also failed to show sliding activity (Figure 34). Granted both mutant complexes only have a small portion (11 and 49 out of 257 amino acid) of the Ino80 ATPase insertion deleted (Figure 23 and 25), we can not rule out the possibility that the structural integrity of the insertion/snf2-like

ATPase domain is required for the proper assembly and functions of the intact INO80 complex.

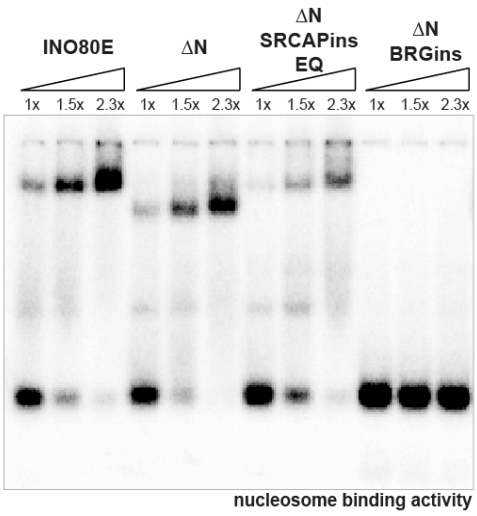

Figure 29. Nucleosome binding ability of INO80 depends on the Ino80 family insertions and associating subunits

Nucleosome binding assays were performed in the presence of varying amounts of the indicated FLAG-immunopurified INO80 complex. Binding of INO80 or INO80 subcomplexes to mononucleosomes results in the emergence of slow-migrating "super-shifted" bands corresponding to mononucleosomes stably bound by INO80 or INO80 subcomplexes.

To explore mechanistic explanations for the incapability of INO80ΔN BRGins and InsΔ1/2 complexes to remodel nucleosomes, we assayed these subcomplexes for their nucleosome-stimulated ATPase and nucleosome binding activities using a Thin Layer Chromatography (TLC) -based ATPase assay (Figure 28B and Figure 30). The activity of Ino80 ATPases accounts for the majority of the DNA and nucleosome stimulated ATP hydrolysis by the INO80 complex, and is essential for the nucleosome remodeling activity of the whole INO80 complex. We did not detect ATPase activity from these three subcomplexes lacking those insertion binding subunits, with or without the presence of

nucleosomes (Figure 30). Our result argues that some or all of those subunits are likely to be required for activating the ATPase activity of Ino80 ATPases, and INO80 complexes; and thereby are required for catalyze ATP-dependent nucleosome remodeling activity by INO80 complexes.

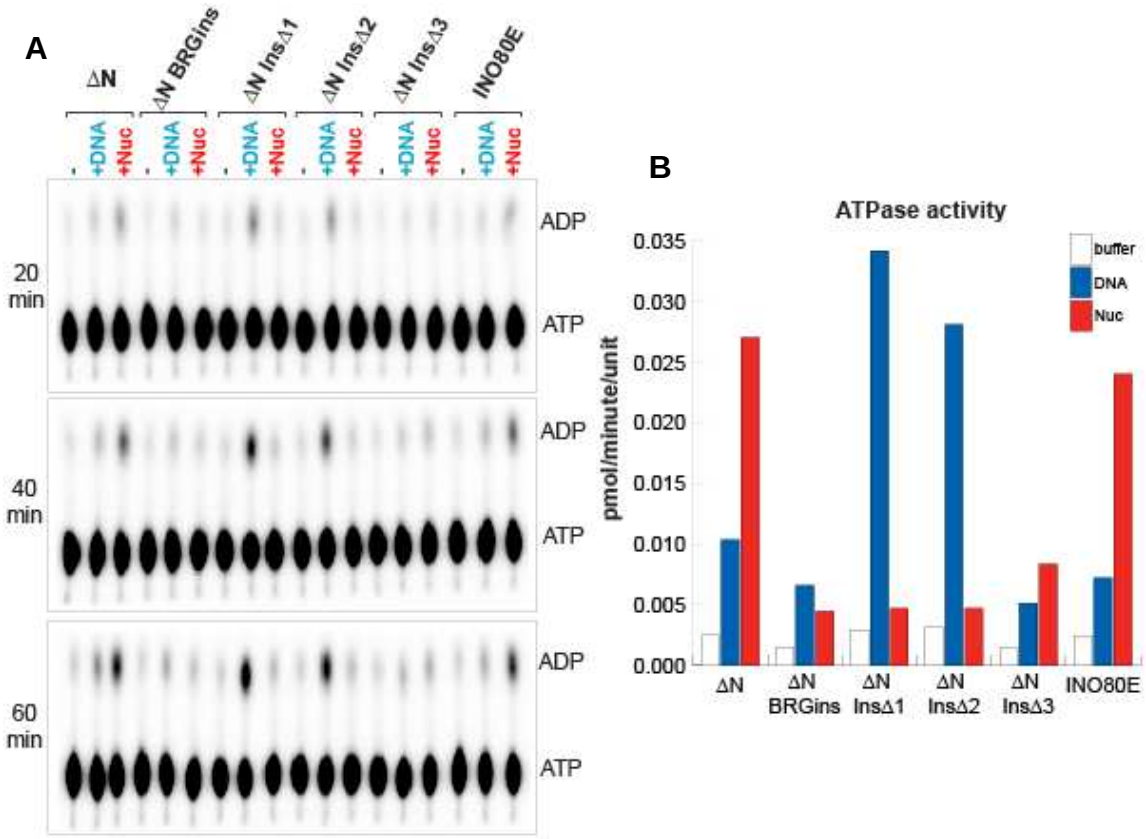

Figure 30. The Ino80 ATPase insertion and its associating subunits are required for optimal nucleosome stimulated ATPase activity of INO80 complexes

DNA- and nucleosome- stimulated ATPase assays were performed in the presence of similar amounts of the indicated FLAG-immunopurified INO80 complex. (A) Three different time points (20/40/60 min) of the ATPase assay were examined, with the corresponding p^{32} radiographs shown. (B) The rate of ATP hydrolysis was calculated from the data collected, and graphed as a bar graph. Noticeably, unexpected high DNA-, but not mock- or nucleosomes-, stimulated ATPase activity were observed in INO80ΔN InsΔ1/2 complexes. We are in the process to test whether this hyper-activated ATPase activity is Ino80 dependent, or is due to co-purified ATPase specifically associating with FLAG Ino80ΔN InsΔ1 and Δ2.

In addition, we inferred the nucleosome binding ability of aforementioned INO80 subcomplexes by monitoring the formation of stable INO80-nucelosome intermediates in electrophoretic mobility shift assays (EMSA) (79, 130). Binding of wild type INO80 or INO80 subcomplexes to nucleosomal substrate resulted in the emergence of slow-migrating "super-shifted" bands, which correspond to mononucleosomes stably bound by INO80 or INO80 subcomplexes. Noticeably, the relative mobility of the super-shifted bands is determined by the size of the complexes tested. Moreover, the super-shifted bands by all the INO80 complexes are relatively mono-dispersed, suggesting that these immunopurified complexes are relatively uniform in their stoichiometry (Figure 9B).

We observed, first of all, the subcomplex INO80ΔN that lacks NTD metazoan-specific INO80 module can supershift mononucleosomes to a degree that is comparable with the complete INO80 complexes immunopurified through FLAG tagged INO80E, suggesting the NTD module is dispensable for the nucleosome binding property of INO80 complexes (Figure 29).

The non-involvement of the NTD module in nucleosome binding ability of INO80 may provide a mechanistic explanation for the published data that the whole NTD module of INO80 is dispensable for the nucleosome remodeling and ATPase activities of the human INO80; while the remaining conserved region of Ino80, including HSA domain and Ino80 snf2-like ATPase domain, assemble a subcomplex that is sufficient to support the optimal nucleosome binding ability of INO80, thus the full potential to remodel nucleosomes. However, we can not rule out the possibility that the NTD module may be

involved in specific recognition of a particular DNA sequence, histone modification, or chromatin structure that were not reflected in our assays.

In addition, the subcomplexes INO80ΔN BRGins and InsΔ1/2 were not able to exhibit significant nucleosome binding activity, as shown in Figure 31 and data not shown. Since these subcomplexes lack ATPase-binding subunits Ies2, Ies6, Arp5, and Tip49a/b, but retain the normal assembly of the HSA module subunits YY1, Arp8, and Baf53a, our observation is consistent with the possibility that some or all of the insertion binding subunits are required for the optimal nucleosome binding of INO80, which can not be sufficiently recapitulated by an INO80 subcomplex only containing HSA module subunits YY1, Arp8, and Baf53a.

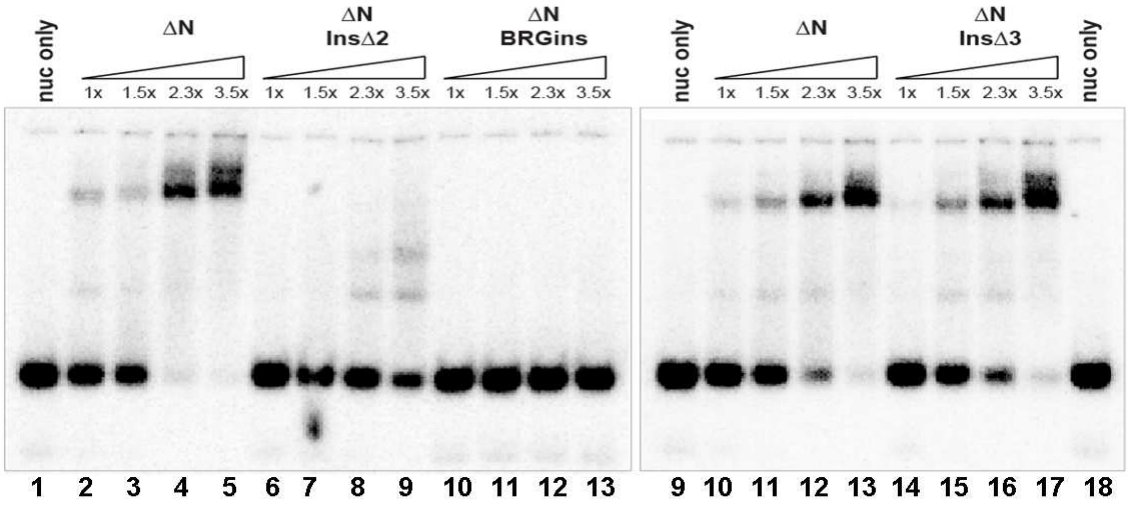

Figure 31. Ino80 ATPase insertion-binding subunits, except Ies2, are important for INO80 nucleosome binding

Nucleosome binding assays were performed in the presence of varying amounts of the indicated FLAG-immunopurified INO80 complex. Binding of INO80 or INO80 subcomplexes to mononucleosomes results in the emergence of slow-migrating "super-shifted" bands corresponding to mononucleosomes stably bound by INO80 subcomplexes. Note that INO80ΔN InsΔ2 and BRGins complexes lacking Arp5, Ies6, Ies2, Tip49a and Tip49b did not bind efficiently to nucleosomes (lanes 5-13); whereas INO80ΔN InsΔ3 complex only lacking the Ies2 subunit was able to bind nucleosomes normally(lanes 14-17).

Surprisingly, once the Srcap insertion and its associating subunits were introduced into the INO80ΔN BRGins complex, the nucleosome binding activity was evidently restored at least to a certain degree in the resulting INO80ΔN SRCAPins EQ complexes (Figure 29). (We were not able to generate INO80ΔN SRCAPins complexes with wild type ATPase binding pocket, whose expression level is below detection). Given that the "grafted" subunits ZnHIT1, YL1, Arp6, and Tip49a/b are closely related to those counterparts in the INO80 complex, we hypothesize that Ino80 family insertions assemble a module of subunits, including AAA ATPases, actin-related proteins, and Yl1-like proteins, that is essential to support INO80 binding to nucleosomes. The reduced binding affinity of INO80ΔN SRCAPins EQ compared to INO80ΔN may reflect the difference in binding affinity between INO80 and SRCAP complexes to the nucleosomal substrates used in the assay.

In summary, we observed that several INO80 subcomplexes that lack all the insertion binding subunits Ies2, Ies6, Arp5, and Tip49a/b exhibit defective nucleosome binding, and nucleosome-dependent ATPase activities, thus showing compromised nucleosome remodeling activity. Our result suggests some or all of Ies2, Ies6, Arp5 and Tip49a/b are required for INO80 activity by involving in either binding to nucleosomes, or catalyzing ATP hydrolysis.

The contribution of Ies2, Ies6, and Arp5 to the nucleosome remodeling process of INO80

To further dissect the individual contribution of Ies2, Ies6 and Arp5 to the nucleosome remodeling activities of INO80, we analyzed the DNA- and nucleosome- dependent ATPase activities of INO80ΔN:: Ies2-si, Ies6-si, and Arp5-si with INO80ΔN:: control-si subcomplexes (Figure 32). To our surprise, INO80ΔN::Ies6-si and Arp5-si subcomplexes depleted of the Ies6 and Arp5 heterodimer can catalyze DNA- and nucleosome-dependent ATP hydrolysis in a rate comparable with the INO80ΔN::control-si, suggesting the Ies6 and Arp5 are not absolutely required for ATP hydrolysis by INO80 complexes. In the contrary, INO80ΔN::Ies2-si subcomplexes exhibit a much slower rate of ATP hydrolysis to a degree similar to the catalytic mutant version INO80ΔN EQ, suggesting Ies2 is required for the robust DNA- and nucleosome- dependent ATPase activity of INO80. Additionally, the INO80ΔN InsΔ3 subcomplex assembles with less Ies2, but associates with normal level of Ies6, Arp5, and Tip49a/b, likewise failed to catalyze robust DNA- and nucleosome- stimulated ATP hydrolysis, agreeing with the possibility that the compromised ATPase activity of INO80ΔN InsΔ3 complexes may be caused by reduced assembly of Ies2 into the complexes (Figure 30).

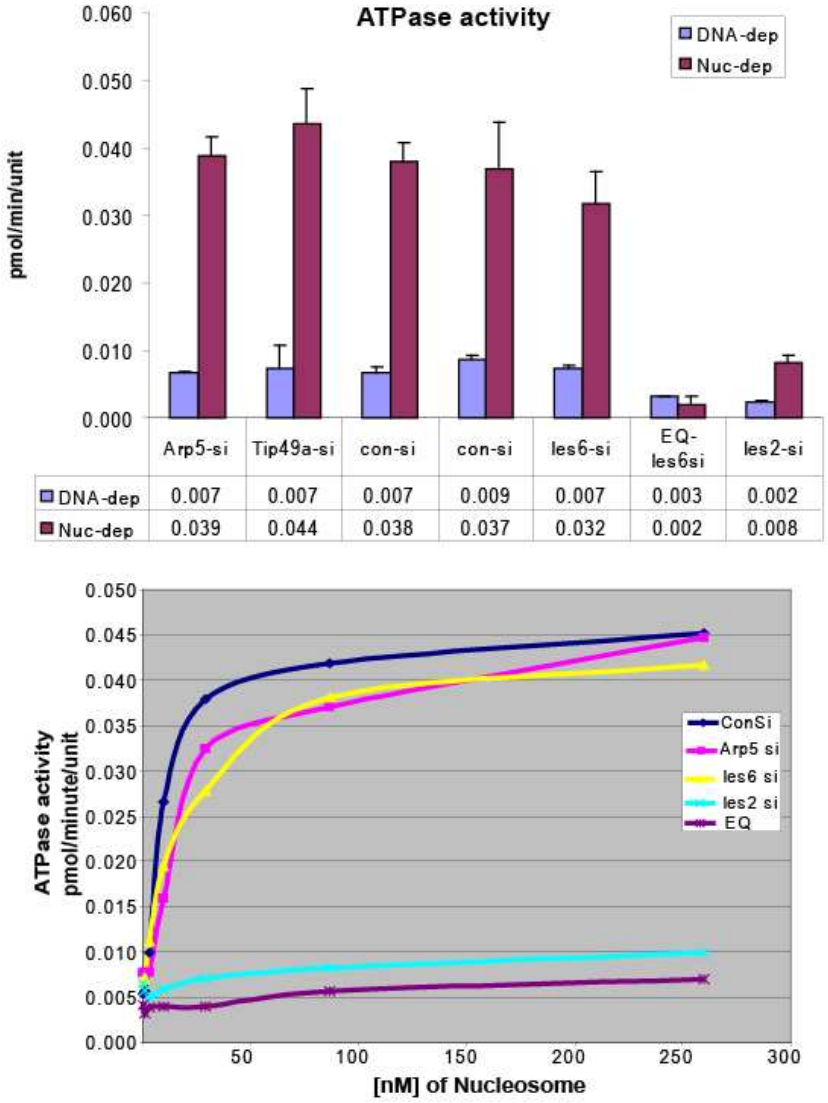

Figure 32. Ies2, but not Ies6 and Arp5, is absolutely required for the ATPase activity of INO80

Either Ies2, or Ies6 and Arp5 were depleted from INO80ΔN complexes by siRNA knockdowns. The immunoprecipitated complexes were subjected to DNA- and nucleosome-stimulated ATPase assays (saturating condition) to address the contribution of the depleted subunit(s) to the catalytic activity of INO80. The activity measured from the mock treated complexes served as a positive control, and INO80ΔN-EQ::si-Ies6 complexes served as a negative control (Upper). We also compared the nucleosome-stimulated ATPase activities of different complexes by titrating nucleosome cofactors over a wide concentration range (lower).

Consistent with the important role played by Ies2 during catalysis of INO80, we observe greatly compromised nucleosome remodeling efficiency when both INO80ΔN::Ies2-si

and INO80ΔN InsΔ3 were measured in nucleosome sliding assays (Figure 33A and Figure 34A). When recombinant Ies2 proteins were supplemented into these two defective nucleosome sliding reactions, both INO80ΔN::Ies2-si and InsΔ3 exhibited elevated remodeling activity (Figure 33B and Figure 34B), but not when a control protein similarly prepared was added in both assays. The recombinant Ies2 proteins used in these assays are free of any detectable nucleosome sliding capability, and were obtained via either Nickel purification of a poly-histidine (6xHIS) tagged Ies2 from E. coli cells, or anti-Myc agarose chromatography of a Myc tagged Ies2 from an extract made form baculovirus infected insect cells.

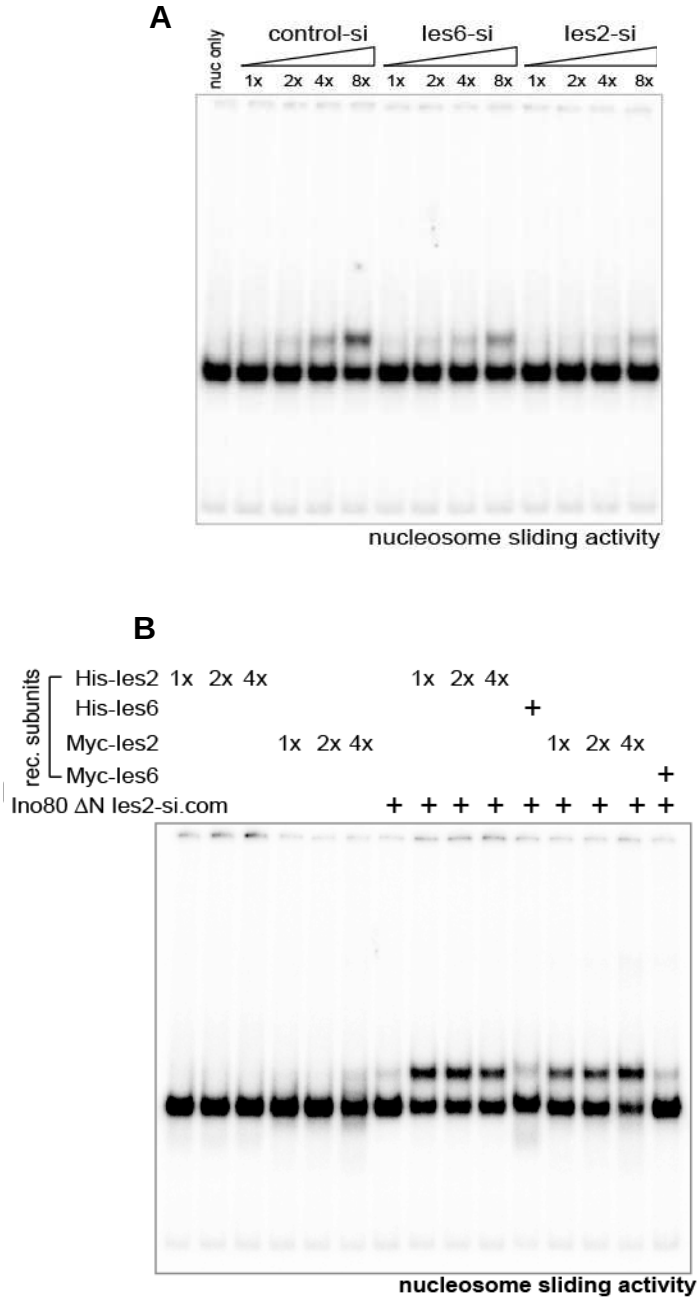

Figure 33. Ies2, Ies6 and Arp5 are required for the optimal INO80 chromatin remodeling activity

(A) Either Ies2, or Ies6 and Arp5 were depleted from INO80ΔN complexes by siRNA knockdowns. The varying amount of each immunoprecipitated complexes were subjected to nucleosome sliding assay. (B) Recombinant Ies2 proteins were added back to the reactions containing INO80ΔN::Ies2-si complexes to test whether the sliding activity can be restored. His-Ies2 and Ies6 were purified from E. coli cell extracts; Myc-Ies2 and Ies6 were purified from insect cell extracts infected by baculoviruses. Ies6 proteins were used as a control.

Our Ies2 “adding back” experiments confirmed that the reduction in remodeling activity of these two subcomplexes was truly due to loss of Ies2. The observation is consistent with the possibility that free Ies2 was able to assemble with the “Ies2-less” INO80 subcomplexes *in trans*, and facilitate their nucleosome sliding ability by stimulating ATP catalysis of INO80.

In addition, the amount of Myc tagged Ies2 that was able to stimulate the sliding activity of INO80ΔN InsΔ3 subcomplexes failed to exert any effect when added with InsΔ2 subcomplexes, which are defective in catalysis, and lack Ies6, Arp5, and Tip49a/b, besides Ies2. This observation is consistent with the possibility that Ies2 alone is not sufficient to stimulate nucleosome remodeling of INO80, other potential contributions from Ies6, Arp5, and Tip49a/b might be needed. In addition, the observation that INO80ΔN InsΔ3 subcomplexes can still be activated (Figure 34B), and carry out nucleosome remodeling activity argues against the possibility that the small deletion in the Ino80 insertion regions of INO80ΔN InsΔ3 subcomplexes may cause an overall folding defect in the Ino80 ATPase domain.

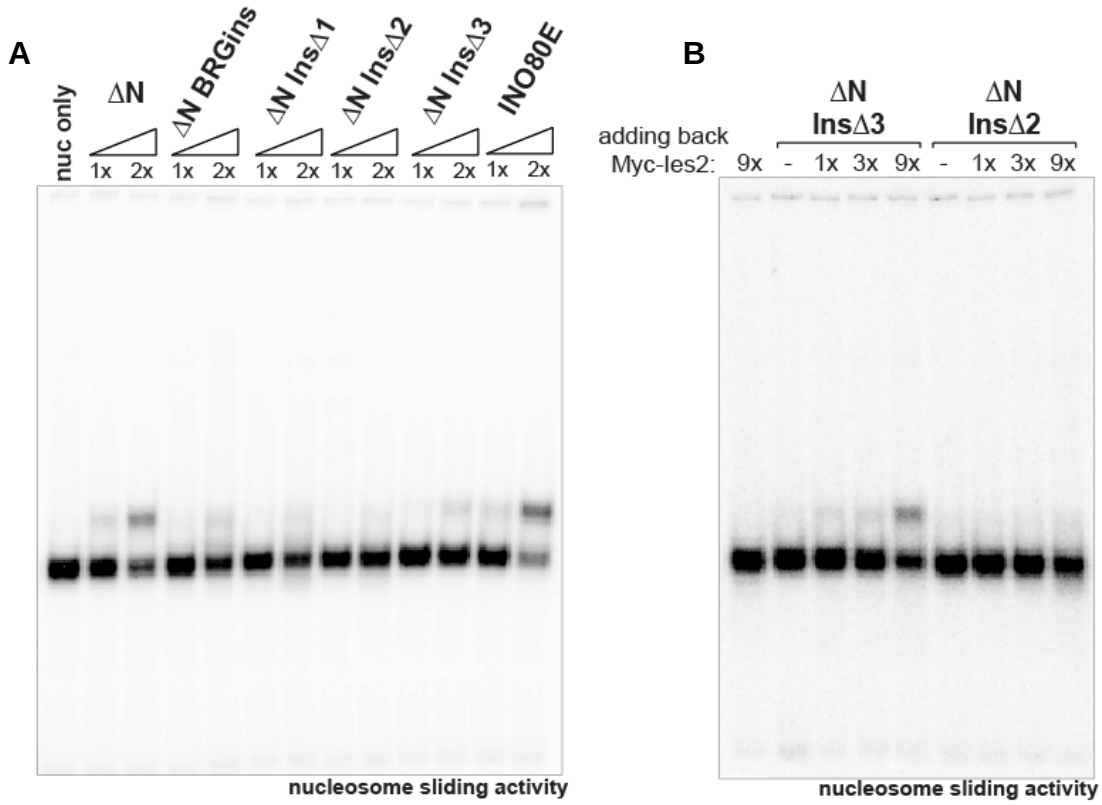

Figure 34. Ino80 insertion module is critical for the INO80 nucleosome sliding activity

(A) Nucleosome sliding assays were performed in the presence of varying amounts of the indicated FLAG-immunopurified INO80 complex. Insertion deletion mutants all exhibited compromised activity than complexes purified via Ino80ΔN and INO80E. (B) Addition of the recombinant Myc tagged Ies2 can restore the sliding activity of INO80ΔN InsΔ3 complexes to a certain degree, but not INO80ΔN InsΔ2 complexes that lacks Ies6, Arp5, Tip49a and Tip49b.

To test whether the important role of Ies2 for INO80 ATPase and remodeling activities is due to its contribution for the complex's affinity for nucleosomes, we subjected INO80ΔN InsΔ3 subcomplexes to the EMSA assay, and observed the ability of INO80ΔN InsΔ3 to supershift the nucleosomes is comparable to INO80ΔN complexes (Lane 10-17, Figure 31), suggesting Ies2 is dispensable for the optimal nucleosome binding ability of the INO80 complexes. Therefore, Ies2 is required for proper ATP

hydrolysis and nucleosome remodeling activities of INO80 complexes, but not required for INO80's nucleosome binding ability.

Since the Arp5 and Ies6 heterodimer can be significantly depleted from the INO80 complex without affecting its catalytic activity, we further explore the dimer's contribution to other aspects of the complex's activities using nucleosome sliding and binding assays. We observed a reduction in INO80 nucleosome sliding activity when Ies6 and Arp5 were depleted from the INO80ΔN subcomplexes (Figure 33A), suggesting the dimer is required for the optimal nucleosome remodeling activity of INO80. Since the same complex exhibited competent ATPase activity under saturating amount of nucleosome substrate, we tested whether Arp5 and Ies6 may be involved in the nucleosome binding by INO80. We purified INO80ΔN complexes from cells that stably express a short hairpin RNA (sh-RNA) targeting Ies6 (Figure 35B), and found that the binding affinity of the complexes toward nucleosome was indeed compromised upon the reduction in Arp5 and Ies6 (Figure 35C). Consistent with the possibility that the dimer is required for optimal nucleosome binding of INO80, we observed a slight but reproducible reduction in nucleosome dependent ATPase activity when a non-saturating amount of nucleosomes were used in the reaction. In addition, we plotted the rate of nucleosome stimulated ATP hydrolysis of various INO80ΔN siRNA complexes as a function of nucleosome concentration over a wide range, and observed an slight increase in Km value of complexes treated with siRNA targeting Ies6 and Arp5 in comparison of control siRNA treated complexes (Figure 32), suggesting reduced affinity of INO80 toward nucleosome substrates in the absence of Ies6 and Arp5. Our observations are

consistent with the possibility that Arp5 and Ies6 are required for the optimal nucleosome remodeling of INO80 by contributing to its nucleosome binding.

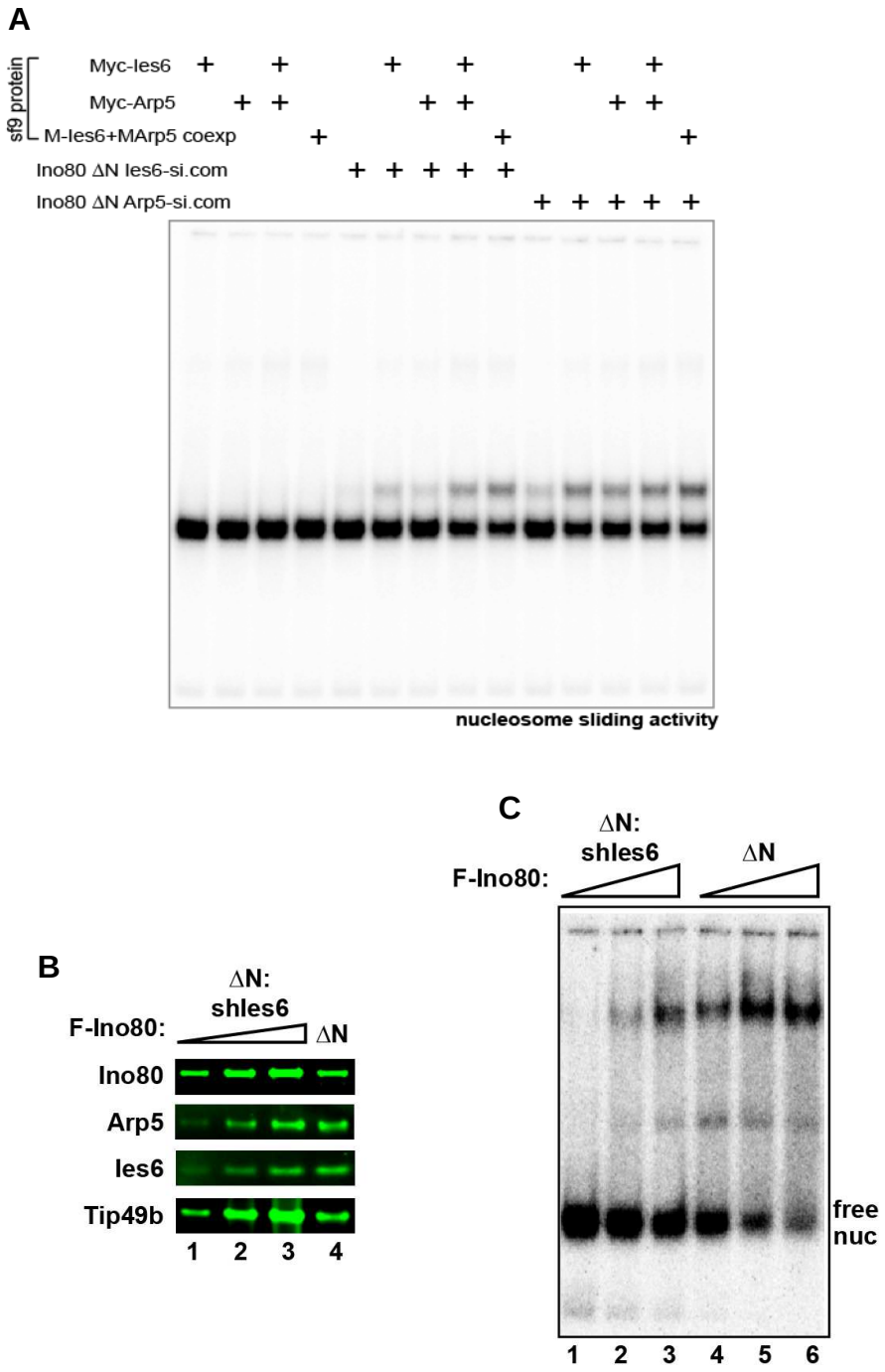

Figure 35. Ies6 and Arp5 are critical for nucleosome binding and chromatin remodeling activities of INO80

(A) The recombinant Ies6 and Arp5 can rescue compromised nucleosome sliding activity of INO80 complexes that lack Ies6 and Arp5. Nucleosome sliding assays were performed with purified INO80ΔN Arp5-si and Ies6-si complexes. The addition of recombinant human Ies6 and Arp5 made from insect cells

restored the sliding activity of both complexes to certain degrees. (C) Nucleosome binding assays were performed with increasing amount of complete INO80 complexes INO80E, and INO80ΔN complexes purified from cells stably expressing a small hairpin RNA (shRNA) targeting Ies6 (INO80ΔN: shIes6), whose subunit composition was analyzed in (B). It took 3 fold more INO80ΔN: shIes6 complexes to supershift comparable amount of nucleosome substrate.

Chapter V. Discussion

Modular organization of the human INO80 chromatin remodeling complex

Our findings suggest that the hINO80 complex is composed of at least three modules that assemble on distinct regions of the hIno80 protein. Two of these modules assemble on the conserved HSA/PTH and ATPase domains of the hIno80 protein and, together, are sufficient to reconstitute the ATP-dependent nucleosome remodeling activity of the hINO80 complex. Associated with the hIno80 ATPase domain are a subset of the conserved subunits, including the AAA^+ ATPases Tip49a and Tip49b, Ies2 and Ies6, and the actin-related protein Arp5, while the remaining conserved subunits Arp4, Arp8, and YY1 assemble on the HSA/PTH domain. HSA/PTH domains are found in multiple chromatin remodeling complexes from yeast to human and have been shown to function as docking sites for actin-related proteins (38, 117, 125). Evidence from this and prior studies argues that HSA/PTH domains are required for maximal ATPase and/or nucleosome remodeling activities catalyzed by HSA/PTH domain-containing Snf2 family ATPases (117, 125, 141); however, the exact function(s) of HSA/PTH domains and of their associated proteins are not known. Based on the observations (i) that yeast INO80 complexes lacking actin, Arp4, and Arp8 are defective in DNA binding, ATPase, and nucleosome remodeling activities (117), and (ii) that Arp4 and Arp8 can bind histones

(55, 117), it is possible that the INO80 HSA/PTH-containing module may contribute to recognition of DNA and/or nucleosome substrates. In this regard, it is noteworthy that YY1 is a DNA-binding protein that in at least some contexts can target the hINO80 complex to YY1-responsive elements in cells (17, 60). Whether YY1's DNA binding activity contributes to the nucleosome remodeling or ATPase activities of the INO80 complex remains to be determined.

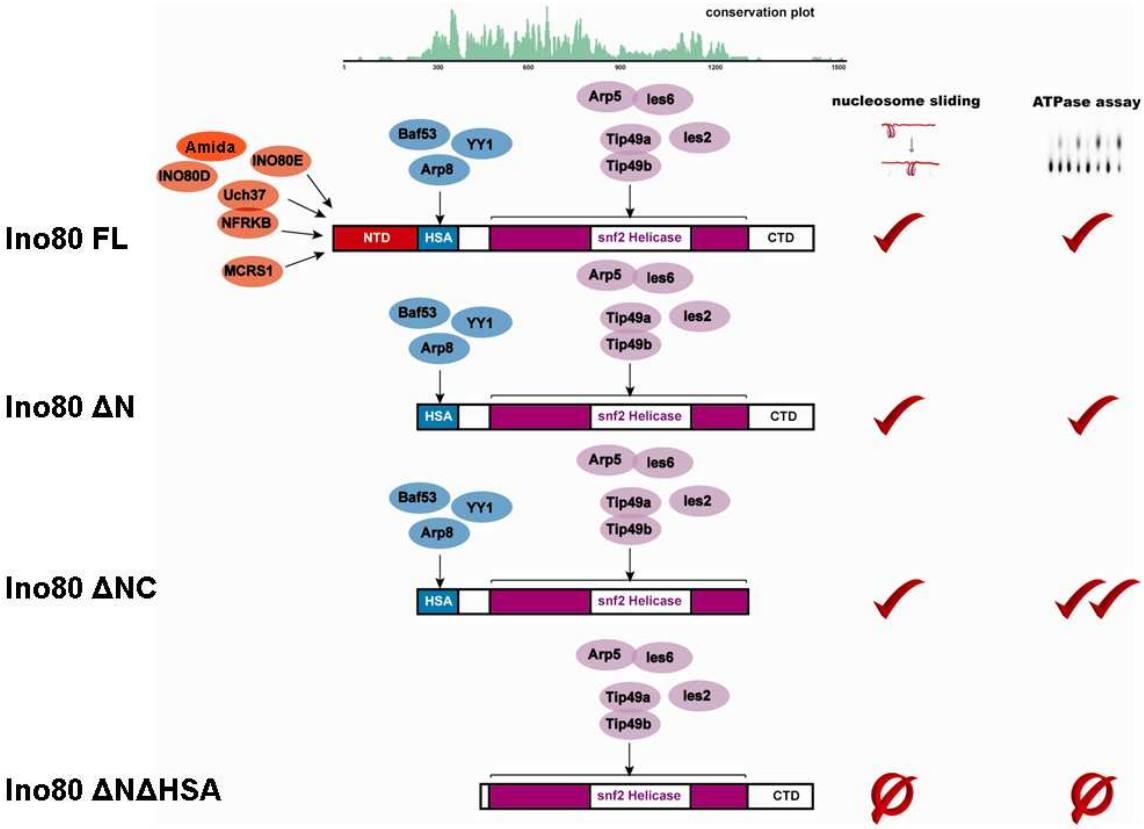

Figure 36. A summary of the modularity of INO80 chromatin remodeling complexes

The Ino80 ATPase contains regions that function as modular scaffolds on which the other INO80 subunits assemble. Subunits shown in red associate with the Ino80 NTD (N-terminal domain); subunits shown in blue associate with the Ino80 HSA (Helicase SANT Associated) domain; subunits shown in purple associate with the SNF2 ATPase domain, composed of SNF2N and HelicC regions (purple) separated by a long insertion region (white). Conserved subunits of INO80 bind to conserved region of Ino80, and reconstitute the conserved ATP-dependent nucleosome remodeling activity.

The hIno80 NTD nucleates assembly of the third hINO80 module, which includes all of the metazoan-specific subunits. Notably, while this hIno80 region is not conserved from yeast to humans, comparison of the sequences of human and insect Ino80 proteins reveals several conserved sequence blocks, and in the future it will be of interest to address the possibility that these sequences direct assembly of the metazoan-specific module. Our finding that the hIno80 NTD and the metazoan-specific subunits that assemble on it are dispensable for the ATPase and nucleosome sliding activities of the hINO80 complex suggests that these subunits are likely to have regulatory roles *in vivo* and paves the way for future studies on their contribution(s) to the function of the hINO80 complex in cells.

Previous studies demonstrated the Ies2, Ies6, Arp5, and Tip49a and Tip49b are components of a core human INO80 complex that is sufficient to carry out full ATP-dependent nucleosome remodeling activity; in the presented report, we provided evidence to further define the requirement for assembly of Ies2, Ies6, Arp5, Tip49a and Tip49b, and distinguish their functional contribution to ATP-dependent chromatin remodeling activities of the INO80 complex.

ATP-dependent nucleosome remodeling of human INO80 complex can be envisioned as a multi-step process that starts with assembly of INO80 subunits to form functional complexes, followed by engagement of INO80 complexes to nucleosomes, activation of ATP hydrolysis by the Ino80 ATPase, translocation of the remodeler and nucleosome repositioning. To define the contribution of Ies2, Ies6, Arp5, and Tip49a/b in the multistep process of nucleosome remodeling, we generated a collection of INO80

subcomplexes that carry structural mutations in the insertion region of the ATPase domain, or contain reduced level of a given subunit, and analyzed these INO80 subcomplexes for their subunit composition and enzymatic activities using several *in vitro* biochemical assays, including DNA- and nucleosome- dependent ATPase assay, nucleosome binding assay, and ATP-dependent nucleosome sliding assay.

We obtained evidence that the ATPase insertion regions of INO80 family ATPases are necessary for assembly of ATPase-associating subunits, which requires the presence of the eIF3B-related sequence within the Ino80 insertion. The missing or inclusion of this insertion module correlates with loss or gain of nucleosome binding capacity of the INO80 subcomplexes, suggesting they contribute to nucleosome binding. Consistent with this hypothesis, the subcomplexes missing the insertion module were not able to bind to nucleosome, thus were deficient in nucleosome-stimulated ATPase, and ATP dependent nucleosome remodeling activities. Within the insertion module, Ies6 and Arp5 form a heterodimer, and are mutually dependent for assembly into INO80. The dimer is dispensable for INO80's ATPase activity, but is required for the optimal nucleosome remodeling, presumably via its contribution to nucleosome binding. On the contrary, Ies2 assembles independently of the Arp5-Ies6 dimer, and is absolutely required for the catalytic activities of the INO80 complex, while dispensable for its binding affinity to nucleosomes.

The Helical Domain 2 (HD2; Protrusion2) region of Ino80 is important for the activities of the complex

The insertion regions of Ino80 and Srcap are located within the Helical Domain 2 (HD2; protrusion2) of the Rad54 ATPase structure (127), based on sequence homology. In an effort to define the insertion regions of the human Ino80, SRCAP, and Brg1 ATPases, we aligned their primary sequences using Jalview software (137). We also included the sequence of zebrafish Rad54 protein, whose structural information has been published (127), in this multi-sequence alignment. According to the annotated Snf2-like structural features of Rad54, and the apparent sequence similarity, we identified a major insertion site located in the Helical Domain 2 (HD2; protrusion 2) within the ATPase domain, in which long patches of non-homologous sequences of Ino80 and Srcap ATPases were inserted after the first two conserved helixes. As shown in this report and elsewhere (140, 141), the loss of the insertion regions within Ino80 and Srcap, or small deletions within Ino80 insertion rendered the remaining complexes catalytic inactive.

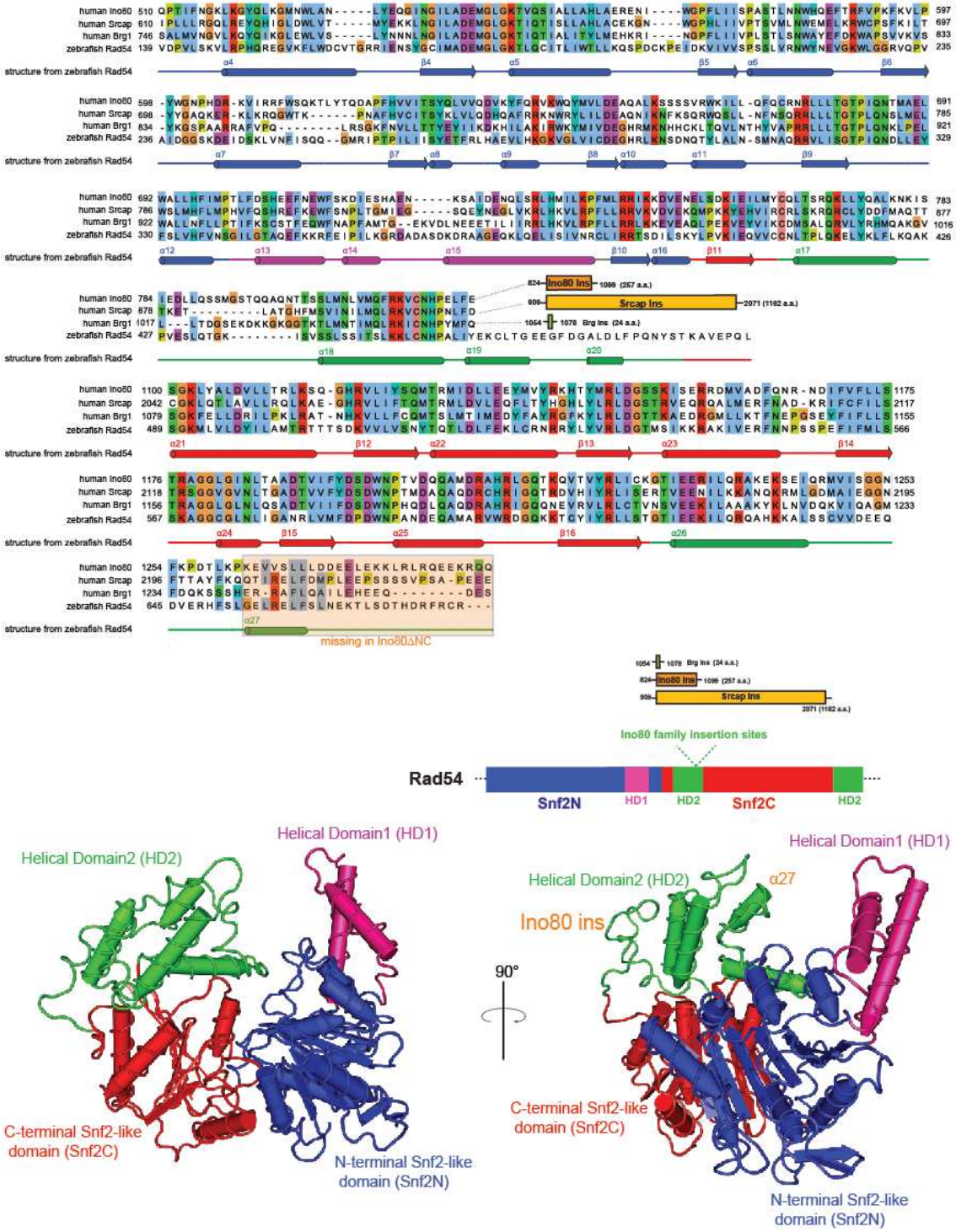

Figure 37. Modeling of human Ino80 structure based on zebrafish Rad54

(top) sequence alignment of human Ino80 (Q9ULG1), Srcap (Q6ZRS2), Brg1 (P51532), and zebrafish Rad54 (Q7ZV09). The secondary structures and the marked Snf2 family insertion site were annotated based on

sequence similarity with the published structural data of zebrafish Rad54 (127). (Bottom) Structure of zebrafish Rad54: the localization of predicted Ino80 insertion and α27 triangular brace (NegC) are indicated. The schematic diagram of Rad54 structural arrangement was shown in the insert. Snf2-like ATPase N-terminal domain is depicted in blue; Snf2-like ATPase C-terminal domain is depicted in red; Helical domain 1 (HD1) is depicted in pink, and HD2 is depicted in green.

An inhibitory region within Ino80 C Terminal Domain (CTD) is also located in the HD2 region of the ATPase structure. Previously, we reported that the CTD of Ino80 can negatively regulate the ATPase activity of INO80. Through extensive mutagenesis effort, we managed to narrow this inhibitory activity down to a string of 27 amino acids (1261-1288), located at the end of the conserved Snf2-C domain. The deletion of this region caused a dramatic increase in the DNA- and nucleosome stimulated INO80 ATPase activation (see Figure 22). Interestingly, the homologous region of the Rad54 protein adopts structural folds (after the 26th α-helix) that is spatially positioned near the HD2 region, according to the structural model. Interestingly, a recently described "NegC" region within ISWI family remodelers (26) has been shown to negatively regulate the ability of ISWI to couple ATP hydrolysis with the process of DNA translocation. This "NegC" motif was inserted immediate after the homologous region of the Rad54 26th α-helix (Figure 37).

The HD2 fold consists of two anti-parallel helixes α17 and α18, which are conserved across different Snf2 remodelers. The Ino80 insertions and the inhibitory α27 position spatially "sandwich" the anti-paralleled helical core, (Figure 37) suggesting a potential regulatory relationship. Thus, the insertion regions of INO80 family ATPases, and inhibitory regions of Ino80 and Iswi are predicted to position in the same structural fold domain, arguing that this HD2 (protrusion2) region of the snf2-like ATPase plays an

important role in modulating protein interactions and enzymatic activities of various remodelers.

Insertion regions of INO80 family snf2 like ATPase direct subunit assembly

We studied the structural requirement for recruitment of ATPase-associating INO80 subunits by insertion-swapping experiments. We demonstrated that the Ino80 insertion is required to recruit Ies2, Ies6, Arp5, Tip49a, and Tip49b into the complex; whereas the INO80 HSA, Snf2-N and Snf2-C domains are insufficient. Moreover, the homologous Srcap insertion of the SRCAP complex sufficiently recruited SRCAP subunits ZnHIT1, Yl1, Arp6, Tip49a, and Tip49b into the INO80ΔN SRCAPins subcomplex.

Our results suggest that the recruitment specificity of these ATPase-associating subunits of INO80 and SRCAP complexes are likely embedded within the insertion region of the Ino80 and Srcap ATPases, respectively. Moreover, since both Tip49a and Tip49b are shared subunits between two complexes, it is less likely that they play major roles in specifying complex-specific subunits in the insertion module.

The ATPase insertion region and its homologous binding subunits in respective INO80 and SRCAP complexes comprise a similar molecular environment; therefore, the shared structure properties between the homologous subunits and the ATPase insertions of both complexes may play an important role in assembly of this “insertion module” of INO80 family remodeling complexes. Arguing that the Yl1-like domain contributes to the assembly of Ies6 into INO80, the Yl1-like domain of Ies6 alone, when expressed in cells,

can associate with an INO80 complex with full set of its subunits (data not shown). It is of interests to test whether the homologous domain of YL1 alone can sufficiently associate with SRCAP complexes. Additionally, we detect strong association of Yl1 with SRCAP in our western blotting using Yl1 specific antibody, but we do also detect a trace amount of Yl1 in our INO80ΔN complexes, suggesting a smaller population of YL1 can mediate interaction with Ino80 insertions under certain condition. Consistent with the possibility that certain shared sequence features embedded in both insertion regions may be responsible for the assembly of some or all of the insertion-binding subunit(s), deletion of the InsΔ3 box in the Ino80 insertion resulted in specific reduction of Ies2 in the INO80ΔN InsΔ3, but not other subunits.

Organization of the insertion module

Blast search of the insertion sequence of Ino80 uncovered a sequence motif that shares similarity with the eIF3B protein, which happens to be an integral subunit of a multi-protein complex that also associates with Tip49a, and Tip49b. The deletion of the EIF3B-like sequence from the Ino80 insertion indeed results in loss of Tip49a and Tip49b from the INO80ΔNInsΔ1/2.com. Unexpectedly Ies2, Ies6, and Arp5 are also depleted from these mutant INO80. Noticeably, a transient depletion of Tip49a and Tip49b led to the concomitant depletion of Arp5 from the budding yeast INO80 complexes (67); however, the same report did not include Ies2 and Ies6 as potential proteins that associate with INO80. These observations suggest that Tip49a and Tip49b, together with the complex-specific insertions, are required for the binding of other ATPase binding subunits to INO80, consistent with a chaperon-like activity of the AAA+ ATPases Tip49a and

Tip49b in the assembly of various protein and/or RNA complexes (63, 89, 134), though we can not rule out the alternative possibility that the assembly of insertion module subunits depends on the structural integrity of the entire Ino80 ATPase domain.

We studied the molecular interactions of the insertion module in more detail. Dutta lab (67) reported that Arp5 can associate with Tip49a/b in an Ino80 and ATP dependent manner. Arguing that the association between Arp5 and Tip49a/b is indirect and likely though other INO80 subunits, our insect cell coexpression data showed no detectable mutual interactions, either with or without ATP; instead, under the same condition, Ies6 interacts with Arp5, and forms stable heterodimers. Also, the addition of Ies6, but not Tip49a and Tip49b, can facilitate Arp5's association with the Ino80 ATPase. Consistently, knockdown of either Arp5 or Ies6 by siRNAs resulted in depletion of both subunits from the rest of INO80, highlighting an essential structural role played by the Ies6 and Arp5 heterodimer. Tip49a and Tip49b are mutually dependent on each other to assemble into INO80 (67). Their assembly appears to be independent of Ies2, or Ies6-Arp5 dimer. Additionally, Ies2 associates with INO80 at a normal level in the absence of the Ies6-Arp5 heterodimer. Its optimal assembly requires the presence of the missing sequences in Ino80 InsΔ3, in addition to the eIF3B sequence (InsΔ1/2) required by all the insertion subunits. Our result is consistent with a hierarchical assembly model in which Tip49a and Tip49b assemble with the eIF3B-related region of the Ino80 ATPase insertion prior to the rest of subunits, which together reconstitute a proper structural conformation that allows the independent assembly of an obligatory heterodimer of Ies6 and Arp5, and Ies2 by itself.

Ino80 insertion region recruits a module of subunits that supports nucleosome binding

To address the functional role of the insertion module subunits, we generated a chimeric complex INO80ΔN BRGins that contains normal subunits in the HSA module, but lacks the INO80 insertion module subunits Ies2, Ies6, Arp5, Tip49a, and Tip49b. This chimeric complex was not able to exhibit detectable nucleosome binding activity, but regained such activity when the homologous subunits of the SRCAP complex were recruited with the insertion region of Srcap. Our data is consistent with the possibility that the insertion regions of both complexes assemble a set of core subunits that are necessary and sufficient for the INO80 family complexes to bind to nucleosomes.

In addition, the Bromo domain is an acetyl-lysine-recognition motif that can specifically recognize acetylated histone tails at lysine residues (36). Brg1 ATPases contain a C terminal bromo domain, which has been shown to be necessary for the stable occupancy of the orthologous yeast SWI/SNF2 complex on acetylated nucleosome arrays (57). The chimeric ATPase Ino80ΔN BRGins lacks the C terminal bromo domain, but shares homologous snf2-like ATPase domain and HSA domain with human Brg1. Consistent with the essential role of Bromo in nucleosome binding of Brg1 complexes, the chimeric ATPase assembles a complex that was not able to associate with nucleosomes stably. It would be of interests to graft the Brg1 bromo domain back into the Ino80ΔN BRGins chimera, and test whether the nucleosome binding ability of the resulting complex has been rescued or not.

Therefore, our observations raise the possibility that the Ino80 family insertion, together with its binding subunits, form a structural module that is functional equivalent to the bromo domain of the Brg1 ATPase, or SANT-SLIDE domain of the Iswi ATPase (50) in supporting the binding of the remodeling complexes to nucleosomes.

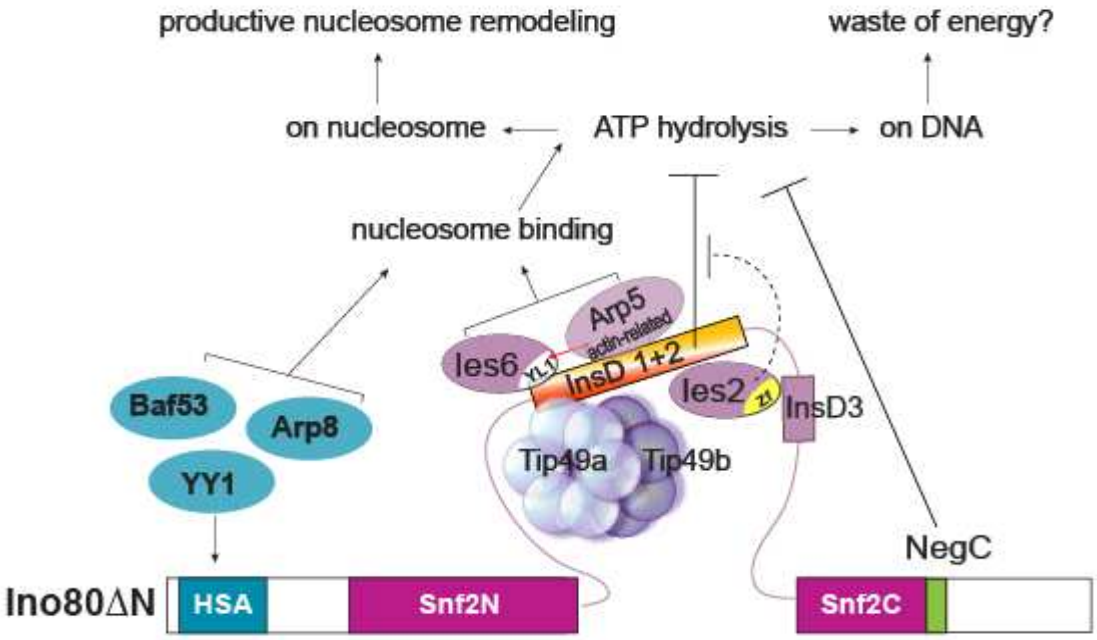

Figure 38. A proposed model explaining the structural and functional relationship of INO80 core subunits

The insertion region of the Ino80 ATPase is depicted in a pink ribbon, on which the five conserved INO80 subunits assemble. The inhibitory regulation of the InsΔ1 +2 domains on ATP hydrolysis was deduced from the hyper-active DNA-stimulated ATPase activity in INO80ΔN InsΔ1/2 complexes, though further confirmation is required. Additionally, Ies2 was evidently missing from the de-repressed INO80ΔN InsΔ1 and Δ2 complexes, arguing against a direct activating role by Ies2, but a role to counter the negative regulation posed by InsΔ1 and InsΔ2 sequences. "NegC" corresponds to the 27 amino acid CTD inhibitory triangle brace region in Ino80 identified in Figure 22.

Arps and HSA domain in nucleosome remodeling

Arp4 (Baf53a), Arp8, Arp5, and β-actin subunits are important for INO80 activities both *in vitro* and *in vivo*. Arp4 (Baf53a), Arp8, and actin assemble with the HSA domain;

while Arp5 assembles with the ATPase insertion region of Ino80 in a Tip49a/b dependent manner. Non-mutually exclusive mechanisms by which actin and Arps contribute to nucleosome remodeling activities of INO80 and other remodeling complexes have been proposed.

Most Arps assemble interdependently with either actin or another Arp into nucleosome remodeling complexes, thus maintaining structural integrity of these Arps-containing complexes. Arp7-Arp9, and Arp4 (Baf53a)-actin form obligatory dimers in order to assemble into yeast RSC, and human Brg1 complexes, respectively (90, 126). Moreover, Arp8 is required for the proper incorporation of Arp4 and actin into the yeast INO80 complexes (117), and recently been shown to exist as both a monomer and dimer (108). It is so far unknown whether the insertion-binding Arp5 of INO80 and Arp6 of SRCAP have assembly interdependency. In this study, we presented compelling evidence to support a model in which Arp5 and Ies6, a protein unrelated to Arp, form an obligatory heterodimer, and are interdependent for their association with INO80 complexes. Consistently, Arp6 has been demonstrated to be required for assembly of Swc2/3/6 into SRCAP complexes (140). It is of interest to test whether Ies6 shares any similar property with actin and Arps, and whether homologous subunits YL1 (Swc2) and Arp6 also assemble interdependently. In addition, we observed weak, but detectable interactions between Arp5 and Arp8, Arp4, and Arp5 itself, but not with other non-Arp subunits, raising the possibility that actin and Arps may form inter- or intra- complex contact with other actin and Arp pairs.

Consistent with the possibility that Arps and actin may function as nucleosomes-binding interfaces for INO80 complexes, multiple lines of evidence suggest that recombinant Arp4 and Arp8 can bind to core histones *in vitro* (48, 55, 90, 108, 117). Consistently, yeast INO80 complexes containing mutated β-actin (69), or lacking Arp5 or Arp8 (117) exhibited reduced or diminished DNA and nucleosome binding activities. Interestingly, complete removal of Arp5 from yeast INO80 complexes only resulted in a moderate reduction (~50%) in nucleosome binding affinity of INO80 complexes. We observed a similar reduction in INO80's nucleosome binding affinity when Ies6 and Arp5 were co-depleted from the mutant INO80 subcomplexes by RNAi knockdown. We argue the remaining binding activity of our Arp5-depleted INO80 is less likely due to the residual Arp5, but due to other additional nucleosome-binding interfaces in INO80. Indeed, additional reduction of nucleosome binding was evident when we tested insertion mutant INO80 subcomplexes that lack the entire insertion module, suggesting the rest of the INO80 insertion module could also participate in binding of nucleosomes. In addition, given that yeast INO80 lacking Arp8, Arp4, and actin showed little or no nucleosome binding activity (117) and insertion mutants subcomplexes containing normal assembly of the HSA module failed to exhibit detectable nucleosome binding activity, suggests that HSA-binding Arps are insufficient in supporting the optimal nucleosome binding activity of INO80. Recently, a RSC subcomplex containing the Sth1 HSA domain and Arp7/9 was not able to exhibit specific binding to nucleosomes (112). Therefore, these observations agree with the possibility that multiple nucleosome interfaces exist in INO80, and they are collectively required for the full nucleosome binding potential of the complex.

Alternatively, compensatory mutagenesis analysis from the Cairns lab (125) supported a model that HSA-binding Arps of the RSC complex may form regulatory contact with the snf2-like ATPase domain, thereby modulating the catalysis of the nucleosome remodeling complexes. Multiple lines of studies in different families of remodeling complexes lacking HSA domain or Arps supports that actin and Arps are indispensible for the optimal ATPase activities of the remodeling complexes, though the degree to which actin and Arps are needed differs from complex to complex. Some of the reports challenged the remodeling complex lacking Arps with a single activity measurement, either for ATP hydrolysis or nucleosome remodeling. While establishing a requirement of the missing Arp in a given activity, these results lend little support to demonstrate a direct role of the missing Arp in the process of a multi-step chromatin remodeling process.

Our biochemical analysis of INO80 subcomplexes depleted with Arp5 suggests that the insertion-binding Arp5 plays an essential role in nucleosome binding and remodeling activities of the complex, which is consistent with the published data in yeast INO80. Arguing that Arp5 is less likely to play a direct role in activating INO80 ATPase activity, INO80 subcomplexes with greatly depleted Arp5 and Ies6 were able to hydrolyze ATP at a rate comparable to the maximum rate by the complete complex, under saturating condition. We do observe slightly reduced ATPase activity when non-saturating amount of nucleosome substrate were used, which could be explained by the aforementioned reduction in nucleosome binding affinity (increase in Km) caused by depletion of Arp5 and Ies6 from INO80 complexes.

Ies2 and Ies6 as bona fide components of INO80 complexes

We presented compelling evidence to support functional roles played by conserved subunits Ies2 and Ies6 in the nucleosome remodeling process by human INO80 complexes. Homologous subunits Swc6 (for Ies2) and Swc2 (for Ies6) of yeast SWR1 complexes are essential for the ATP dependent histone H2Az exchange activity (140), consistent with the important function played by Ies2 and Ies6 for human INO80 chromatin remodeling activities. It is somehow surprising that Ies2 and Ies6 orthologs were not detected in yeast INO80 complexes (116) under high salt washing condition (500 mM KCl). Additionally, these complexes associate with Arp5, and were able to bind and remodel nucleosomes, and hydrolyze ATP (117). The discrepancy between the two results could be reconciled by simple gain of new functions by Ies2 and Ies6 through evolutionary selection; or alternatively, Ies2 and Ies6 bind to INO80 in a salt sensitive way, likely as peripheral subunits. High salt washed INO80 complexes carried an amount of Ies2 and Ies6 that were below detection sensitivity by silver staining and mass spectrometry analysis in the earlier study. Consistently, we observed small, but noticeable, stimulation of INO80 remodeling activity upon the addition of recombinant Ies2, Ies6 and Arp5 dimers (data not shown), raising the possibility that Ies2 and Ies6 may be sub-stoichiometric components of human INO80 chromatin remodeling complex.

Swc2 (Yl1), Ies6's homolog in SWR1 complexes, has been shown to interact directly with histone variant H2Az (140, 141). Given that the yeast INO80 complex has been reported to catalyze histone exchange activity (97), it would be interesting to test whether these ATPase insertion–binding subunits Ies2, Ies6 and Arp5 contribute to proper H2Az deposition *in vitro* and *in vivo*.

Chapter VI. REFERENCES

1. **Ahn, S. H., W. L. Cheung, J. Y. Hsu, R. L. Diaz, M. M. Smith, and C. D. Allis.** 2005. Sterile 20 kinase phosphorylates histone H2B at serine 10 during hydrogen peroxide-induced apoptosis in S. cerevisiae. Cell **120:**25-36.
2. **Aoyagi, S., and J. J. Hayes.** 2002. hSWI/SNF-catalyzed nucleosome sliding does not occur solely via a twist-diffusion mechanism. Molecular and cellular biology **22:**7484-7490.
3. **Armstrong, J. A., O. Papoulas, G. Daubresse, A. S. Sperling, J. T. Lis, M. P. Scott, and J. W. Tamkun.** 2002. The Drosophila BRM complex facilitates global transcription by RNA polymerase II. The EMBO journal **21:**5245-5254.
4. **Bao, Y., and X. Shen.** 2007. INO80 subfamily of chromatin remodeling complexes. Mutation research **618:**18-29.
5. **Bao, Y., and X. Shen.** 2007. SnapShot: chromatin remodeling complexes. Cell **129:**632.
6. **Bernstein, B. E., T. S. Mikkelsen, X. Xie, M. Kamal, D. J. Huebert, J. Cuff, B. Fry, A. Meissner, M. Wernig, K. Plath, R. Jaenisch, A. Wagschal, R. Feil, S. L. Schreiber, and E. S. Lander.** 2006. A bivalent chromatin structure marks key developmental genes in embryonic stem cells. Cell **125:**315-326.
7. **Bhaumik, S. R., E. Smith, and A. Shilatifard.** 2007. Covalent modifications of histones during development and disease pathogenesis. Nature structural & molecular biology **14:**1008-1016.
8. **Bjorklund, S., G. Almouzni, I. Davidson, K. P. Nightingale, and K. Weiss.** 1999. Global transcription regulators of eukaryotes. Cell **96:**759-767.
9. **Blosser, T. R., J. G. Yang, M. D. Stone, G. J. Narlikar, and X. Zhuang.** 2009. Dynamics of nucleosome remodelling by individual ACF complexes. Nature **462:**1022-1027.
10. **Bouazoune, K., A. Mitterweger, G. Langst, A. Imhof, A. Akhtar, P. B. Becker, and A. Brehm.** 2002. The dMi-2 chromodomains are DNA binding modules important for ATP-dependent nucleosome mobilization. The EMBO journal **21:**2430-2440.
11. **Bowen, N. J., N. Fujita, M. Kajita, and P. A. Wade.** 2004. Mi-2/NuRD: multiple complexes for many purposes. Biochimica et biophysica acta **1677:**52-57.
12. **Boyer, L. A., R. R. Latek, and C. L. Peterson.** 2004. The SANT domain: a unique histone-tail-binding module? Nature reviews. Molecular cell biology **5:**158-163.
13. **Brehm, A., K. R. Tufteland, R. Aasland, and P. B. Becker.** 2004. The many colours of chromodomains. BioEssays : news and reviews in molecular, cellular and developmental biology **26:**133-140.
14. **Brizzard, B. L., R. G. Chubet, and D. L. Vizard.** 1994. Immunoaffinity purification of FLAG epitope-tagged bacterial alkaline phosphatase using a novel monoclonal antibody and peptide elution. BioTechniques **16:**730-735.
15. **Brosh, R. M., Jr., and S. W. Matson.** 1995. Mutations in motif II of Escherichia coli DNA helicase II render the enzyme nonfunctional in both mismatch repair and excision repair with differential effects on the unwinding reaction. Journal of bacteriology **177:**5612-5621.
16. **Cai, Y., J. Jin, A. J. Gottschalk, T. Yao, J. W. Conaway, and R. C. Conaway.** 2006. Purification and assay of the human INO80 and SRCAP chromatin remodeling complexes. Methods **40:**312-317.

17. **Cai, Y., J. Jin, T. Yao, A. J. Gottschalk, S. K. Swanson, S. Wu, Y. Shi, M. P. Washburn, L. Florens, R. C. Conaway, and J. W. Conaway.** 2007. YY1 functions with INO80 to activate transcription. Nature structural & molecular biology **14:**872-874.
18. **Cairns, B. R.** 2004. Around the world of DNA damage INO80 days. Cell **119:**733-735.
19. **Cairns, B. R., Y. J. Kim, M. H. Sayre, B. C. Laurent, and R. D. Kornberg.** 1994. A multisubunit complex containing the SWI1/ADR6, SWI2/SNF2, SWI3, SNF5, and SNF6 gene products isolated from yeast. Proceedings of the National Academy of Sciences of the United States of America **91:**1950-1954.
20. **Calo, E., and J. Wysocka.** 2013. Modification of enhancer chromatin: what, how, and why? Molecular cell **49:**825-837.
21. **Chaban, Y., C. Ezeokonkwo, W. H. Chung, F. Zhang, R. D. Kornberg, B. Maier-Davis, Y. Lorch, and F. J. Asturias.** 2008. Structure of a RSC-nucleosome complex and insights into chromatin remodeling. Nature structural & molecular biology **15:**1272-1277.
22. **Chambers, A. L., G. Ormerod, S. C. Durley, T. L. Sing, G. W. Brown, N. A. Kent, and J. A. Downs.** 2012. The INO80 chromatin remodeling complex prevents polyploidy and maintains normal chromatin structure at centromeres. Genes & development **26:**2590-2603.
23. **Chen, L., Y. Cai, J. Jin, L. Florens, S. K. Swanson, M. P. Washburn, J. W. Conaway, and R. C. Conaway.** 2011. Subunit organization of the human INO80 chromatin remodeling complex: an evolutionarily conserved core complex catalyzes ATP-dependent nucleosome remodeling. The Journal of biological chemistry **286:**11283-11289.
24. **Cheung, P., C. D. Allis, and P. Sassone-Corsi.** 2000. Signaling to chromatin through histone modifications. Cell **103:**263-271.
25. **Clapier, C. R., and B. R. Cairns.** 2009. The biology of chromatin remodeling complexes. Annual review of biochemistry **78:**273-304.
26. **Clapier, C. R., and B. R. Cairns.** 2012. Regulation of ISWI involves inhibitory modules antagonized by nucleosomal epitopes. Nature **492:**280-284.
27. **Clapier, C. R., K. P. Nightingale, and P. B. Becker.** 2002. A critical epitope for substrate recognition by the nucleosome remodeling ATPase ISWI. Nucleic acids research **30:**649-655.
28. **Conaway, R. C., and J. W. Conaway.** 2009. The INO80 chromatin remodeling complex in transcription, replication and repair. Trends in biochemical sciences **34:**71-77.
29. **Corona, D. F., and J. W. Tamkun.** 2004. Multiple roles for ISWI in transcription, chromosome organization and DNA replication. Biochimica et biophysica acta **1677:**113-119.
30. **Cote, J., J. Quinn, J. L. Workman, and C. L. Peterson.** 1994. Stimulation of GAL4 derivative binding to nucleosomal DNA by the yeast SWI/SNF complex. Science **265:**53-60.
31. **Dang, W., M. N. Kagalwala, and B. Bartholomew.** 2007. The Dpb4 subunit of ISW2 is anchored to extranucleosomal DNA. The Journal of biological chemistry **282:**19418-19425.
32. **Dechassa, M. L., B. Zhang, R. Horowitz-Scherer, J. Persinger, C. L. Woodcock, C. L. Peterson, and B. Bartholomew.** 2008. Architecture of the SWI/SNF-nucleosome complex. Molecular and cellular biology **28:**6010-6021.

33. **Delmas, V., D. G. Stokes, and R. P. Perry.** 1993. A mammalian DNA-binding protein that contains a chromodomain and an SNF2/SWI2-like helicase domain. Proceedings of the National Academy of Sciences of the United States of America **90:**2414-2418.
34. **Denslow, S. A., and P. A. Wade.** 2007. The human Mi-2/NuRD complex and gene regulation. Oncogene **26:**5433-5438.
35. **Dephoure, N., C. Zhou, J. Villen, S. A. Beausoleil, C. E. Bakalarski, S. J. Elledge, and S. P. Gygi.** 2008. A quantitative atlas of mitotic phosphorylation. Proceedings of the National Academy of Sciences of the United States of America **105:**10762-10767.
36. **Dhalluin, C., J. E. Carlson, L. Zeng, C. He, A. K. Aggarwal, and M. M. Zhou.** 1999. Structure and ligand of a histone acetyltransferase bromodomain. Nature **399:**491-496.
37. **Dignam, J. D., R. M. Lebovitz, and R. G. Roeder.** 1983. Accurate transcription initiation by RNA polymerase II in a soluble extract from isolated mammalian nuclei. Nucleic acids research **11:**1475-1489.
38. **Dion, V., K. Shimada, and S. M. Gasser.** 2010. Actin-related proteins in the nucleus: life beyond chromatin remodelers. Current opinion in cell biology **22:**383-391.
39. **Dorigo, B., T. Schalch, A. Kulangara, S. Duda, R. R. Schroeder, and T. J. Richmond.** 2004. Nucleosome arrays reveal the two-start organization of the chromatin fiber. Science **306:**1571-1573.
40. **Ebbert, R., A. Birkmann, and H. J. Schuller.** 1999. The product of the SNF2/SWI2 paralogue INO80 of Saccharomyces cerevisiae required for efficient expression of various yeast structural genes is part of a high-molecular-weight protein complex. Molecular microbiology **32:**741-751.
41. **Falbo, K. B., and X. Shen.** 2012. Function of the INO80 chromatin remodeling complex in DNA replication. Frontiers in bioscience : a journal and virtual library **17:**970-975.
42. **Fiorini, F., M. Boudvillain, and H. Le Hir.** 2013. Tight intramolecular regulation of the human Upf1 helicase by its N- and C-terminal domains. Nucleic acids research **41:**2404-2415.
43. **Flaus, A., D. M. Martin, G. J. Barton, and T. Owen-Hughes.** 2006. Identification of multiple distinct Snf2 subfamilies with conserved structural motifs. Nucleic acids research **34:**2887-2905.
44. **Florens, L., and M. P. Washburn.** 2006. Proteomic analysis by multidimensional protein identification technology. Methods in molecular biology **328:**159-175.
45. **Foury, F., and A. Goffeau.** 1979. Genetic control of enhanced mutability of mitochondrial DNA and gamma-ray sensitivity in Saccharomyces cerevisiae. Proceedings of the National Academy of Sciences of the United States of America **76:**6529-6533.
46. **Gangaraju, V. K., and B. Bartholomew.** 2007. Dependency of ISW1a chromatin remodeling on extranucleosomal DNA. Molecular and cellular biology **27:**3217-3225.
47. **Gangaraju, V. K., P. Prasad, A. Srour, M. N. Kagalwala, and B. Bartholomew.** 2009. Conformational changes associated with template commitment in ATP-dependent chromatin remodeling by ISW2. Molecular cell **35:**58-69.
48. **Gerhold, C. B., D. D. Winkler, K. Lakomek, F. U. Seifert, S. Fenn, B. Kessler, G. Witte, K. Luger, and K. P. Hopfner.** 2012. Structure of Actin-related protein 8 and its contribution to nucleosome binding. Nucleic acids research **40:**11036-11046.
49. **Gorbalenya, A. E., and E. V. Koonin.** 1993. Helicases: amino acid sequence comparisons and structure-function relationships. Current opinion in structural biology **3:**419-429.

50. **Grune, T., J. Brzeski, A. Eberharter, C. R. Clapier, D. F. Corona, P. B. Becker, and C. W. Muller.** 2003. Crystal structure and functional analysis of a nucleosome recognition module of the remodeling factor ISWI. Molecular cell **12:**449-460.
51. **Haber, J. E., and B. Garvik.** 1977. A new gene affecting the efficiency of mating-type interconversions in homothallic strains of Saccharomyces cerevisiae. Genetics **87:**33-50.
52. **Hamiche, A., J. G. Kang, C. Dennis, H. Xiao, and C. Wu.** 2001. Histone tails modulate nucleosome mobility and regulate ATP-dependent nucleosome sliding by NURF. Proceedings of the National Academy of Sciences of the United States of America **98:**14316-14321.
53. **Han, M., and M. Grunstein.** 1988. Nucleosome loss activates yeast downstream promoters in vivo. Cell **55:**1137-1145.
54. **Hanson, P. I., and S. W. Whiteheart.** 2005. AAA+ proteins: have engine, will work. Nature reviews. Molecular cell biology **6:**519-529.
55. **Harata, M., Y. Oma, S. Mizuno, Y. W. Jiang, D. J. Stillman, and U. Wintersberger.** 1999. The nuclear actin-related protein of Saccharomyces cerevisiae, Act3p/Arp4, interacts with core histones. Molecular biology of the cell **10:**2595-2605.
56. **Hargreaves, D. C., and G. R. Crabtree.** 2011. ATP-dependent chromatin remodeling: genetics, genomics and mechanisms. Cell research **21:**396-420.
57. **Hassan, A. H., P. Prochasson, K. E. Neely, S. C. Galasinski, M. Chandy, M. J. Carrozza, and J. L. Workman.** 2002. Function and selectivity of bromodomains in anchoring chromatin-modifying complexes to promoter nucleosomes. Cell **111:**369-379.
58. **Hewish, D. R., and L. A. Burgoyne.** 1973. Chromatin sub-structure. The digestion of chromatin DNA at regularly spaced sites by a nuclear deoxyribonuclease. Biochemical and biophysical research communications **52:**504-510.
59. **Hirschhorn, J. N., S. A. Brown, C. D. Clark, and F. Winston.** 1992. Evidence that SNF2/SWI2 and SNF5 activate transcription in yeast by altering chromatin structure. Genes & development **6:**2288-2298.
60. **Hogan, C. J., S. Aligianni, M. Durand-Dubief, J. Persson, W. R. Will, J. Webster, L. Wheeler, C. K. Mathews, S. Elderkin, D. Oxley, K. Ekwall, and P. D. Varga-Weisz.** 2010. Fission yeast Iec1-ino80-mediated nucleosome eviction regulates nucleotide and phosphate metabolism. Molecular and cellular biology **30:**657-674.
61. **Horn, P. J., L. M. Carruthers, C. Logie, D. A. Hill, M. J. Solomon, P. A. Wade, A. N. Imbalzano, J. C. Hansen, and C. L. Peterson.** 2002. Phosphorylation of linker histones regulates ATP-dependent chromatin remodeling enzymes. Nature structural biology **9:**263-267.
62. **Hur, S. K., E. J. Park, J. E. Han, Y. A. Kim, J. D. Kim, D. Kang, and J. Kwon.** 2010. Roles of human INO80 chromatin remodeling enzyme in DNA replication and chromosome segregation suppress genome instability. Cellular and molecular life sciences : CMLS **67:**2283-2296.
63. **Jha, S., and A. Dutta.** 2009. RVB1/RVB2: running rings around molecular biology. Molecular cell **34:**521-533.
64. **Jiang, Y., X. Wang, S. Bao, R. Guo, D. G. Johnson, X. Shen, and L. Li.** 2010. INO80 chromatin remodeling complex promotes the removal of UV lesions by the nucleotide excision repair pathway. Proceedings of the National Academy of Sciences of the United States of America **107:**17274-17279.

65. **Jin, J., Y. Cai, T. Yao, A. J. Gottschalk, L. Florens, S. K. Swanson, J. L. Gutierrez, M. K. Coleman, J. L. Workman, A. Mushegian, M. P. Washburn, R. C. Conaway, and J. W. Conaway.** 2005. A mammalian chromatin remodeling complex with similarities to the yeast INO80 complex. The Journal of biological chemistry **280:**41207-41212.
66. **Jones, D. T.** 1999. Protein secondary structure prediction based on position-specific scoring matrices. Journal of molecular biology **292:**195-202.
67. **Jonsson, Z. O., S. Jha, J. A. Wohlschlegel, and A. Dutta.** 2004. Rvb1p/Rvb2p recruit Arp5p and assemble a functional Ino80 chromatin remodeling complex. Molecular cell **16:**465-477.
68. **Kagalwala, M. N., B. J. Glaus, W. Dang, M. Zofall, and B. Bartholomew.** 2004. Topography of the ISW2-nucleosome complex: insights into nucleosome spacing and chromatin remodeling. The EMBO journal **23:**2092-2104.
69. **Kapoor, P., M. Chen, D. D. Winkler, K. Luger, and X. Shen.** 2013. Evidence for monomeric actin function in INO80 chromatin remodeling. Nature structural & molecular biology **20:**426-432.
70. **Kennison, J. A., and J. W. Tamkun.** 1988. Dosage-dependent modifiers of polycomb and antennapedia mutations in Drosophila. Proceedings of the National Academy of Sciences of the United States of America **85:**8136-8140.
71. **Klymenko, T., B. Papp, W. Fischle, T. Kocher, M. Schelder, C. Fritsch, B. Wild, M. Wilm, and J. Muller.** 2006. A Polycomb group protein complex with sequence-specific DNA-binding and selective methyl-lysine-binding activities. Genes & development **20:**1110-1122.
72. **Kornberg, R. D.** 1974. Chromatin structure: a repeating unit of histones and DNA. Science **184:**868-871.
73. **Kossel, A.** 1884. Ueber einen peptoartigen bestandheil des zellkerns. . Z. Physiol. Chem. **8**.
74. **Kouzarides, T.** 2007. Chromatin modifications and their function. Cell **128:**693-705.
75. **Laurent, B. C., and M. Carlson.** 1992. Yeast SNF2/SWI2, SNF5, and SNF6 proteins function coordinately with the gene-specific transcriptional activators GAL4 and Bicoid. Genes & development **6:**1707-1715.
76. **Laurent, B. C., M. A. Treitel, and M. Carlson.** 1991. Functional interdependence of the yeast SNF2, SNF5, and SNF6 proteins in transcriptional activation. Proceedings of the National Academy of Sciences of the United States of America **88:**2687-2691.
77. **Laurent, B. C., X. Yang, and M. Carlson.** 1992. An essential Saccharomyces cerevisiae gene homologous to SNF2 encodes a helicase-related protein in a new family. Molecular and cellular biology **12:**1893-1902.
78. **Leschziner, A. E., B. Lemon, R. Tjian, and E. Nogales.** 2005. Structural studies of the human PBAF chromatin-remodeling complex. Structure **13:**267-275.
79. **Li, B., M. Gogol, M. Carey, D. Lee, C. Seidel, and J. L. Workman.** 2007. Combined action of PHD and chromo domains directs the Rpd3S HDAC to transcribed chromatin. Science **316:**1050-1054.
80. **Lorch, Y., J. W. LaPointe, and R. D. Kornberg.** 1987. Nucleosomes inhibit the initiation of transcription but allow chain elongation with the displacement of histones. Cell **49:**203-210.

81. **Lorch, Y., B. Maier-Davis, and R. D. Kornberg.** 2010. Mechanism of chromatin remodeling. Proceedings of the National Academy of Sciences of the United States of America **107:**3458-3462.
82. **Lorch, Y., M. Zhang, and R. D. Kornberg.** 1999. Histone octamer transfer by a chromatin-remodeling complex. Cell **96:**389-392.
83. **Lowary, P. T., and J. Widom.** 1998. New DNA sequence rules for high affinity binding to histone octamer and sequence-directed nucleosome positioning. Journal of molecular biology **276:**19-42.
84. **Luger, K., A. W. Mader, R. K. Richmond, D. F. Sargent, and T. J. Richmond.** 1997. Crystal structure of the nucleosome core particle at 2.8 A resolution. Nature **389:**251-260.
85. **Mizuguchi, G., X. Shen, J. Landry, W. H. Wu, S. Sen, and C. Wu.** 2004. ATP-driven exchange of histone H2AZ variant catalyzed by SWR1 chromatin remodeling complex. Science **303:**343-348.
86. **Mohrmann, L., and C. P. Verrijzer.** 2005. Composition and functional specificity of SWI2/SNF2 class chromatin remodeling complexes. Biochimica et biophysica acta **1681:**59-73.
87. **Morrison, A. J., J. Highland, N. J. Krogan, A. Arbel-Eden, J. F. Greenblatt, J. E. Haber, and X. Shen.** 2004. INO80 and gamma-H2AX interaction links ATP-dependent chromatin remodeling to DNA damage repair. Cell **119:**767-775.
88. **Neigeborn, L., and M. Carlson.** 1984. Genes affecting the regulation of SUC2 gene expression by glucose repression in Saccharomyces cerevisiae. Genetics **108:**845-858.
89. **Newman, D. R., J. F. Kuhn, G. M. Shanab, and E. S. Maxwell.** 2000. Box C/D snoRNA-associated proteins: two pairs of evolutionarily ancient proteins and possible links to replication and transcription. Rna **6:**861-879.
90. **Nishimoto, N., M. Watanabe, S. Watanabe, N. Sugimoto, T. Yugawa, T. Ikura, O. Koiwai, T. Kiyono, and M. Fujita.** 2012. Heterocomplex formation by Arp4 and beta-actin is involved in the integrity of the Brg1 chromatin remodeling complex. Journal of cell science **125:**3870-3882.
91. **Noll, M.** 1974. Subunit structure of chromatin. Nature **251:**249-251.
92. **O'Gorman, S., D. T. Fox, and G. M. Wahl.** 1991. Recombinase-mediated gene activation and site-specific integration in mammalian cells. Science **251:**1351-1355.
93. **Olins, A. L., and D. E. Olins.** 1974. Spheroid chromatin units (v bodies). Science **183:**330-332.
94. **Oudet, P., M. Gross-Bellard, and P. Chambon.** 1975. Electron microscopic and biochemical evidence that chromatin structure is a repeating unit. Cell **4:**281-300.
95. **Owen-Hughes, T., R. T. Utley, D. J. Steger, J. M. West, S. John, J. Cote, K. M. Havas, and J. L. Workman.** 1999. Analysis of nucleosome disruption by ATP-driven chromatin remodeling complexes. Methods in molecular biology **119:**319-331.
96. **Papamichos-Chronakis, M., and C. L. Peterson.** 2008. The Ino80 chromatin-remodeling enzyme regulates replisome function and stability. Nature structural & molecular biology **15:**338-345.
97. **Papamichos-Chronakis, M., S. Watanabe, O. J. Rando, and C. L. Peterson.** 2011. Global regulation of H2A.Z localization by the INO80 chromatin-remodeling enzyme is essential for genome integrity. Cell **144:**200-213.

98. **Park, E. J., S. K. Hur, and J. Kwon.** 2010. Human INO80 chromatin-remodelling complex contributes to DNA double-strand break repair via the expression of Rad54B and XRCC3 genes. The Biochemical journal **431:**179-187.
99. **Pause, A., and N. Sonenberg.** 1992. Mutational analysis of a DEAD box RNA helicase: the mammalian translation initiation factor eIF-4A. The EMBO journal **11:**2643-2654.
100. **Peterson, C. L., and I. Herskowitz.** 1992. Characterization of the yeast SWI1, SWI2, and SWI3 genes, which encode a global activator of transcription. Cell **68:**573-583.
101. **Peterson, C. L., and J. L. Workman.** 2000. Promoter targeting and chromatin remodeling by the SWI/SNF complex. Current opinion in genetics & development **10:**187-192.
102. **Phillips, D. M., and E. W. Johns.** 1965. A Fractionation of the Histones of Group F2a from Calf Thymus. The Biochemical journal **94:**127-130.
103. **Racki, L. R., J. G. Yang, N. Naber, P. D. Partensky, A. Acevedo, T. J. Purcell, R. Cooke, Y. Cheng, and G. J. Narlikar.** 2009. The chromatin remodeller ACF acts as a dimeric motor to space nucleosomes. Nature **462:**1016-1021.
104. **Ramachandran, A., M. Omar, P. Cheslock, and G. R. Schnitzler.** 2003. Linker histone H1 modulates nucleosome remodeling by human SWI/SNF. The Journal of biological chemistry **278:**48590-48601.
105. **Ramakrishnan, V.** 1997. Histone H1 and chromatin higher-order structure. Critical reviews in eukaryotic gene expression **7:**215-230.
106. **Saeki, H., K. Ohsumi, H. Aihara, T. Ito, S. Hirose, K. Ura, and Y. Kaneda.** 2005. Linker histone variants control chromatin dynamics during early embryogenesis. Proceedings of the National Academy of Sciences of the United States of America **102:**5697-5702.
107. **Saha, A., J. Wittmeyer, and B. R. Cairns.** 2005. Chromatin remodeling through directional DNA translocation from an internal nucleosomal site. Nature structural & molecular biology **12:**747-755.
108. **Saravanan, M., J. Wuerges, D. Bose, E. A. McCormack, N. J. Cook, X. Zhang, and D. B. Wigley.** 2012. Interactions between the nucleosome histone core and Arp8 in the INO80 chromatin remodeling complex. Proceedings of the National Academy of Sciences of the United States of America **109:**20883-20888.
109. **Sauer, B.** 1994. Site-specific recombination: developments and applications. Current opinion in biotechnology **5:**521-527.
110. **Schalch, T., S. Duda, D. F. Sargent, and T. J. Richmond.** 2005. X-ray structure of a tetranucleosome and its implications for the chromatin fibre. Nature **436:**138-141.
111. **Schmid, S. R., and P. Linder.** 1992. D-E-A-D protein family of putative RNA helicases. Molecular microbiology **6:**283-291.
112. **Schubert, H. L., J. Wittmeyer, M. M. Kasten, K. Hinata, D. C. Rawling, A. Heroux, B. R. Cairns, and C. P. Hill.** 2013. Structure of an actin-related subcomplex of the SWI/SNF chromatin remodeler. Proceedings of the National Academy of Sciences of the United States of America **110:**3345-3350.
113. **Schwanbeck, R., H. Xiao, and C. Wu.** 2004. Spatial contacts and nucleosome step movements induced by the NURF chromatin remodeling complex. The Journal of biological chemistry **279:**39933-39941.
114. **Seet, B. T., I. Dikic, M. M. Zhou, and T. Pawson.** 2006. Reading protein modifications with interaction domains. Nature reviews. Molecular cell biology **7:**473-483.

115. **Sha, Z., L. M. Brill, R. Cabrera, O. Kleifeld, J. S. Scheliga, M. H. Glickman, E. C. Chang, and D. A. Wolf.** 2009. The eIF3 interactome reveals the translasome, a supercomplex linking protein synthesis and degradation machineries. Molecular cell **36:**141-152.
116. **Shen, X., G. Mizuguchi, A. Hamiche, and C. Wu.** 2000. A chromatin remodelling complex involved in transcription and DNA processing. Nature **406:**541-544.
117. **Shen, X., R. Ranallo, E. Choi, and C. Wu.** 2003. Involvement of actin-related proteins in ATP-dependent chromatin remodeling. Molecular cell **12:**147-155.
118. **Shogren-Knaak, M., H. Ishii, J. M. Sun, M. J. Pazin, J. R. Davie, and C. L. Peterson.** 2006. Histone H4-K16 acetylation controls chromatin structure and protein interactions. Science **311:**844-847.
119. **Shogren-Knaak, M., and C. L. Peterson.** 2006. Switching on chromatin: mechanistic role of histone H4-K16 acetylation. Cell cycle **5:**1361-1365.
120. **Simon, J. A., and R. E. Kingston.** 2009. Mechanisms of polycomb gene silencing: knowns and unknowns. Nature reviews. Molecular cell biology **10:**697-708.
121. **Steinberg, T. H.** 2009. Protein gel staining methods: an introduction and overview. Methods in enzymology **463:**541-563.
122. **Strohner, R., M. Wachsmuth, K. Dachauer, J. Mazurkiewicz, J. Hochstatter, K. Rippe, and G. Langst.** 2005. A 'loop recapture' mechanism for ACF-dependent nucleosome remodeling. Nature structural & molecular biology **12:**683-690.
123. **Struhl, K.** 1998. Histone acetylation and transcriptional regulatory mechanisms. Genes & development **12:**599-606.
124. **Subramanya, H. S., L. E. Bird, J. A. Brannigan, and D. B. Wigley.** 1996. Crystal structure of a DExx box DNA helicase. Nature **384:**379-383.
125. **Szerlong, H., K. Hinata, R. Viswanathan, H. Erdjument-Bromage, P. Tempst, and B. R. Cairns.** 2008. The HSA domain binds nuclear actin-related proteins to regulate chromatin-remodeling ATPases. Nature structural & molecular biology **15:**469-476.
126. **Szerlong, H., A. Saha, and B. R. Cairns.** 2003. The nuclear actin-related proteins Arp7 and Arp9: a dimeric module that cooperates with architectural proteins for chromatin remodeling. The EMBO journal **22:**3175-3187.
127. **Thoma, N. H., B. K. Czyzewski, A. A. Alexeev, A. V. Mazin, S. C. Kowalczykowski, and N. P. Pavletich.** 2005. Structure of the SWI2/SNF2 chromatin-remodeling domain of eukaryotic Rad54. Nature structural & molecular biology **12:**350-356.
128. **Tse, C., T. Sera, A. P. Wolffe, and J. C. Hansen.** 1998. Disruption of higher-order folding by core histone acetylation dramatically enhances transcription of nucleosomal arrays by RNA polymerase III. Molecular and cellular biology **18:**4629-4638.
129. **Tsukiyama, T.** 2002. The in vivo functions of ATP-dependent chromatin-remodelling factors. Nature reviews. Molecular cell biology **3:**422-429.
130. **Udugama, M., A. Sabri, and B. Bartholomew.** 2011. The INO80 ATP-dependent chromatin remodeling complex is a nucleosome spacing factor. Molecular and cellular biology **31:**662-673.
131. **Ura, K., H. Kurumizaka, S. Dimitrov, G. Almouzni, and A. P. Wolffe.** 1997. Histone acetylation: influence on transcription, nucleosome mobility and positioning, and linker histone-dependent transcriptional repression. The EMBO journal **16:**2096-2107.
132. **van Attikum, H., O. Fritsch, B. Hohn, and S. M. Gasser.** 2004. Recruitment of the INO80 complex by H2A phosphorylation links ATP-dependent chromatin remodeling with DNA double-strand break repair. Cell **119:**777-788.

133. **van der Westhuyzen, D. R., and C. von Holt.** 1971. A new procedure for the isolation and fractionation of histones. FEBS letters **14:**333-337.
134. **Venteicher, A. S., Z. Meng, P. J. Mason, T. D. Veenstra, and S. E. Artandi.** 2008. Identification of ATPases pontin and reptin as telomerase components essential for holoenzyme assembly. Cell **132:**945-957.
135. **Vincent, J. A., T. J. Kwong, and T. Tsukiyama.** 2008. ATP-dependent chromatin remodeling shapes the DNA replication landscape. Nature structural & molecular biology **15:**477-484.
136. **Washburn, M. P., D. Wolters, and J. R. Yates, 3rd.** 2001. Large-scale analysis of the yeast proteome by multidimensional protein identification technology. Nature biotechnology **19:**242-247.
137. **Waterhouse, A. M., J. B. Procter, D. M. Martin, M. Clamp, and G. J. Barton.** 2009. Jalview Version 2--a multiple sequence alignment editor and analysis workbench. Bioinformatics **25:**1189-1191.
138. **Wu, J. I., J. Lessard, and G. R. Crabtree.** 2009. Understanding the words of chromatin regulation. Cell **136:**200-206.
139. **Wu, S., Y. Shi, P. Mulligan, F. Gay, J. Landry, H. Liu, J. Lu, H. H. Qi, W. Wang, J. A. Nickoloff, and C. Wu.** 2007. A YY1-INO80 complex regulates genomic stability through homologous recombination-based repair. Nature structural & molecular biology **14:**1165-1172.
140. **Wu, W. H., S. Alami, E. Luk, C. H. Wu, S. Sen, G. Mizuguchi, D. Wei, and C. Wu.** 2005. Swc2 is a widely conserved H2AZ-binding module essential for ATP-dependent histone exchange. Nature structural & molecular biology **12:**1064-1071.
141. **Wu, W. H., C. H. Wu, A. Ladurner, G. Mizuguchi, D. Wei, H. Xiao, E. Luk, A. Ranjan, and C. Wu.** 2009. N terminus of Swr1 binds to histone H2AZ and provides a platform for subunit assembly in the chromatin remodeling complex. The Journal of biological chemistry **284:**6200-6207.
142. **Yang, J. G., T. S. Madrid, E. Sevastopoulos, and G. J. Narlikar.** 2006. The chromatin-remodeling enzyme ACF is an ATP-dependent DNA length sensor that regulates nucleosome spacing. Nature structural & molecular biology **13:**1078-1083.
143. **Yao, T., L. Song, J. Jin, Y. Cai, H. Takahashi, S. K. Swanson, M. P. Washburn, L. Florens, R. C. Conaway, R. E. Cohen, and J. W. Conaway.** 2008. Distinct modes of regulation of the Uch37 deubiquitinating enzyme in the proteasome and in the Ino80 chromatin-remodeling complex. Molecular cell **31:**909-917.
144. **Ye, J., A. R. Osborne, M. Groll, and T. A. Rapoport.** 2004. RecA-like motor ATPases--lessons from structures. Biochimica et biophysica acta **1659:**1-18.
145. **Yoshinaga, S. K., C. L. Peterson, I. Herskowitz, and K. R. Yamamoto.** 1992. Roles of SWI1, SWI2, and SWI3 proteins for transcriptional enhancement by steroid receptors. Science **258:**1598-1604.
146. **Yu, E. Y., O. Steinberg-Neifach, A. T. Dandjinou, F. Kang, A. J. Morrison, X. Shen, and N. F. Lue.** 2007. Regulation of telomere structure and functions by subunits of the INO80 chromatin remodeling complex. Molecular and cellular biology **27:**5639-5649.